Cells reshape habitability of temperature by secreting antioxidants to help each other replicate and avoid population extinction

Diederik S. Laman Trip[1,2] and Hyun Youk[1,2,3,*]

[1]Kavli Institute of Nanoscience,
[2]Department of Bionanoscience, Delft University of Technology, Delft 2628CJ, The Netherlands
[3]CIFAR, CIFAR Azrieli Global Scholars Program, Toronto ON M5G 1M1, Canada
[*]Corresponding author. Email: h.youk@tudelft.nl

Note: *Low resolution figures with captions are embedded within the main text. High resolution figures are at the end of the main text and preceded by their captions.*

SUMMARY

How the rising global temperatures affect organisms is a timely question. The conventional view is that high temperatures cause microbes to replicate slowly or die, both autonomously. Yet, microbes co-exist as a population, raising an underexplored question of whether they can cooperatively combat rising temperatures. Here we show that at high temperatures, budding yeasts help each other and future generations of cells replicate by secreting and extracellularly accumulating glutathione - a ubiquitous heat-damage-reducing antioxidant. Yeasts thereby collectively delay and can halt population extinctions at high temperatures. As a surprising consequence, even for the same temperature, a yeast population can either exponentially grow, never grow, or grow after unpredictable durations (hours-to-days) of stasis, depending on its population density. Furthermore, reducing superfluous expression of one gene can extend life-permitting temperature by several Celsius, thereby restoring population growths. Despite theory stating that heat-shocked cells autonomously die, non-growing populations at high temperatures - due to cells cooperating via glutathione - continuously decelerate and can eventually stop their approach to extinction, with higher population-densities stopping faster. A mathematical model recapitulates all these features. These results show how cells can collectively extend boundaries of life-permitting temperatures.

(190 words)

INTRODUCTION

Many model organisms are typically studied at a particular temperature that is "optimal" for that organism's growth. For example, the budding yeast is often studied at 30 ^{O}C while *E. coli* and mammalian cells are usually studied at 37 ^{O}C. Yet, an organism can live and replicate at a range of "habitable temperatures" (*1-3*). Understanding why an organism cannot replicate and eventually dies for temperatures outside the habitable range - called "unlivable temperatures" - would provide insights into life's vulnerabilities and how temperature, a fundamental physical quantity, drives processes of life. Moreover, given the rising global temperatures, a timely and practical question is how organisms do or can combat high temperatures to avoid extinction. For microbes and mammalian cells, the conventional view is that as the habitable temperature increases above some optimal value and approaches unlivable temperatures, cells need more time to replicate and that once the temperature enters the unlivable temperature regime, cells fail to replicate and eventually die (*1-4*) (Figures 1A-B). This view states that at sufficiently high temperatures, crucial proteins unfold and other heat-induced damages occur (e.g., damages by reactive oxygen species) (*5-7*), all of which disrupt cell replications. Moreover, it states that whether a cell can replicate or not at a high temperature depends on its autonomous ability to repair heat-induced damages by using its heat-shock response system, which is conserved across species (*8*). It is thought that while cells can autonomously repair heat-induced damages at moderately high, still-habitable temperatures which are just below the unlivable temperatures, they fail to do so at temperatures that are too high (i.e., at unlivable temperatures). Thus, this view states that one cell's ability to replicate and its lifespan are both independent of any other cell's lifespan and ability to replicate (*4*) (Figure 1C). Yet a cell rarely exists alone - it lives within a population and can cooperate with other cells. Indeed, microbes can use mechanisms such as quorum sensing to coordinate their behaviors (*9*), share food (*10*), and collectively tune their extracellular pH (*11*). These findings motivated us to ask whether microbes use collective strategies to combat rising temperatures and if so, what such strategies are (Figure 1D). These questions remain unaddressed for many microbial species. We sought to address them for the budding yeast, *Saccharomyces cerevisiae*. Surprisingly, we discovered that budding yeasts use a collective strategy to help each other replicate, help future generations of cells replicate, and thereby delay and even prevent population extinctions at high temperatures that are conventionally defined to be unlivable for yeast.

As our starting point, we reproduced the well-known, textbook picture of how temperature affects yeast and microbial growth (*4,12-14*) by using populations of a laboratory-standard ("wild-

type") strain of haploid budding yeast (Figure 1B and Figure S1). In this picture, the yeasts' growth rate becomes zero - the population density negligibly changes - for temperatures of 40 ^{O}C and higher, which would thus be defined as "unlivable temperatures" for budding yeast (Figure 1B - dark red region; Figure S1C). Despite being evidently true - since we reproduced it here - we discovered that this cell-autonomous view of yeast replication (Figure 1C) is misleading. For example, we discovered that yeast populations, depending on their population densities, can actually grow at "unlivable" temperatures (e.g., at 40 ^{O}C) and not grow at "habitable" temperatures (e.g., at 38 ^{O}C). As we will show, we discovered a picture that revises the cell-autonomous view: yeasts help each other and their future generations of cells replicate at high temperatures by secreting and accumulating an extracellular pool of glutathione - a versatile antioxidant that is widely used by many species - which reduces damages caused by reactive oxygen species that high temperatures create. Thus, yeasts collectively set the habitability of each temperature (Figure 1D). A surprising consequence of this is that a temperature which is unlivable for a relatively few yeasts becomes habitable if there are enough yeasts in a population that work together to help each other replicate. As another surprising consequence, we found that a yeast population - due to its cells gradually building up extracellular glutathione - decelerates and can eventually stop its approach to extinction at high temperatures. In fact, we found that a population of a higher density can more rapidly decelerate and halt its approach to extinction due to more cells cooperating through their secreted glutathione. This goes against the prevalent theory which states that cells autonomously die at high temperatures. Intriguingly, we discovered that yeast populations at one particular temperature - a special temperature that places yeasts at a cusp of being able to replicate and unable to replicate - exhibit behaviors that are akin to those of biomolecular (*15,16*) and physical systems (*17*) that undergo phase transitions at special (critical) temperatures. Our paper ends by describing a mathematical model that we developed. The model recapitulates all the experimental results and quantitatively explains the origin of these phase-transition-like features by using, as the mechanism, cells cooperatively accumulating extracellular glutathione. Glutathione, antioxidants, and heat-induced reactive oxygen species are common to many organisms, including humans. Hence the cooperative mechanism for budding yeast that we uncovered here - involving glutathione's previously underappreciated role as a secreted factor at high temperatures - raises the possibility that cells of other species do or can also collectively combat rising temperatures in a similar manner. Taken together, our work shows how the habitability of a temperature emerges as a community-level property for a specie - determined by intraspecies interactions - rather than determined solely by the specie's autonomous features.

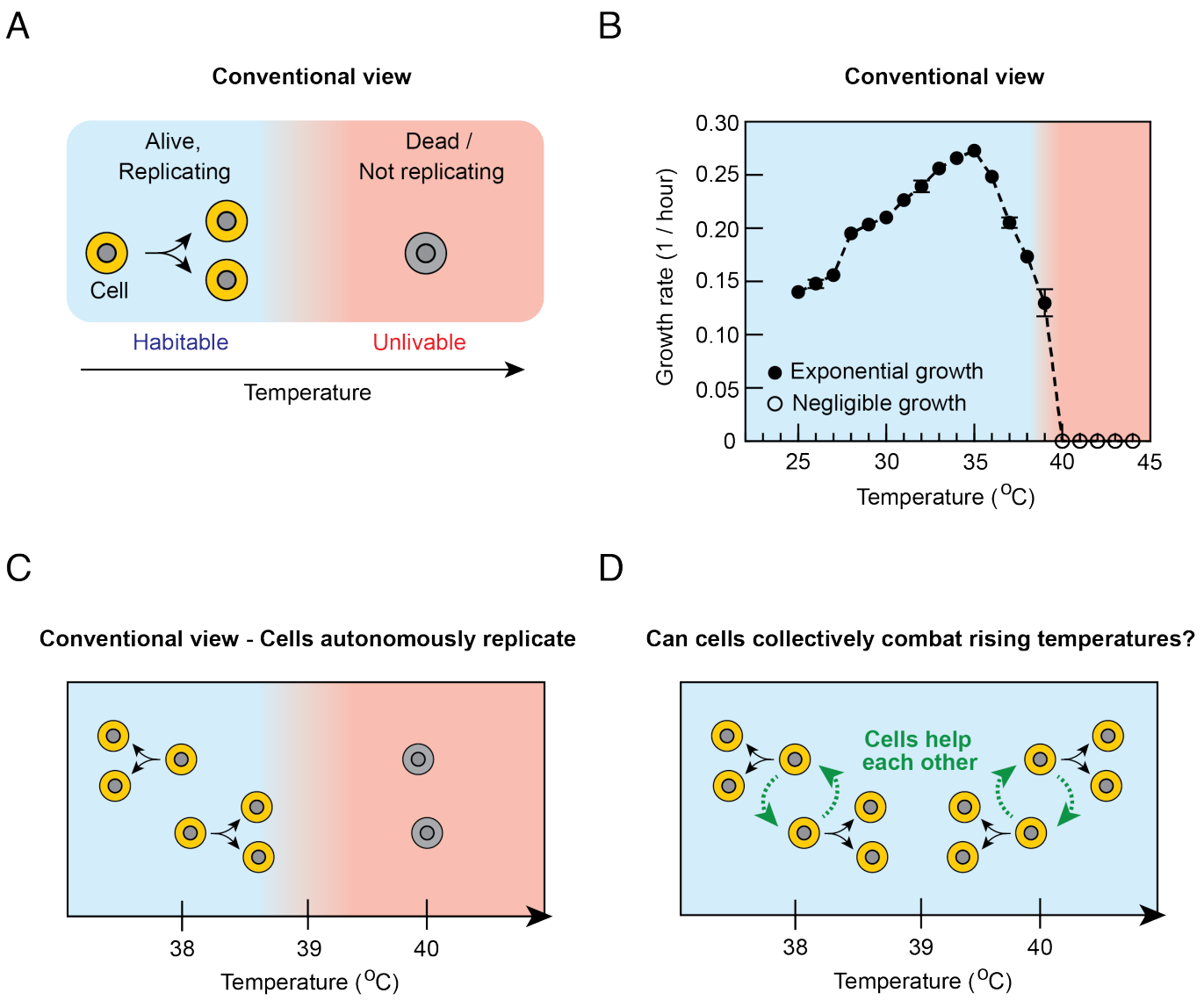

Figure 1. Conventional, cell-autonomous view of temperature-dependent cell-replications.
(A) The conventional view states that cells autonomously replicate at "habitable temperatures" (blue region) and that at sufficiently high temperatures (i.e., "unlivable temperatures"), cells fail to replicate and can eventually die (red region). This view states that whether a cell can replicate or not at a given temperature depends on the cell's autonomous ability to use its heat-shock response system to sufficiently deal with various heat-induced damages. **(B)** Growth rate as a function of temperature for populations of wild-type yeast cells. Black data points in the blue region are for populations with sustained, exponential growth over time and white data points in the red region are for populations without sustained exponential growth. 39 ^{O}C is near a boundary of blue and red regions (also see Figure S1). **(C)** The conventional view (explained in (A)) applied to budding yeast, based on the data in (B). **(D)** Question that we investigated in our study: can cells (budding yeasts) cooperatively combat rising temperatures so that they can turn a temperature that is unlivable for a few cells (e.g., 40 ^{O}C shown in (C)) into a habitable temperature if there are sufficiently many cells working together to fight off extinction?

RESULTS

Population density determines replicability of cells and habitability of each temperature

We re-examined the conventional, cell-autonomous picture by incubating populations of wild-type yeasts at a conventionally-defined habitable temperature (38 ^{O}C), unlivable temperature (40 ^{O}C), and a transition temperature in between the two (39 ^{O}C). We first grew the yeasts at 30 ^{O}C in 5 mL of standard minimal-media and then transferred some of these cells to a fresh minimal media which we then incubated at a desired temperature, just as we did to obtain the conventional picture (Figure 1B). This time, however, we took care to transfer a precise number of cells to the fresh minimal media so that we could vary the initial population density (# of cells/mL) over a wide range whereas to obtain the conventional picture, we kept the initial population density within a fixed range of values for all temperatures (as one often does) (Figure S1). With a flow cytometer, we counted the integer numbers of cells per volume to determine the population density at each time point. For each temperature, we incubated multiple liquid cultures that all started with the same population density with cells that all came from a single liquid culture that exponentially grew at 30 ^{O}C. These experiments revealed surprising behaviors that deviated from the conventional picture. Specifically, at the supposedly-habitable temperature of 38 ^{O}C, none of the populations that started with a relatively low population density (200 cells/mL) grew at all during ~12 days of incubation except for a small, transient growth that occurred for a few hours right after the transfer from 30 ^{O}C (Figure 2A - red curves). At the same temperature (38 ^{O}C), setting the initial population density to be just five times larger (1,000 cells/mL) than these non-growing populations yielded a population whose behavior was completely unpredictable: it could either grow until it reached the carrying capacity (i.e., ~10^7 cells/mL) or not grow at all after the initial transient-growth (Figure 2A - green curves). When the population did grow, it could wait 4 days or 8 days or some other, unpredictable time before starting to grow (Figure 2A - multiple green curves). Still, at the same temperature (38 ^{O}C), setting the initial population density to be just five times larger (5,000 cells/mL) than these randomly-growing populations yielded populations that always grew exponentially over time, all in the same way, until they reached the carrying capacity (Figure 2A - blue curves). Thus, among the three initial population densities at 38 ^{O}C, only the largest one led to the deterministic, population-level growth that the conventional picture states should be exhibited by every population density at habitable temperatures (*1,12-14*).

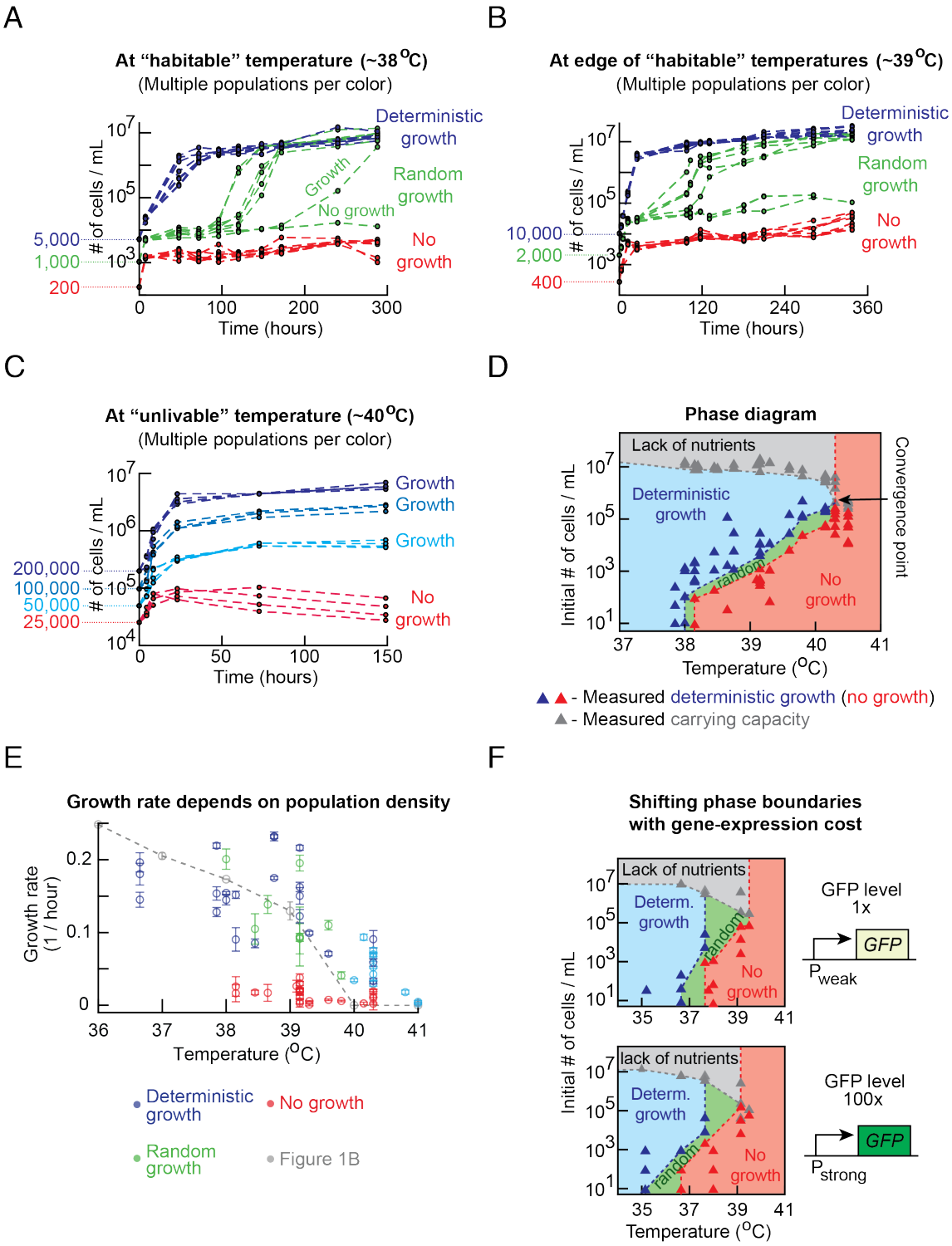

Figure 2. Population density determines replicability of cells and habitability of each temperature.

(A-C) Population density (number of cells / mL) measured over time with a flow cytometer for populations of wild-type yeast of differing initial population-densities at (**A**) a conventionally-defined habitable temperature (38.4 °C), (**B**) near the edge of conventionally-defined habitable and unlivable temperatures (39.1 °C), (**C**) and at a conventionally-defined unlivable temperature (40.3 °C). Figure 1B sets the conventional definition of a temperature's habitability. For (**A-B**): Each color shows eight populations

that start with the same initial population-density. Red curves show no-growth beyond initial transient growths (i.e., "no growth"). Green curves show unpredictable growths (i.e., "random growth"). Blue curves show deterministic, exponential growths whereby all populations identically grow (i.e., "deterministic growth"). For (**C**): Each color shows four populations with the same initial population-density. All colors except the red show growth by ~10-fold. **(D)** Phase diagram constructed from measurements. Colors represent the behaviors mentioned in (B) - blue region marks deterministic growth, green region marks random-growth, red region marks no-growth, and grey region marks populations not growing as they have more cells than the carrying capacity. Each triangle represents an experiment of type shown in (A-C), performed at a specific initial population-density and temperature (Figures S2-3). A triangle's color represents the phase exhibited by populations. See caption of Figure S3 for a description of how we deduced the phase boundaries from the measurements. **(E)** Growth rates of populations in the no-growth phase (red), random-growth phase (green) and deterministic-growth phase (blue) as a function of temperature (error bars are s.e.m., n = 6 or more for temperatures less than 40 ^{O}C, and n = 3 for higher temperatures). Grey data reproduces the growth rates of the conventional view shown in Figure 1B. **(F)** Phase diagrams constructed for engineered yeast strains that constitutively express GFP at the indicated levels (1x and 100x - see Figure S4A). Triangles indicate experimental data (samples of growth data represented by these triangles are in Figures S4B-I).

We also observed the same three population-level features - no growth, random growth, and deterministic growth - as a function of the initial population density for a temperature (~39 ^{O}C) that is near the boundary of the "habitable" and "unlivable" regimes (Figure 2B). Moreover, at a supposedly-unlivable temperature (~40 ^{O}C), we found that a population with an initial density of at least 50,000 cells/mL do, in fact, grow by ~10-fold and then remains stable for several days without reaching the carrying capacity (Figure 2C - non-red curves). In contrast, if the initial population density was just half of this value (25,000 cells/mL), then the population density, instead of plateauing, continuously decreased over several days after an initial, transient growth (Figure 2C - red curves). This shows that just a two-fold difference in the initial population density can determine whether there is a net cell-death or net cell-growth at ~40 ^{O}C, which the conventional picture of autonomous cell-replications cannot explain.

Phase diagram shows allowed population-level behaviors across temperatures

Above results (Figures 2A-C) show that in order to determine whether a population grows or not, one must know *both* the temperature and the initial population-density. We can summarize this in a "phase diagram" that we constructed by performing the above growth experiments at multiple, additional temperatures and with multiple, initial population densities (Figure 2D and Figures S2-3). The phase diagram consists of four phases - deterministic growth, random growth, no growth, and no-growth due to insufficient nutrients (i.e., the initial population density is beyond the carrying capacity) - as a function of the initial population density and temperature. It shows that the

173 conventional picture (Figures 1B-C) mistakenly arises because one typically ignores the initial
174 population density or sets it to be within some narrow range when studying population growth
175 across temperatures. This leads to, for example, the growth rate *appearing* to decrease as the
176 temperature increases within a given temperature range (e.g., 36.5 ^{O}C ~ 39 ^{O}C) (Figure 1B). But
177 in fact, for the same temperature range, we found that the populations' growth rates - when they
178 grew in the deterministic-growth and random-growth phases - were poorly correlated with
179 temperature and could highly vary between populations even for the same temperature if we
180 varied the initial population density (Figure 2E). In constructing the phase diagram, we determined
181 at least how many cells are necessary to guarantee that a population grows for each temperature
182 (i.e., minimum number of cells required for a deterministic growth). This is set by the boundary
183 between the deterministic-growth and random-growth phases in Figure 2D. We also determined
184 at most how many cells are necessary to guarantee that a population never grows for each
185 temperature. This is set by the boundary between the random-growth and no-growth phases in
186 Figure 2D. We found that both of these values - the minimum required to guarantee growth and
187 the maximum allowed for no-growth - are extremely sensitive (i.e., "ultra-sensitive" (*18,19*)) to
188 temperature. For example, the phase diagram revealed that each of these two values change by
189 ~100-fold as the temperature increases from 39 ^{O}C to 40 ^{O}C. The random-growth phase, in the
190 phase diagram, lies between the no-growth and deterministic-growth phases - one might see it as
191 a hybrid of the growth and no-growth phases - and is thin along the axis that represents the initial
192 population density. Its thinness reflects our previous observation that a small change (5-fold or
193 less) in the initial population density can transform either a no-growth or a deterministic growth
194 into a random growth (Figure 2A) (i.e. populations are ultra-sensitive to their initial densities).
195 Intriguingly, the phase boundaries - the borders between the four different phases - all converge
196 at a single, "convergence point" whose coordinate is (40.3 ^{O}C, 1 x 10^5 cells/mL) in the phase
197 diagram (Figure 2D), leaving only the no-growth phase for temperatures higher than 40.3 ^{O}C.
198 Thus, a population cannot grow regardless of its initial density for temperatures higher than 40.3
199 ^{O}C. The convergence point is special for another reason which we will later turn to - one that is
200 reminiscent of critical points in phase diagrams of physical systems.
201
202
203 **Tuning the cost of expressing a single superfluous gene reshapes habitability of**
204 **temperature**
205 To explore possible ways of manipulating the phase diagram (i.e., where the phase boundaries
206 are), we genetically engineered the wild-type yeast so that it constitutively expressed the Green

Fluorescent Protein (GFP), which serves no function for cell growth. We constructed two such strains - one expressing GFP at a relatively low amount (defined as 1x) and another at a relatively high amount (~100x) (Figure S4A). We repeated the growth experiments with these two strains, for multiple temperatures and initial population-densities, and used these results to construct a phase diagram for each strain (Figure 2F and Figures S4B-I). The resulting phase diagrams revealed that increasing the GFP expression shifts the phase boundaries in such a way that a population growth is no longer possible, regardless of the initial population density, at lower temperatures than the wild-type strain. Specifically, this means that the random-growth and no-growth behaviors are possible for GFP-expressing strains at lower temperatures than for the wild-type strain (Figure 2F). For example, at ~36 ^{O}C, a population with high GFP-levels (100x) can be in the random-growth and no-growth phases whereas the yeasts with the low GFP-levels (1x) can only deterministically grow regardless of how few cells there are. Therefore, a population that could grow at a given temperature can no longer grow at that same temperature because its cells express GFP. One needs to either increase the initial population-density or decrease the temperature to observe its growth. These results show that the cost of expressing superfluous genes (*20*) can markedly alter the phase boundaries' locations and shapes. In particular, this means that reducing the cost of expressing a single, unnecessary gene can increase the life-permitting temperature by several degrees Celsius.

Single-cell measurements reveal that a few "pioneer" cells initiate replications in randomly growing populations and sustenance of transiently replicating sub-populations in non-growing populations

To gain further insights, we turned to single-cell-level measurements. Unlike the GFP-expressing strains, the wild-type strain lacks a functional *ADE2* gene for synthesizing adenine. Since we incubated yeasts in the minimal media with all the essential amino acids and nitrogenous sources - including adenine that represses their adenine-biosynthesis - the wild-type cells could still grow. But, as is well-known, having a defective *ADE2* gene turns yeasts red if they have not divided for some time because they have accumulated red pigments - these are by-products of the not-fully-repressed and defective adenine-biosynthesis (*21*). The cells can only dilute away the red pigments through cell divisions. Defective *ADE2* gene cannot be a reason for any of the population-density-dependent growth behaviors that we observed because the GFP-expressing strains do have the functional *ADE2* gene and yet exhibit the same, surprising behaviors as the wild-type cells (Figure 2F). But the red pigments were useful because, for the wild-type

241 populations, we could use our flow cytometer's red-fluorescence detector to count how many non-
242 replicators (red ells) and how many replicators (non-red, "white cells") co-existed a population at
243 each time point (Figure S5A). As a result, we discovered that, in every population and at every
244 temperature, nearly all cells were red at the start of each growth experiment due to the cells having
245 just been transferred from cultures that grew to saturation in 30 ^{O}C to the higher temperature.
246 Subsequently, the number of replicators increased to about 10-30% of the population during the
247 initial, transient growth in which the cells from 30 ^{O}C adjust to the higher temperature (Figure S5B).
248 Afterwards, the number of replicators varied depending on which phase the population has. For a
249 deterministically growing population, the number of replicators kept increasing over time until it
250 reached the carrying capacity (Figure S5C) whereas it typically decreased until very few cells (~1-
251 5 % of population) remained as replicators for random-growth and no-growth populations (Figure
252 S5C). Subsequently, two behaviors were possible depending on whether the population was in
253 the no-growth or random-growth phase. For populations in the random-growth phase, the number
254 of replicators, after unpredictable hours or days, suddenly started to increase by orders of
255 magnitude until the population reached the carrying capacity (Figure S5C). On the other hand, for
256 populations in the no-growth phase, the number of replicators sustainably remained low (~1-5%
257 of the population) and fluctuated up and down by a few-fold during the incubation (~300 hours in
258 our experiments) (Figure S5C). These fluctuations were too small to noticeably change the total
259 population density over time. Yet, this result revealed that there is always a small sub-population
260 of transiently replicating cells and that these transient replications are such that the fraction of
261 replicators in the population could stably remain in low numbers (e.g., ~1% of total population).
262 We will later return to these single-cell data when we introduce a mathematical model that
263 recapitulates them.
264
265
266 **Cells collectively delay and prevent population extinctions at high temperatures**
267 We next asked whether cell deaths, like its counterpart - cell replication, also depend on the initial
268 population density. At several temperatures, we measured how the number of surviving cells
269 changed over time for a population that we kept in the no-growth phase (i.e., population with not
270 enough cells to trigger its own random or deterministic growth). We counted the number of
271 survivors by taking out an aliquot of cells from the population at different incubation times,
272 spreading it onto an agar pad at 30 ^{O}C, and then counting how many colonies formed (Figure
273 S6A). Surprisingly, these measurements deviated qualitatively - not just quantitatively - from the
274 conventional theory of cell deaths which states that deaths of heat-shocked cells are autonomous.

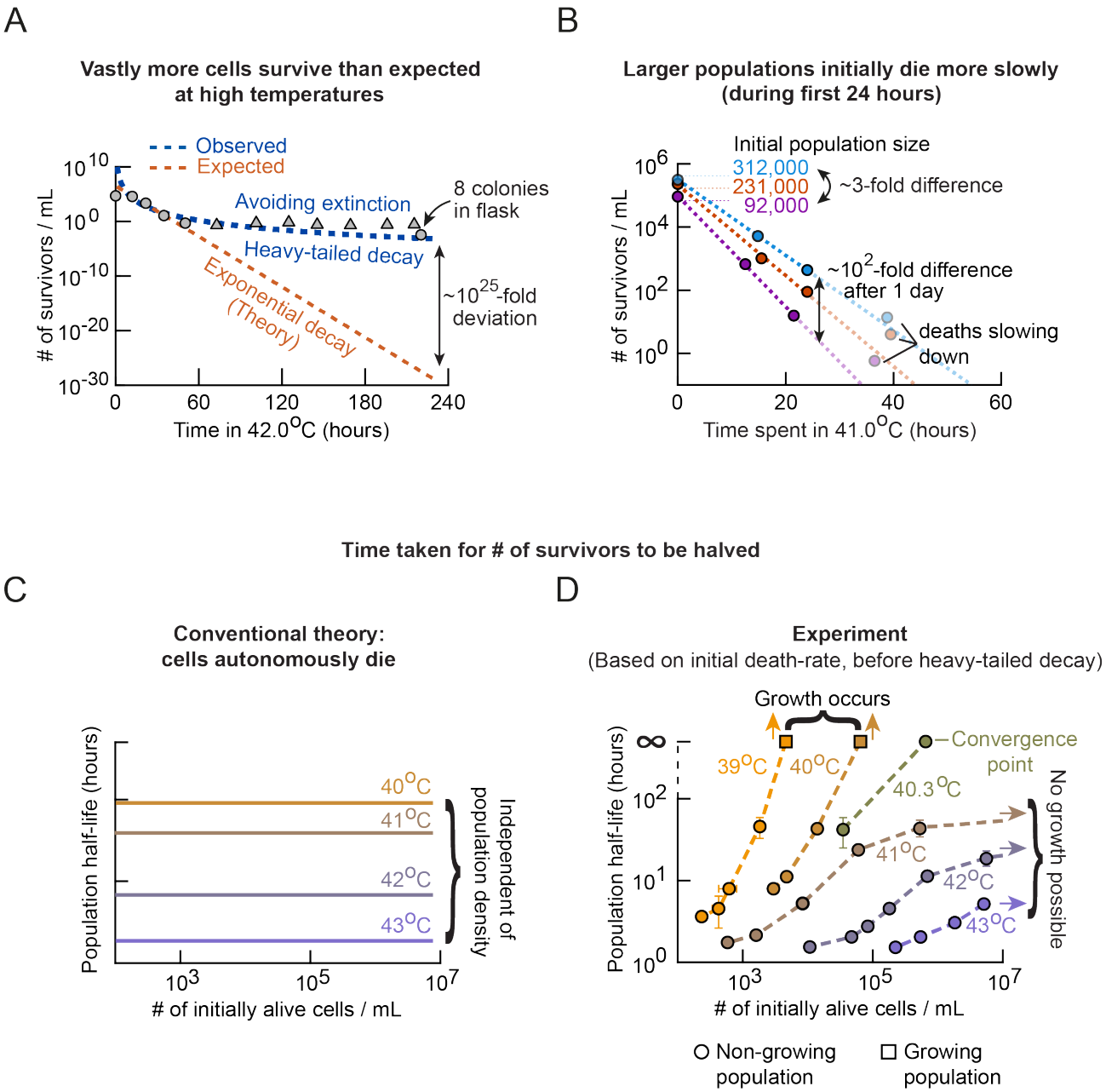

Figure 3. Cell deaths depend on initial population-density and are not autonomous: populations of higher initial densities decelerate and halt their approach to extinction more rapidly.

(**A**) We determined the number of survivors per mL over time in a non-growing population at 42.0 °C (i.e., population in the no-growth phase) by transferring an aliquot of the liquid culture to an agar pad at different time points, incubating the agar pad at 30 °C, and then counting the number of colony forming units ("# of survivors/mL") (see Figure S6A). Circles represent measured numbers of survivors. Triangles are also from measurements and are overestimates (i.e., the aliquots did not yield any colonies at 30 °C, meaning that an aliquot of a larger volume was required to observe at least one colony. Hence the triangles represent an overestimate of the number of survivors per mL). Brown dashed line is an exponentially decaying function fitted to the three circles between 10 and 50 hours. Blue dashed curve is a power-law fit to the same circles. Also see Figure S6. (**B**) Number of survivors per mL for three populations of differing initial population-density - all in the no-growth phase at 41.0 °C - measured as in (A).

Initial population-densities are 92,000 cells / mL (purple), 231,000 cells / mL (orange), and 312,000 cells / mL (blue). Dashed lines are exponentially decreasing functions fitted to first three timepoints that share the same color (i.e., deaths that occur during the first day of incubation). Also see Figure S6. (**C**) The conventional view states that cells autonomously die and that every cell has the same probability of dying per unit time. This leads to the population half-life (i.e., the time taken for a population density to be halved) to be independent of the initial population-density for a given temperature. (**D**) Population half-life, plotted here as a function of initial population-density, is defined as the time taken for a population density to be halved, based on fitting exponentially decreasing functions to the number of survivors during the first 24 hours of incubation that follows a ~20-hours of transient growth (transient growth is due to the cells coming from 30 ^{O}C and adjusting to the new temperature). Hence, we measured the number of survivors at approximately 20 hrs, 28 hrs, 36 hrs, and 44 hrs after we incubated the populations at the desired high temperature. Usually, the 44-hr data already deviated from exponential decay and thus we usually omitted them from the exponential fits. Shown here are the half-lives of populations at 39.1 ^{O}C, 40 ^{O}C, 40.3 ^{O}C, 40.8 ^{O}C, 42 ^{O}C, and 43 ^{O}C. Error bars are the s.e.m. (n = 3 for all data points). Circles represent populations in the no-growth phase. The two squares (for 39.1 ^{O}C and 40 ^{O}C) represent populations that grew because they had sufficient densities to trigger their own growth, in accordance with the phase diagram (Figure 2D).

Specifically, it says that the number of survivors should exponentially decrease over time at a constant exponential rate until the population becomes extinct due to every cell having the same, fixed probability of dying per unit time regardless of the population density (*4*) (Figure 3A - brown line). Yet, we discovered that the rate at which the cells die itself continuously decreases over time as a heavy-tailed (power-law-like) function, instead of as an exponential decay (Figure 3A - blue curve). Consequently, the number of survivors seems to decrease exponentially at a constant exponential rate for the first day but then, after a few days, decreases exceptionally slowly as a heavy-tailed decay. The heavy-tailed decay means that the population continuously decelerates and then eventually ceases its approach to extinction. This causes the number of survivors to plateau after some time. For example, the number of survivors at 42 ^{O}C did not noticeably decrease over a period of ~1 week (~180 hours) after some deaths in the first day and deviated by ~10^{25}-fold from the number of survivors that the theory states one should have after nine days of incubation (Figure 3A - last time point; Figures S6B-H). Moreover, we discovered that the rate at which cells die during the first day of incubation at a high temperature depends on the initial population density (Figure 3B and Figures S6B-H). During the first day, the number of survivors seems to exponentially decrease over time before it noticeably enters a heavy-tailed decay regime on later days (Figure 3B). Hence, we can assign a constant, exponential rate of decay to each population to describe how the number of survivors decreases during the first day. We found that this rate - which we will call the "initial death-rate" - depends on the initial population density. Namely, we discovered that as the initial population density increases, the initial death-rate decreases, meaning that number of survivors decreases more slowly during the first day for higher initial population-densities (Figure 3B - three dashed lines with differing slopes). For example, after

one day of incubation at 41.0 ^{O}C, a population that started with ~92,000 cells had about 100-fold less survivors than a population that started with about three times more cells (Figure 3B - compare blue and purple lines). Yet, the prevalent theory states that it should be 3-fold less, not 100-fold less. Taken together, these results establish that a population that starts with a higher density has a larger fraction of its cells remaining as survivors after one day and, due to the heavy-tailed decay, has vastly more survivors than a population that started with a lower density (Figure 3B - last, faded data points for each color). This population-density dependent effect - a small initial difference in population density amplifying to a large, nonlinear change in the final population density - suggests a highly nonlinear cooperative effect that cells have on each other's survival.

A special temperature that defines convergence point in phase diagram separates two extinction-avoidance regimes

The conventional theory - which imposes a constant, exponential death rate - says that the time taken for the number of survivors to be halved decreases with increasing temperature and that it is independent of the initial population density (Figure 3C). Yet, our experiments revealed a starkly different story (Figure 3D). We can see this by extracting the initial half-life, which we define to be the amount of time taken for the number of survivors to be halved based on the initial death-rate (Figure 3D). The initial half-life is inversely proportional to the initial death-rate. We discovered that while increasing the initial population density always increases the population's initial half-life, it is the temperature that determines how sensitively the initial half-life depends on the initial population density. In particular, we found that a population's initial half-life has two regimes of sensitivities, depending on whether the temperature is below or above 40.3 ^{O}C. Intriguingly, 40.3 ^{O}C is the temperature where the convergence point lies in the phase diagram (Figure 2D). For temperatures below 40.3 ^{O}C, we found that the initial half-life can increase from a few hours to a few days when the initial population density changes by just a few fold (e.g., 3-fold) (Figure 3D - yellow and brown curves for 39 ^{O}C and 40 ^{O}C respectively). Moreover, as we keep increasing the initial population density, the initial half-life keeps increasing and eventually reaches infinity, due to the fact that a sufficiently high-density population would grow at these temperatures (Figure 2D). For temperatures above 40.3 ^{O}C, we discovered an opposite trend: increasing the initial population density above some value hardly changes the initial half-life, leading to the half-life eventually plateauing at a finite value as we keep increasing the initial population density (Figure 3D - purple curves for 41 ^{O}C ~ 43 ^{O}C). Thus, after some amount, increasing the initial population density does not yield much gain in the initial half-life. This occurs because a population can never

332 grow regardless of its density at these temperatures (Figure 2D). Exactly at 40.3 ^{O}C, we found
333 that a population whose initial density matches that of the convergence point (~1 x 10^5 cells/mL)
334 neither replicates nor dies. It is unable to grow yet can indefinitely maintain its number of survivors
335 at a nearly constant value (i.e., its initial half-life is infinite because its initial death-rate is zero).
336 The convergence point is the only combination of temperature (40.3 ^{O}C) and population density
337 (~1 x 10^5 cells/mL) for which an infinite initial half-life is possible without the population growing.
338 This makes the convergence point special: a population at the convergence can - on average and
339 subject to fluctuations - indefinitely maintain its cell numbers at a constant value.
340
341 Taken together, the conventional theory of autonomous cell deaths (*4*) cannot explain the
342 features of cell deaths that we uncovered (Figures 3A-D). Likewise, known mechanisms for
343 yielding long-lived populations under stress - such as those for antibiotic persistence (*22*) - also
344 cannot explain our data for cell deaths. There are two reasons for their inability to do so. Firstly,
345 how fast cells die over time depends on the initial population density (rather than being
346 independent of the initial population density as in the case of antibiotic persistence). Secondly, the
347 rate at which cells die changes over time (rather than remaining constant over time as in the
348 conventional theory).
349
350
351 **Extracellular factor dictates cell replications at high temperatures**
352 Having established that replications and deaths of cells depend on the initial population density,
353 we sought underlying mechanisms. We first focused on finding a mechanism that is responsible
354 for cell replication. As we will show, this mechanism also explains the cell deaths. Broadly, we can
355 consider two classes of mechanisms. One is that the "factors" that dictate a cell's replication, at a
356 high temperature, resides purely within that cell (i.e., purely intracellular factors dictate cell
357 replications). In this case, cell replication would be a purely cell-autonomous process and the
358 reason that it depends on population-density (Figures 2A-C) would be that if we have more cells,
359 then it is more likely that at least one cell would manage to replicate. The other possibility is that
360 an extracellular factor dictates cell replications. In this case, a cell's replication would depend on
361 elements outside of that cell which may include the other cells of the population. To distinguish
362 these two classes of mechanisms, we performed experiments in which we physically separated
363 the cells from their extracellular environment. Specifically, in one experiment, we took cells that
364 were exponentially growing at a particular temperature and then, at that same temperature,
365 transferred them to a fresh medium that never harboured any cells before. This experiment would

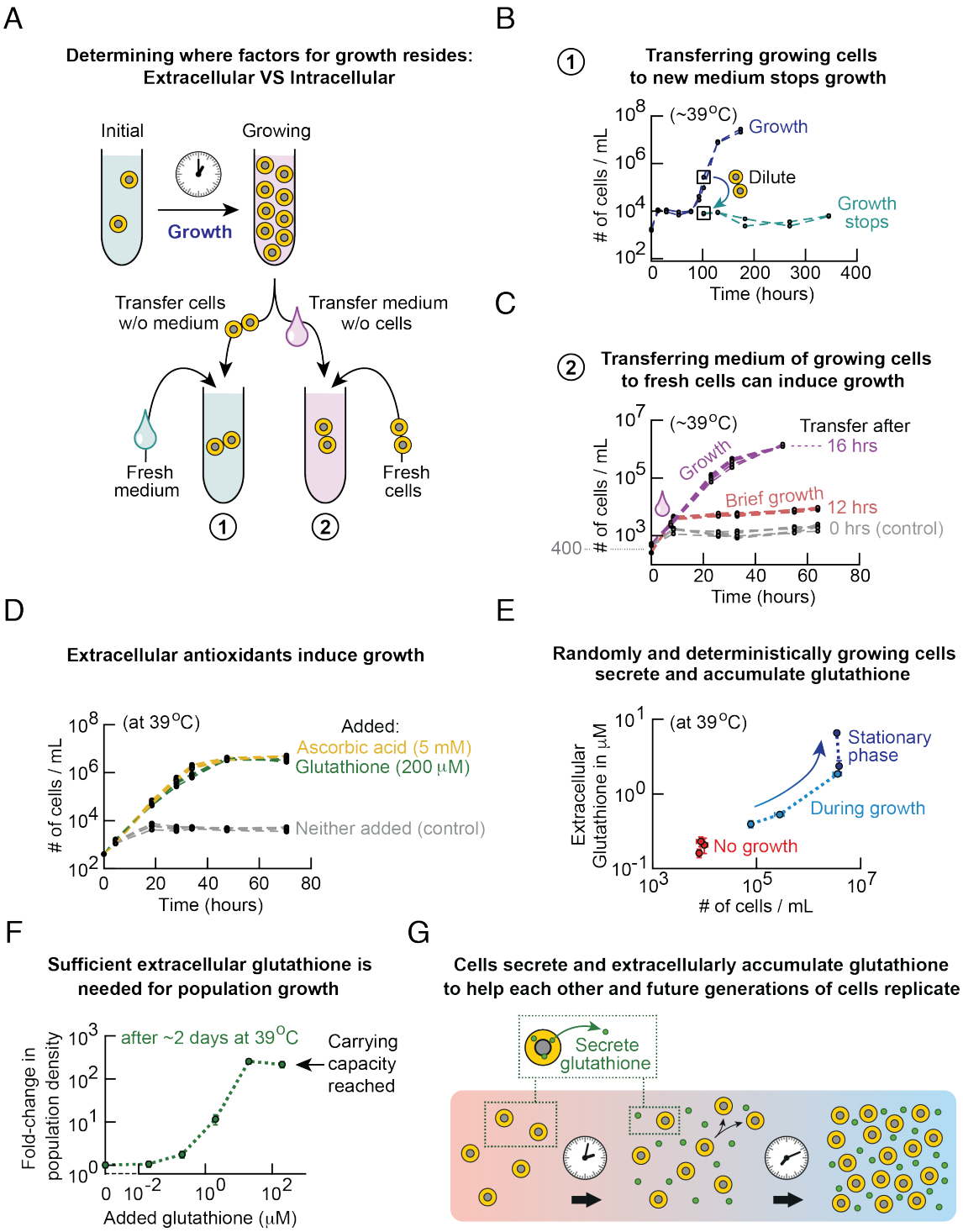

Figure 4. Cells secrete and extracellularly accumulate glutathione to help each other and future generations of cells replicate at high temperatures.

(A) Schematic description of experiments (in (B) and (C)) to distinguish two classes of mechanisms: transfer growing cells into a fresh medium (to determine if intracellular factors dictate population growth) or take out only the growth medium of a growing population and incubate fresh cells in it (to determine if extracellular factors dictate population growth). **(B)** At ~39 ^{o}C. Blue curves show two populations of wild-type yeasts that start to exponentially grow when their population-density reaches ~10,000 cells/mL

in the new culture, represented by the two green curves (two replicate populations). **(C)** At ~39 ^{O}C. Population density over time for populations of wild-type yeasts that were incubated in a growth medium that previously harbored a population of exponentially growing cells at ~39 ^{O}C for 0 hours (grey curves), 12 hours (red curves), and 16 hours (purple curves). Each color shows at least 6 replicate populations. Also see Figures S7A-D. **(D)** At 39.1 ^{O}C. All populations start at 400 cells/mL, which is too low of a density to permit growth. Adding either ascorbic acid (5 mM - yellow) or glutathione (200 μM - green) to the growth media induces growths. Without adding either one, population does not grow (grey). **(E)** At 39.1 ^{O}C. Measured the concentration of extracellular glutathione for populations in no-growth phase (initially 400 cells/mL - red data), random-growth phase (initially 2,000 cells/mL), and deterministic-growth phase (10,000 cells/mL). Three biological replicates each phase (*n*=3; error bars are s.e.m.). Measured three timepoints for each phase. Plotted here are the concentrations of extracellular glutathione as a function of the population density over time. Arrow shows both population density and concentration of extracellular glutathione increasing together over time (see also Figure S10). **(F)** Sensitivity of no-growth populations (initially ~400 cells/mL) at 39.1 ^{O}C to glutathione that we added into the growth medium. Shown here is the fold-change of the population density after two days of incubation with added glutathione. as function of supplemented glutathione. Last two data points show ~200-fold change, which represents the populations having fully grown to reach the carrying capacity (see also Figure S10). **(G)** Cartoon illustrating the mechanism deduced by (A-F). Yeasts secrete glutathione at high temperatures. The extracellular glutathione accumulates. When its concentration reaches at least a threshold amount (~0.3 μM from (F)), the population replicates at high temperatures by noticeable amounts.

367 determine whether the cells could keep on growing and thus support the idea that intracellular
368 factors dictate cell replications (Figure 4A - bottom left tube). In another experiment, we took away
369 the growth medium from cells that were growing at a particular temperature and then, at that same
370 temperature, transplanted into it fresh, non-growing cells whose initial population density was too
371 low for growth. This experiment would determine if the transferred medium, from growing cells,
372 can induce growth in cells that should not grow according to the phase diagram, thus supporting
373 the idea that extracellular factors dictate cell replications (Figure 4A - bottom right tube). As an
374 example of an experiment in which we transferred the growing cells instead of their growth
375 medium, we took some wild-type cells from a population that was exponentially growing at a
376 particular temperature (~39 ^{O}C; Figure 4B - blue curves) and then transplanted them to a fresh
377 medium at the same temperature so that this newly created population started with a population
378 density (10,000 cells/mL) that should permit growth according to the phase diagram (Figure 2D).
379 Surprisingly, we found that these cells stopped growing in the fresh medium soon after the transfer
380 (Figure 4B - green curves). This strongly suggests that extracellular factors dictate cell
381 replications.
382
383 To further test the idea that extracellular factors dictate cell replications, we transferred the
384 growth medium from cells that were growing at a particular temperature (~39 ^{O}C) to fresh, non-
385 growing cells and tested whether these cells could also grow at that same temperature. Strikingly,

386 we found that these fresh cells could grow after being transplanted into the medium (Figure 4C -
387 purple curves), even though they initially had a low population-density (400 cells/mL) that - without
388 the transplanted medium - prohibits growth according to the phase diagram. Crucially, whether
389 the transferred medium induced growth or not depended, in a highly sensitive manner, on the
390 amount of time that the medium harboured exponentially growing cells before the transfer (Figure
391 4C and Figures S7A-D). For instance, at ~39 ^{O}C, if cells exponentially grew for 12 hours or less
392 before we transferred their growth medium to fresh cells, then the fresh cells did not grow in the
393 transferred medium (Figure 4C - grey and red curves and Figures S7A-C). However, if cells had
394 grown for 16 hours or more before we transferred their growth medium to fresh cells, then the
395 fresh cells grew in the transferred medium (Figure 4C - purple curves and Figure S7D). These
396 results support the following idea: for a population to grow by an appreciable amount at high
397 temperatures, the concentration(s) of growth-inducing extracellular factor(s) must be above some
398 threshold value(s). The next question then is whether these extracellular factors must be secreted
399 or depleted by cells to induce population growths.
400
401 To test whether it is a depletion of some extracellular factors that induce population
402 growths, we performed several experiments (Figures S7E-H and Figure S8). In one experiment,
403 we took a fresh growth medium that contains all the essential amino acids, diluted it with water by
404 different amounts, added a saturating level (2%) of glucose to it, and then incubated cells in it at
405 high temperatures (Figure S8A). We found that a population could not grow in any of these diluted
406 media. The same was true if we decreased only the glucose in the fresh medium - without diluting
407 other factors such as amino acids - and then incubated cells in it (Figure S8B). Together, these
408 results strongly indicate that a secretion of factor(s), rather than depletion of key resources in the
409 media, induces population growths. As a complementary experiment, we took the growth medium
410 that harboured growing cells at 30 ^{O}C for various amounts of time, from a few hours to 12 hours.
411 We then transferred the media from these 30 ^{O}C cultures, after filtering the media to eliminate any
412 cells from them, to a fresh cell-population at a high temperature (39 ^{O}C). These newly created
413 populations all had the same initial population density that was too low for growth at 39 ^{O}C (i.e.,
414 400 cells/mL) (Figures S7E-G). We found that the transferred media taken from the log-phase
415 cultures at 30 ^{O}C did not cause the fresh cell-population to grow at 39 ^{O}C. This further supports a
416 secretion, not depletion, of factor(s) inducing population growths. Intriguingly, if the transferred
417 medium was from a population at 30 ^{O}C that was in a stationary phase after a log-phase growth
418 and a diauxic shift, then the fresh cell-population incubated in the transferred medium did grow at
419 39 ^{O}C (Figure S7H). Taken together, these results indicate that certain factors that yeasts secrete

420 at 30 ^{O}C during their stationary phase (following a diauxic shift) can induce population growths at
421 high temperatures. We reasoned that these secreted factors may also be the same factors that
422 we concluded must be secreted by log-phase cells at high temperatures.
423
424
425 **Extracellular antioxidants - glutathione and ascorbic acid - enable yeasts to replicate at**
426 **high temperatures**
427 To help us identify the secreted extracellular factor(s) responsible for cell replications at high
428 temperatures, we performed a transcriptome analysis (RNA-seq) on wild-type yeast at different
429 parts of its phase diagram (Figure S9). We found that deterministically growing cells at high
430 temperatures, compared to those growing at 30 ^{O}C, had downregulated the genes involved in the
431 central carbon metabolism and the majority of genes in general. But we also found that they had,
432 compared to those growing at 30 ^{O}C, upregulated the genes that are associated with DNA damage
433 response, translation initiation, and biogenesis and assembly of cell membranes. These changes
434 in gene expressions are similar to those seen for yeasts experiencing environmental stresses in
435 general (*23*,*24*). We hypothesized that a cell upregulates these genes to repair damages to
436 various cellular components. Furthermore, we hypothesized that reactive oxygen species may
437 cause these damages at high temperatures. Reactive oxygen species are known to damage
438 nucleic acids (*25*), proteins (*26*), and lipids in the cell membrane (*27*). A previous study suggests
439 that high temperatures primarily lead to reactive oxygen species that damage the cell (*28*).
440 Consistent with this idea is that we found many genes associated with the mitochondria to be
441 downregulated for the replicating cells at high temperatures compared to the cells at 30 ^{O}C. Since
442 respiration creates reactive oxygen species in the mitochondria, downregulating respiratory
443 mitochondrial genes may decrease the amount of reactive oxygen species that form and, as a
444 result, allow the yeast to replicate at high temperatures (*29*,*30*). A way to combat the reactive
445 oxygen species is by producing antioxidants. Antioxidants reduce oxidative-stress-related
446 damages by capturing and then deactivating reactive oxygen species. We hypothesized that
447 budding yeasts may be secreting antioxidants at high temperatures and that sufficiently high
448 concentrations of antioxidants - and thus sufficiently large population densities - are required to
449 sufficiently reduce oxidative damages and thereby induce population growth. Strengthening this
450 hypothesis is that heat shocks are known to induce budding yeasts to produce intracellular
451 glutathione. Glutathione is a widely used antioxidant by many species, including humans, and is
452 the primary, intracellular antioxidant in budding yeast (*30*,*31*). Also strengthening our hypothesis
453 is the fact that after a diauxic shift from log-phase growth to a stationary phase in 30 ^{O}C, budding

454 yeasts are known to produce glutathione, most of which is intracellularly kept and very low
455 amounts of it have been detected in their extracellular medium (*32*). Glutathione's extracellular
456 role remains understudied and it is viewed mainly as an intracellular antioxidant for budding yeast.
457 But we reasoned that the very low concentration of extracellular glutathione, if it indeed exists in
458 the growth medium of the stationary-phase population at 30 ^{O}C, may have induced the growth of
459 the fresh cell-population at 39 ^{O}C that we previously observed (Figure S7H). It is unclear, however,
460 whether yeasts at high temperatures secrete glutathione.
461
462 To first test whether antioxidants can even induce population growths at high
463 temperatures, we added either glutathione, ascorbic acid, and trehalose - three prominent
464 antioxidants in yeasts (*31*) - at various concentrations to the growth medium that contained low
465 density of wild-type cells. Strikingly, we found that both glutathione and ascorbic acid can induce
466 population growth as long as either one of them is at high concentrations (e.g., glutathione at 200
467 μM and ascorbic acid at 5 mM) (Figure 4D). Furthermore, we determined that trehalose cannot
468 induce population growth at high temperatures (Figure S8C). These results establish that at high
469 temperatures, glutathione and ascorbic acid are sufficient for inducing growth in a low-density
470 population that would not have grown without them (i.e., 400 cells/mL, Figure 2D). Moreover, these
471 results establish that reactive oxygen species causing damages is the primary reason that yeasts
472 fail to replicate at high temperatures and that not all antioxidants can sufficiently reduce those
473 damages (e.g., trehalose).
474
475
476 **Cells secrete glutathione to help each other replicate at high temperatures**
477 Although ascorbic acid acts as an antioxidant in eukaryotes, its role in budding yeast (i.e.,
478 erythroascorbate in budding yeast) remains unclear as researchers have not detected appreciable
479 amounts of it in yeast (*33*). Therefore, we reasoned that glutathione is the more likely candidate
480 as the secreted extracellular factor. To test if yeast populations secrete glutathione at high
481 temperatures, we measured the glutathione concentration in the growth medium for
482 deterministically growing, randomly growing, and no-growth-phase populations at high
483 temperatures (Figure 4E and Figures S10A-C). For populations in the no-growth phase at high
484 temperatures (e.g., 39 ^{O}C), glutathione concentration barely increased during ~50 hours of
485 incubation. The population did not grow during this time. In contrast, for populations in the random-
486 growth and the deterministic-growth phase at high temperatures, we detected a continuous
487 increase in the extracellular glutathione concentration over the ~50 hours of incubation, leading to

488 ~10-fold increases in the extracellular glutathione concentration. After these populations reached
489 their carrying capacities and stopped growing, their extracellular glutathione concentration still
490 continued to increase (Figure 4E). These results establish that both log-phase and stationary-
491 phase yeasts at high temperatures secrete glutathione. On the other hand, at 30 ^{O}C, we found
492 that only stationary-phase yeasts after a diauxic shift, but not log-phase yeasts, secrete
493 glutathione (Figure S10D).
494
495
496 **Extracellular glutathione concentration must be above a threshold concentration to induce**
497 **population growth**
498 We next addressed how sensitive yeasts are to extracellular glutathione at high temperatures. At
499 high temperatures (e.g., 39 ^{O}C), we added various concentrations of glutathione to a growth
500 medium and then incubated a low density, no-growth phase population in it. By measuring the
501 fold-change in the population density after two days of incubation, we obtained a highly non-linear
502 relationship between glutathione concentration and the fold-change in the resulting population
503 density (Figure 4F). Namely, when the extracellular glutathione concentration was just above 0.3
504 μM, population grew by ~10-fold, whereas when the extracellular glutathione concentration was
505 either just below or much lower than 0.3 μM, the population hardly grew even after two days.
506 Moreover, when the extracellular glutathione concentrations were much higher than 0.3 μM (e.g.,
507 ~10 μM), populations deterministically grew and reached their carrying capacities (i.e., ~200-fold
508 growth). These results show that a population must accumulate enough glutathione in the
509 extracellular medium - above some threshold concentration (~0.3 μM) - in order to grow (Figure
510 4G).
511
512
513 **Minimal mathematical model recapitulates all the experimental observations**
514 To test if the glutathione secretion can tie together and quantitatively explain all the experimental
515 data, we developed a mathematical model. In this model, cells secrete glutathione at a constant
516 rate - this is the simplest possible scenario and we found that not assuming a constant secretion
517 rate does not qualitatively alter the model's outcomes (see Supplemental text). Moreover, aside
518 from always secreting glutathione, a cell in the model takes one of three actions: replicate, die, or
519 stay alive without replicating (Figure 5A). A probability for each action determines what the cell
520 does next (i.e., a cell "rolls" a three-sided, loaded dice to determine its next action). Specifically,
521 we let the probability that a cell dies in the next time step to be fixed by temperature and thus it

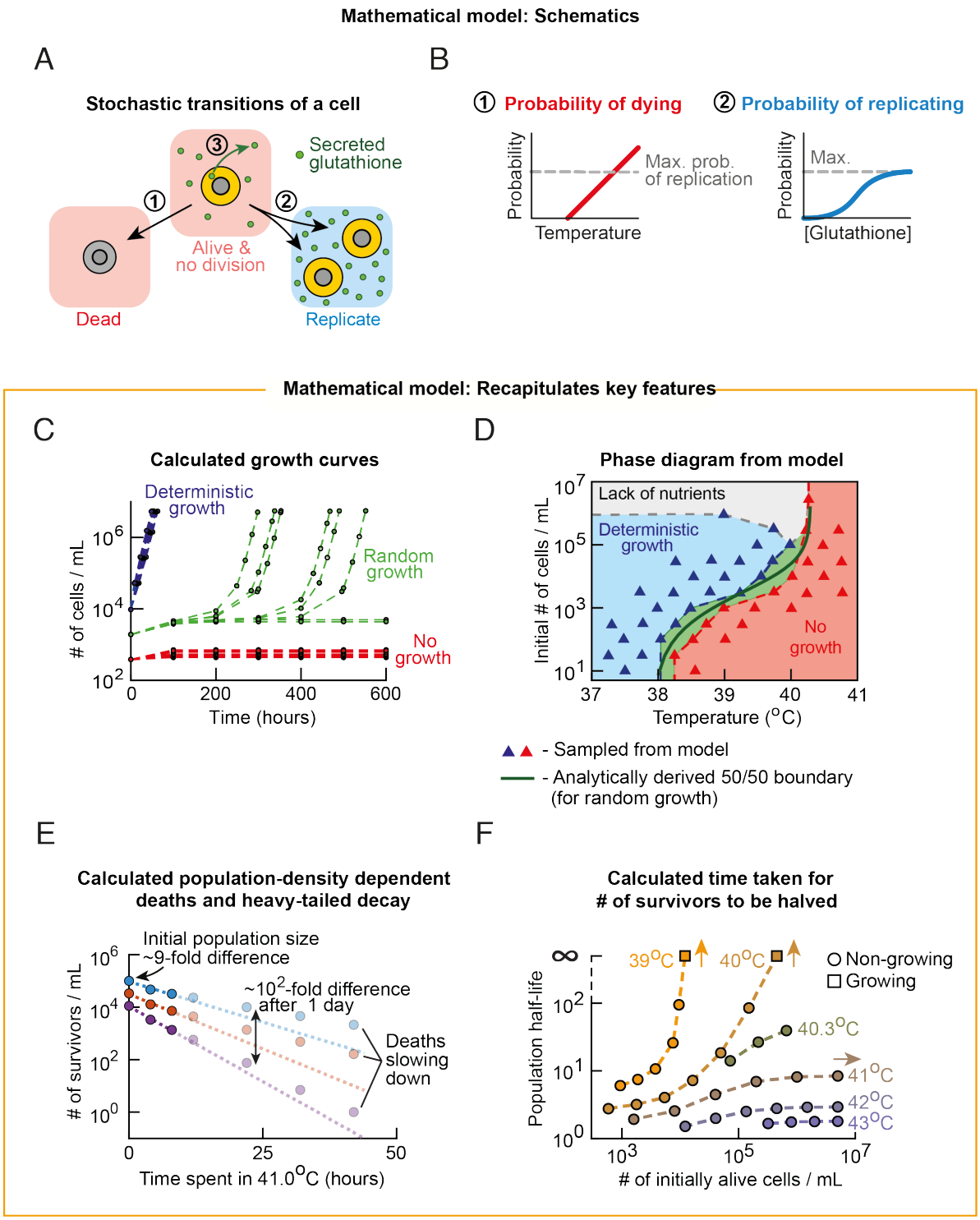

Figure 5. Mathematical model with just one free parameter recapitulates all the experimental data under one framework. (**A-B**) Description of the mathematical model (see full description of the model in the Supplemental text). (**A**) Schematic description of the three states that a cell (yellow circle) can be in. In each time step, any alive cell either stays alive without replicating, replicates, or dies. Alive cells constantly secrete glutathione (green circle). (**B**) Schematic description of the probabilities that describe each of the state transitions shown in (A). Left panel: The probability of a cell dying (red line) is fixed

by the temperature and does not change over time. It increases linearly with temperature and, beyond some temperature, it exceeds the maximum possible value that the probability of a cell replicating can have (grey line). Right panel: The probability of a cell replicating (blue curve) nonlinearly increases as the concentration of the extracellular glutathione increases. Thus, the probability of a cell replicating is initially zero and increases over time up to a maximum possible value (grey horizontal line) as the extracellular glutathione accumulates due to each alive cell constantly secreting glutathione. (**C-F**) Results generated by the model with one, fixed set of parameters. Model recapitulates (C) the population-growth curves (compare with Figure 2A), (D) the phase diagram (compare with Figure 2D), (E) population-density dependent deaths (compare with Figure 3B), (F) population half-life (based on cell deaths during the first day of incubation - compare with Figure 3D), the number of survivors decaying over time as a heavy-tailed function (see Figure S11E), and single-cell-level data on growths (compare Figure S11B with Figures S5C). Also see Figure S11.

523 does not change over time (Figure 5B - left panel). Moreover, we let the probability of dying to
524 linearly increase with temperature but we found that relaxing this assumption - having it non-
525 linearly increase with temperature - does not change the model-produced outcomes (see
526 Supplementary text). We let the probability of a cell replicating in the next time step to be non-
527 linearly (sigmoidally) increasing with glutathione concentration (Figure 5B - right panel). This
528 reflects our experimental observation that glutathione concentration must be above some
529 threshold value to appreciably induce population growths (Figure 4F). The probability of staying
530 alive without dividing is then fixed by the probabilities of dying and of replicating. This model
531 contains four parameters, three of which are rigidly fixed by (directly read-off from) the
532 experimental data without any possibility of us adjusting their values: (1) the maximum growth rate
533 that a population can have (~0.25 / hour from our experiments - Figure 2E), (2) the temperature
534 at which heat-induced deaths begin to be non-negligible (i.e., temperature above which no-growth
535 phase starts to exist - this is ~38 ^{O}C according to the wild-type's phase diagram (Figure 2D) and
536 it is also the temperature at which the red line in Figure 5B starts to increase above zero), and (3)
537 the temperature at which heat-induced deaths are always dominant over cell replications (i.e.,
538 temperature above which only the no-growth phase exists - this is ~40.3 ^{O}C according to the wild-
539 type's phase diagram (Figure 2D) and it is also the temperature at which the highest-possible
540 probability of replicating matches the probability of dying (Figure 5B - grey line)). The only free
541 parameter that we can flexibly fit to our data (i.e., fit to combinations of data rather than directly
542 reading-off from a single measurement) is the glutathione concentration at which the probability
543 of replicating is half its maximum (Figure 5B - blue curve).
544
545 Strikingly, after using our data for the wild-type strain to fit the one free parameter, our
546 highly constrained model qualitatively - and quantitatively - recapitulated all the main experimental
547 data (Figures 5C-F and Figure S11). Specifically, the model recapitulates the population-level

548 growth kinetics with the distinct growth phases (Figure 5C, compare with Figure 2A), the single-
549 cell-level growth kinetics for each growth phase (Figure S11B, compare with Figure S5C), the
550 phase diagram (Figure 5D, compare with Figure 2D), the population-density dependent deaths
551 (including the number of survivors decreasing over time in a heavy-tailed manner) (Figure 5E,
552 compare with Figures 3B), and the relationship between temperature and the population-density
553 dependent deaths (Figure 5F, compare with Figure 3D). Moreover, we used a mathematical
554 argument to establish that our model is the simplest possible class of model that can explain our
555 data (see Supplemental text). To intuitively see how the model reproduces all the experimental
556 data, note that the probability that a cell replicates is initially zero - since the glutathione
557 concentration is initially zero - and increases over time as the glutathione concentration increases
558 due to cells constantly secreting glutathione (Figure 5B and Figure S11A). However, the
559 probability for a cell to die starts at a nonzero value - since it is set only by temperature - and
560 remains constant over time since this value is independent of the extracellular glutathione
561 concentration (Figure 5B and Figure S11A). Therefore, there exists a specific concentration of
562 glutathione - a threshold concentration - above which the probability of replicating exceeds the
563 probability of dying, thereby resulting in a population growth. This sets up a "race" in which a
564 population of cells, starting without any extracellular glutathione, must realize the threshold
565 concentration before going extinct. There are initially more cell deaths than cell replications and
566 thus there is a "ticking time bomb" until extinction. As a result, if the initial population-density is
567 sufficiently high, then population growth wins the race - this occurs in the deterministic-growth
568 phase (Figure S11C). If the initial population-density is sufficiently low, then population extinction
569 wins the race - this occurs in the no-growth phase (Figure S11D). For a population that starts with
570 an intermediate density, the glutathione concentration gets close to the threshold concentration
571 by the time there are very few alive cells remaining. At this point in time, any subsequent, small
572 changes in the number of alive cells determines whether the probability of a cell replicating
573 exceeds the probability of a cell dying (Figure S11A). Hence, when a population would grow and
574 if it can grow are both completely unpredictable because the population-level behavior here is
575 highly sensitive to the stochastic behavior of a few alive cells (*34*) - this occurs in the random-
576 growth phase. In the model, at sufficiently high temperatures (i.e., above ~40.3 ^{O}C), the probability
577 of dying exceeds the highest probability that a cell can have for replicating (Figure 5B - grey
578 dashed line). This occurs precisely at the convergence point in the phase diagram. In the no-
579 growth phase, the model also reproduces the number of survivors decreasing over time in a
580 heavy-tailed manner (Figure 5E and Figure S11E). The mechanism here is that cells keep dying
581 as time progresses - due to the probability of dying being constant over time - but, for the still-alive

582 cells, the probability of replicating increases over time due to each surviving cell continuously
583 secreting glutathione into the environment, making replication more likely for each alive cell as
584 time passes. The competition between the two - a constant probability of dying and an initially
585 lower probability of replicating that gradually approaches the probability of dying - results in a
586 population whose approach to extinction continuously slows down over time, leading to the
587 number of survivors decreasing over time in a heavy-tailed manner that we experimentally
588 observed (see Supplemental text). Taken together, these results show that our relatively simple
589 model, with the secreted and accumulated glutathione helping current and future generations of
590 cells to replicate as the primary ingredient, recapitulates qualitatively and quantitatively all the
591 main features of cell replications and deaths that we experimentally observed (Figure 5C-F).
592
593
594 **DISCUSSION**
595 **Expanding the role of glutathione as extracellular mediator of cooperative cell-replication**
596 **and history-dependent extender of population lifespan at high temperatures**
597 Glutathione (GSH) is a well-known, essential tri-peptide for many organisms, including humans
598 (*31*). It is central to diverse processes such as combating cancer (*35*) and neurodegenerative
599 diseases (*36*), slowing down aging (*37*), detoxifying the liver (*38*), and - relevant to our study -
600 protecting cells from reactive oxygen species that are created by high heat and cause cellular
601 damages (*39*). Much focus on glutathione for yeasts has been on its intracellular role as a protector
602 against reactive oxygen species (i.e., cell-autonomous effects). But glutathione's extracellular role
603 for budding yeast - both at high temperatures and in other contexts - remains poorly understood
604 and has received relatively little attention compared to its intracellular roles. Among the studies
605 that examined extracellular glutathione for yeasts are a recent work which showed that
606 extracellular glutathione can protect yeasts from toxic arsenite (*40*) and a work that showed how
607 extracellular glutathione aids in dealing with nutrient imbalance for certain mutant yeasts that have
608 been evolved to secrete glutathione at 30 ^{O}C (*41*). Moreover, there have been some reports on
609 how yeasts, during stationary-phase that follows a diauxic shift at 30 ^{O}C, uptake and secrete low
610 amounts of glutathione (*32*). Indeed, we confirmed that stationary-phase populations, after many
611 hours, can build up to ~2 μM extracellular glutathione at 30 ^{O}C but that log-phase cells do not
612 secrete glutathione. What was underappreciated before, which we have discovered here, is that
613 yeasts secrete glutathione at high temperatures - during log-phase growth and stationary phases
614 - and that this leads to their cooperative replications and an indefinite extension of a population's
615 lifespan (in the form of heavy-tailed population decay) at high temperatures.

616

617 Furthermore, we found that extracellular glutathione at high temperatures mirror several
618 known features of intracellular glutathione at 30 ^{O}C. Firstly, at 30 ^{O}C, yeasts maintain intracellular
619 glutathione at high, millimolar concentrations and keep most of it in its reduced form by recycling
620 it in a NADPH-dependent manner (*31, 42*). This is because glutathione in its reduced form, rather
621 than its oxidized form, is essential for capturing reactive oxygen species (*31*). Analogously, we
622 found that at high temperatures, log-phase yeast populations maintain ~77% of their extracellular
623 glutathione in the reduced form and the rest in the oxidized form (Figure S10). Secondly, our study
624 establishes that accumulating sufficiently large amounts of extracellular glutathione is crucial to
625 yeasts' survival at high temperatures, just as their survival depends on building up of intracellular
626 glutathione. Specifically, high temperatures cause yeasts to respire, which in turn causes the
627 mitochondria to produce reactive oxygen species (*43*). Thus, it makes sense that - as previous
628 studies established - high temperatures cause yeasts to produce and accumulate high amounts
629 of intracellular glutathione to survive oxidative stress (*30,39*) and that depleting intracellular
630 glutathione causes deaths (*36*). Our work extends these findings by establishing analogous
631 benefits of extracellular glutathione. For example, our work shows that no-growth populations
632 become extinct at high temperatures if they do not build up sufficiently high concentrations of
633 extracellular glutathione. Moreover, our work establishes that accumulating extracellular
634 glutathione, even by the alive cells in the no-growth-phase populations, extends the population's
635 lifespan in a manner that depends on the population's history - namely, how many cells the
636 population started with and how the extracellular glutathione has been accumulating over time. In
637 this way, glutathione extends population's lifespan in a manner that depends on the population's
638 history. Even if the population currently has very few alive cells that are secreting glutathione, it
639 benefits from the extracellular glutathione that the past generations of cells had secreted and
640 accumulated. Given glutathione's utility and secretion in other organisms - for example, human
641 lung epithelial cells secrete it when they are exposed to asbestos (*44*) - future studies may reveal
642 that glutathione serves as a mediator of cooperative survival in other organisms at high
643 temperatures and in other stressful conditions.

644

645

646 **Why cooperate instead of autonomously combatting heat-induced damages?**

647 A natural question is why yeasts secrete glutathione at high temperatures to cooperatively survive
648 instead of each yeast cell autonomously combating heat shocks by intracellularly keeping all the
649 glutathione for itself. A major advantage of secreting glutathione is that glutathione can

650 extracellularly accumulate, thereby allowing cells to help their future generations of cells to
651 replicate, long after the current generation of cells have died off. Indeed, our model shows that it
652 is the accumulation of extracellular glutathione that is responsible for a population to decelerate
653 and eventually stop its approach to extinction.
654
655
656 **Summary and outlook**
657 With the budding yeast, we have demonstrated that cells can avoid extinctions at high
658 temperatures by helping each other and their future generations replicate. As a consequence of
659 this cooperative behavior, we have revealed that a temperature which is unlivable for one
660 population of cells can be habitable for another population of cells of the same specie, depending
661 on whether there are sufficiently many cells that can cooperate to maintain the population alive.
662 Specifically, we have shown that yeasts at high temperatures secrete glutathione and that the
663 extracellularly accumulating glutathione, in turn, increases the probability of a cell replicating. By
664 accumulating extracellular glutathione, yeasts also aid the future generations of cells to replicate,
665 long after they themselves have died. Taken together, our experiments and mathematical model
666 replaces the conventional picture in which whether a yeast cell survives a high temperature or not
667 depends on whether the cell can autonomously use its heat-shock response system to combat
668 heat-induced damages. A surprising consequence of our model, which recapitulates all the main
669 features of the experimental data, is that yeasts can, in fact, replicate - albeit with a vanishingly
670 low probability - at extremely high temperatures (e.g., 45 ^{O}C) for which the population cannot grow
671 (due to only the no-growth phase existing in the population-level phase diagram) (Figure S11F).
672 Previous studies have examined cell growth (*45-48*), gene regulations (*49,50*), and metabolite
673 exchanges among microbes (*51,52*) for various species at their conventionally-defined habitable
674 temperatures. Our work encourages re-examining these features at high temperatures that were
675 previously dismissed as unlivable but which may, in fact, be habitable for sufficiently large
676 populations due to the cells cooperating in ways that have so far been overlooked.
677
678 A common explanation for why cells cannot replicate at high temperatures has been that
679 key proteins unfold at these temperatures. While crucial proteins do unfold at certain high
680 temperatures (*6*), our work suggests that there is more to the story than these proteins unfolding
681 since it is unclear how the initial population-density - which determines whether a population
682 (randomly) grows or not at a given temperature - would affect the thermal stability of key proteins,

683 if it does at all. Moreover, we have shown that the budding yeast can replicate at such high
684 temperatures, albeit with a low probability (Figure S11F).
685
686 From a standpoint of physics, we can interpret the random-growth phase in the phase
687 diagram as a boundary formed by a co-existence of the deterministic growth and no-growth
688 phases. A population that is at the endpoint of this boundary, which we earlier called a
689 convergence point, can indefinitely maintain a steady number of cells without either growing or
690 becoming extinct - its population density can fluctuate but does not change over time on average.
691 The convergence point and the number of surviving cells decreasing over time as a heavy-tailed
692 function for populations that are near the convergence point in the phase diagram, remind us of
693 the power-law functions that often describe the behaviors of non-living systems at critical points
694 which are associated with phase transitions (*15-17*). By exploiting these resemblances and using
695 our data and model, a future study might further advance theories of non-equilibrium phase
696 transitions (*55*) that pertain to biologically realistic, self-replicating systems that constantly drive
697 and keep themselves out of equilibrium. Furthermore, understanding how cells can work together
698 to collectively combat extreme temperatures, as we have done here, may suggest intervention
699 mechanisms to combat climate change as well as advance our understanding of how temperature
700 and climate change can impact unicellular life and multicellular communities.

701 ## Methods

702

703 **Growth media and strains.** The "wild-type", haploid yeast strain that we used is from Euroscarf
704 with the official strain name "20000A", isogenic to another laboratory-standard haploid yeast
705 "W303a", and has the following genotype: *MATa*; *his3-11_15; leu2-3_112; ura3-1; trp1Δ2; ade2-*
706 *1; can1-100*. We built the two strains that constitutively expressed GFP by first using PCR to insert
707 a functional *ADE2* gene into the locus of the defective *ADE2* gene in the wild-type strain, by a
708 homologous recombination, so that the red pigments that would have accumulated without the
709 *ADE2* insertion no longer existed (i.e., the strain can now synthesize adenine) and we could thus
710 detect GFP fluorescence without interferences. After replacing the defective *ADE2* locus with a
711 functional *ADE2*, we constructed the 1x-GFP and 100x-GFP strains (see GFP-expression levels
712 in Fig. S4A) by integrating a single-copy of an appropriate, linearized yeast-integrating plasmid at
713 the *HIS3* locus of the chromosome. Specifically, the 1x-GFP strain had its GFP expression
714 controlled by the constitutive promoter of yeast's *KEX2* gene (621 bases upstream of its ORF)
715 which was on a yeast-integration plasmid (*56*) that constitutively expressed *HIS3* (from *C.*
716 *glabrata*) and integrates into the non-functional *HIS3*-locus of the wild-type strain by a homologous
717 recombination. The 100x-GFP strain had its GFP expression controlled by a strong constitutive
718 promoter pGPD1 (*56*) which was on the same plasmid as the one for the 1x-GFP strain except
719 that the *KEX2* promoter was swapped with pGPD1. We cultured all yeasts in defined, minimal
720 media that consisted of (all from Formedium): Yeast Nitrogen Base (YNB) media, Complete
721 Supplement Mixture (CSM) that contains all the essential amino acids and vitamins, and glucose
722 at a saturating concentration (2% = 2 g per 100 mL). The agar pads that we used for growing
723 yeast colonies, including for the fractal-like colonies, contained 2%-agar (VWR Chemicals), Yeast
724 Extract and Peptone (YEP) (Melford Biolaboratories Ltd.), and 2%-glucose.

725

726 **Growth experiments.** In a typical growth experiment, we first picked a single yeast colony from
727 an agar plate and then incubated it at 30 ^{O}C for ~14 hours in 5-mL of minimal medium, which
728 contained all the essential amino acids and a saturating concentration of glucose (2%).
729 Afterwards, we took an aliquot of a defined volume from the 5-mL culture (typically 20 μL), and
730 then flowed it through a flow cytometer (BD FACSCelesta with a High-Throughput Sampler) to
731 determine the 5-mL culture's population-density (# of cells/mL). We then serially diluted the culture
732 into fresh minimal media to a desired initial population-density for a growth experiment at various
733 temperatures. Specifically, we distributed 5-mL of diluted cells to individual wells in a "brick" with

734 twenty-four 10-mL-wells (Whatman: "24-well x 10mL assay collection & analysis microplate"). This
735 ensured that we had 8 identical replicate cultures for each initial population-density (e.g., in Fig.
736 2A-C). We sealed each brick with a breathable film (Diversified Biotech: Breathe-Easy), covered
737 it with a custom-made Styrofoam-cap for insulation, and incubated it in a compressor-cooled, high-
738 precision thermostatic incubators (Memmert ICP260) that stably maintained their target
739 temperature throughout the course of our growth-experiments, with a typical standard deviation of
740 0.017 ^{O}C over time (deviation measured over several days - see Figure S2). Throughout the
741 incubation, the cultures on the brick were constantly shaken at 400 rpm on a plate shaker
742 (Eppendorf MixMate) that we kept in the incubator. To measure their population densities, we took
743 a small aliquot (typically 50 μL) from each well, diluted it with PBS (Fisher Bioreagents) into a 96-
744 well plate (Sarstedt, Cat. #9020411), and then flowed it through the flow cytometer which gave us
745 the # of cells/mL. We determined the growth rates were by measuring the maximum slope of the
746 log-population density after their initial, transient growths.

747

748 **Flow cytometry.** The flow cytometer that we used was a BD FACSCelesta with a High-
749 Throughput Sampler and lasers with the following wave lengths: 405 nm (violet), 488 nm (blue),
750 and 561 nm (yellow/green). We calibrated the FSC and SSC gates to detect only yeast cells (FSC-
751 PMT=681V, SSC-PMT=264V, GFP-PMT=485V, mCherry-PMT=498V. As a control, flowing PBS
752 yielded no detected events). The number of cells/mL that we plotted in our growth experiments is
753 proportional to the number of events (yeast cells) that the flow cytometer measured in an aliquot
754 of cells with a defined volume. We measured the GFP fluorescence with a FIT-C channel and the
755 "red cells" (Figure S5) with a mCherry channel. We analyzed the flow cytometer data with a custom
756 MATLAB script (MathWorks).

757

758 **Measuring number of surviving cells.** We prepared a 250-mL cultures of wild-type cells in 500-
759 mL Erlenmeyer flasks. We placed a constantly spinning magnetic stir-bar at the bottom of the
760 flasks and placed each flask on top of spinning magnets (Labnet Accuplate - at 220 rpm) inside
761 the thermostatic incubators (Memmert ICP260) that we set at desired high-temperatures. For
762 every time point in Figure 3 and Figures S6B-H, we ensured that these populations were not
763 growing (i.e., all populations were in the no-growth phase) by using the flow cytometer to measure
764 their population-densities over time to verify that their population-densities indeed remained
765 constant over time. For the first 48 hours of incubation, we measured the number of Colony

766 Forming Units (CFUs) by taking out a small-volume aliquot from the liquid cultures at high
767 temperatures and distributed droplets from a serial dilution of the aliquot across an agar pad (2%
768 glucose with YEP) that we then incubated in 30 ^{O}C for several days until (no) colonies appeared.
769 When there were few surviving cells per mL - especially for the last time points in each experiment
770 - we determined, in parallel to the plating method, the number of CFUs by transferring an
771 appropriate volume of the liquid cultures from the incubator to an Erlenmeyer flask and then
772 diluting it with the same volume of fresh minimal media. We sealed this flask with a breathable
773 film (Diversified Biotech: Breathe-Easy) and then left it still without stirring, on a benchtop at ~24-
774 30 ^{O}C - we checked that slightly lower temperatures (e.g., room temperatures) did not affect
775 colony-forming abilities - which allowed any surviving cells to settle down to the bottom of the flask
776 and form colonies. We counted the number of colonies at the bottom of the flask - this is the value
777 that we plotted as the last time point in each experiment (Figures 3 and Figures S6B-H).

778

779 **Medium-transfer experiments.** Details are also in Figure S7. At a given temperature, we first
780 grew populations in the deterministic-growth phase (e.g., initial population-density of 30,000
781 cells/mL at 39.1 ^{O}C). We used the flow cytometer to measure their growing population-densities
782 at different times so that we knew from which part of deterministic growth they were in (e.g., mid-
783 log phase). We then transferred each liquid culture to a 50-mL tube (Sarstedt) and centrifuged it
784 so that the cells formed a pellet at the bottom of the tube. We then took the resulting supernatant,
785 without the cell pellet, and flowed it through a filter paper with 200-nm-diameter pores (VWR: 150-
786 mL Filter Upper Cup) to remove any residual cells from the supernatant. After filtering, we flowed
787 an aliquot of the filtered media through a flow cytometer to verify that there were no cells left in
788 the filtered media. We incubated fresh cells into these filtered media (instead of into fresh minimal
789 media) and proceeded with a growth experiment at a desired temperature as described in "Growth
790 experiments".

791

792 **Measuring the depletion of extracellular nutrients.** See caption for Figure S8.

793

794 **Extracellular glutathione assay.** To quantify the extracellular glutathione concentration, cells
795 were removed from the cultures by extracting the media with a 0.45–μm pore filter (VWR,
796 cellulose-acetate membrane). To ensure and verify that there were no cells in the filtered media,

797 we flowed the filtered media through a flow cytometer which indeed did not detect any cells in
798 them. We measured extracellular glutathione concentrations in the filtered media as described in
799 manufacturers' protocol (38185 quantification kit for oxidized and reduced glutathione, 200 tests).
800 We used "BMG Labtech Spectrostar Nano" to measure the optical absorbance at 415-nm. As a
801 background subtraction for all absorbance measurements, we subtracted the absorbance of
802 minimal medium from the measurements to remove the background signal (which could come
803 from, for example, cysteine in the minimal media). We subsequently determined the extracellular
804 glutathione concentrations by using a calibration curve that we constructed by measuring the
805 absorbance at 415-nm for glutathione that we added by hand into buffer provided by the
806 manufacturer.

807

808 **Cell-transfer experiments.** We incubated a 24-well brick of liquid cultures, in the random-growth
809 phase at a desired temperature (e.g., 10,000 cells/mL at 39.1 ^{O}C), in the thermostatic incubators
810 (Memmert ICP260) as described in "Growth experiments". At ~48 hours, we took three aliquots
811 (250 μL, 500 μL, and 1 mL) from the cultures that were growing in mid-log phase (as checked by
812 flow cytometry) and then diluted each of them into pre-warmed, 50-mL minimal media that were
813 in 500-mL Erlenmeyer flasks (Duran group, Cat. #10056621) so that these newly created
814 populations were in the random-growth regime at the same temperature as the original population
815 that they came from (e.g., 10,000 cells/mL at 39.1 ^{O}C). We sealed each flask with a breathable
816 film (Diversified Biotech: Breathe-Easy) and incubated them at the same temperature as the
817 original population. We performed the growth experiments with these new populations as
818 described in "Growth experiments".

819

820 **RNA-seq.** For each temperature that we studied, we collected cells in 50-mL tubes and spun them
821 in a pre-cooled centrifuge. We then extracted RNA from each cell-pellet with RiboPure Yeast Kit
822 (Ambion, Life Technologies) as described by its protocol. Next, we prepared the cDNA library with
823 the 3' mRNA-Seq library preparation kit (Quant-Seq, Lexogen) as described by its protocol.
824 Afterwards, we loaded the cDNA library on an Illumina MiSeq with the MiSeq Reagent Kit c2
825 (Illumina) as described by its protocol. We analyzed the resulting RNA-Seq data as previously
826 described (*57*): We performed the read alignment with TopHat, read assembly with Cufflinks, and
827 analyses of differential gene-expressions with Cuffdiff. We used the reference genome for *S.*

828 *cerevisiae* from ensembl. We categorized the genes by the Gene Ontologies with AmiGO2 and
829 manually checked them with the Saccharomyces Genome Database (SGD).

830

831 **Mathematical model.** Derivations of equations and a detailed description of the mathematical
832 model together with the parameter values used for simulations are in the Supplemental text.

833

Supplemental Information:

- Supplementary Figures S1-S11
- Detailed description of the mathematical model

Acknowledgements:

We thank Shalev Itzkovitz and Arjun Raj for insightful comments on our manuscript. We also thank the members of the Youk laboratory for helpful discussions and Mehran Mohebbi for help with initial experiments. H.Y. was supported by the European Research Council (ERC) Starting Grant (MultiCellSysBio, #677972), the Netherlands Organisation for Scientific Research (NWO) Vidi award (#680-47-544), the CIFAR Azrieli Global Scholars Program, and the EMBO Young Investigator Award.

Author contributions:

H.Y. initiated this research and designed the initial experiments. D.S.L.T. subsequently conceived and developed the project with guidance from H.Y. D.S.L.T. performed the experiments, developed the mathematical model, and analysed the data with advice from H.Y. D.S.L.T. and H.Y. discussed and checked all the data and wrote the manuscript.

DECLARATION OF INTERESTS

The authors declare no competing interests.

855 **References:**

856 1. M. T. Madigan, J. M. Martinko, D. A. Stahl, & D. Clark. *Brock biology of microorganisms* (13th
857 Ed.) (Pearson, 2011), pp. 162-163.

858 2. R. Milo, & R. Phillips. *Cell biology by the numbers* (1st ed.) (Garland Science, 2015),
859 http://book.bionumbers.org/how-does-temperature-affect-rates-and-affinities/.

860 3. L. Bruslind. *Microbiology*. (Open Oregon State University, 2019),
861 http://library.open.oregonstate.edu/microbiology/chapter/environmental-factors/

862 4. P. M. Doran. *Bioprocess Engineering Principles* (2nd ed.) (Academic Press, 2012), pp. 653-
863 655.

864 5. K. Ghosh, & K. Dill. Cellular proteomes have broad distributions of protein stability. *Biophys J*
865 **99**:3996-4002 (2010).

866 6. P. Leuenberger *et al.,* Cell-wide analysis of protein thermal unfolding reveals determinants of
867 thermostability. *Science* **355,** eaai7825 (2017).
868

869 7. J. Verghese, J. Abrams, Y. Wang, & K. A. Morano. Biology of the heat shock response and
870 protein chaperones: Budding yeast (*Saccharomyces cerevisiae*) as a model system.
871 *Microbiol. Mol. Biol. Rev.* **76**:115-158 (2012).
872

873 8. K. Richter, M. Haslbeck, & J. Buchner. The heat shock response: life on the verge of death.
874 *Mol. Cell* **40**:253-266 (2010).
875

876 9. M. B. Miller, & B. L. Bassler. Quorum sensing in bacteria. *Annu. Rev. Microbiol* **55**:165-199
877 (2001).
878

879 10. J. Gore, H. Youk, & A. van Oudenaarden. Snowdrift game dynamics and facultative cheating
880 in yeast. *Nature* **459**:253-256 (2009).
881

882 11. C. Ratzke, J. Denk, & J. Gore. Ecological suicide in microbes. *Nat. Ecol. Evol.* **2**:867-872
883 (2018).
884

885 12. J. Postmus *et al.*, Quantitative analysis of the high temperature-induced glycolytic flux
886 increase in Saccharomyces cerevisiae reveals dominant metabolic regulation. *J. Biol. Chem.*
887 **283**:23524-23532 (2008).
888
889 13. R. M. Walsh, & P. A. Martin. Growth of saccharomyces cerevisiae and saccharomyces
890 uvarum in a temperature gradient incubator. *J. Inst. Brew.* **83**:169-172 (1977).
891
892 14. D. A. Ratkowsky, R. K. Lowry, T. A. McMeekin, A. N. Stokes, & R. E. Chandler. Model for
893 bacterial culture growth rate throughout the entire biokinetic temperature range. *J. Bacteriol.*
894 **154**:1222-1226 (1983).
895
896 15. A. A. Hyman, C. A. Weber, F. Jülicher. Liquid-liquid phase separation in biology. *Annu. Rev.*
897 *Cell. Dev. Biol.* **30**, 39-58 (2014).
898 16. Y. Shin, C. P. Brangwynne. Liquid phase condensation in cell physiology and disease.
899 *Science* **357,** eaaf4382 (2017).
900
901 17. M. Kardar, *Statistical physics of fields* (1st ed.) (Cambridge University Press, 2007).
902 18. A. Goldbeter, D. E. Koshland Jr. Ultrasensitivity in biochemical systems controlled by covalent
903 modification. Interplay between zero-order and multistep effects. *J. Biol. Chem.* **259**, 14441-
904 14447 (1984).
905
906 19. G. J. Melen, S. Levy, N. Barkai, B. Z. Shilo. Threshold responses to morphogen gradients by
907 zero-order ultrasensitivity. *Mol. Syst. Biol.* **1**:2005.0028 (2005).
908
909 20. E. Dekel, U. Alon. Optimality and evolutionary tuning of the expression level of a protein.
910 *Nature* **436,** 588-592 (2005).
911
912 21. V. Bharathi *et al.* Use of *ade1* and *ade2* mutations for development of a versatile red/white
913 colour assay of amyloid-induced oxidative stress in *Saccharomyces cerevisiae*. *Yeast* **33,**
914 607-620 (2016).
915
916 22. N. Q. Balaban. Persistence: mechanisms for triggering and enhancing phenotypic variability.
917 *Curr. Opin. Genet. Dev.* **21,** 768-775 (2011).

23. H. C. Causton *et al.* Remodeling of yeast genome expression in response to environmental changes. *Mol. Biol. Cell* **12**:323-337 (2001).

24. A. P. Gasch, *et al.* Genomic expression programs in the response of yeast cells to environmental changes. *Mol. Biol. Cell* **11**:4241-4257 (2000).

25. F. M. Yakes, & B. van Houten. Mitochondrial DNA damage is more extensive and persists longer than nuclear DNA damage in human cells following oxidative stress. *Proc. Natl. Acad. Sci. U.S.A.* **94**:514-519 (1997).

26. E. Cabiscol, E. Piulats, P. Echave, E. herrero, & J. Ros. Oxidative stress promotes specific protein damage in Saccharomyces cerevisiae. *J. Biol. Chem.* **275**:27393-27398 (2000).

27. T. Bilinski, J. Litwinska, M. Blaszczynski, & A. Bajus. SOD deficiency and the toxicity of the products of autoxidation of polyunsaturated fatty acids in yeast. *Biochim. Biophys. Acta.* **1001**:102-106 (1989).

28. K. A. Morano, C. M. Grant, & W. S. Moye-Rowley. The response to heat shock and oxidative stress in Saccharomyces cerevisiae. *Genetics* **190**:1157-1195 (2012).

29. A. Ayer, C. W. Gourlay, & I. W. Dawes. Cellular redox homeostasis, reactive oxygen species and replicative ageing in Saccharomyces cerevisiae. *FEMS Yeast Res.* **14**:60-72 (2014).

30. K. Sugiyama, A. Kawamura, S. Izawa, & Y. Inoue. Role of glutathione in heat-shock-induced cell death of Saccharomyces cerevisiae. *Biochem. J.* **352**:71-78 (2000).

31. D. J. Jamieson. Oxidative stress responses of the yeast Saccharomyces cerevisiae. *Yeast* **14**:1511-1527 (1998).

32. G. G. Perrone, C. M. Grant, & I. W. Dawes. Genetic and environmental factors influencing glutathione homeostasis in Saccharomyces cerevisiae. *Mol. Biol. Cell* **16**:218-230 (2005).

951 33. M. C. Spickett, N. Smirnoff, & R. A. Pitt. The biosynthesis of erythroascorbate in
952 Saccharomyces cerevisiae and its role as an antioxidant. *Free Radic. Biol. Med.* **28**:183-192
953 (2000).
954
955 34. J. Coates *et al.* Antibiotic-induced population fluctuations and stochastic clearance of bacteria.
956 *eLife*, **7**:e32976 (2018).
957
958 35. J. Navarro *et al.* Changes in glutathione status and the antioxidant system in blood and in
959 cancer cells associate with tumour growth in vivo. *Free Radic Biol. Med.* **26**:410-418 (1999).
960
961 36. J. B. Schulz, J. Lindenau, J. Seyfried, & J. Dichgans. Glutathione, oxidative stress and
962 neurodegeneration. *Eur. J. Biochem.* **267**:4904-4911 (2000).
963
964 37. P. Maher. The effects of stress and aging on glutathione metabolism. *Ageing Res. Rev.* **4**:288-
965 314 (2005).
966
967 38. Y. Honda *et al.* Efficacy of glutathione for the treatment of nonalcoholic fatty liver disease: an
968 open-label, single-arm, multicenter, pilot study. *BMC Gastroenterol.* **17**:96 (2017).
969
970 39. J. C. Lee *et al.* The essential and ancillary role of glutathione in Saccharomyces cerevisiae
971 analysed using a grande gsh1 dirsuptant strain. *FEMS Yeast Res.* **1**:57-65 (2001).
972
973 40. M. Thorsen *et al.* Glutathione serves an extracellular defence function to decrease arsenite
974 accumulation and toxicity in yeast. *Mol. Microbiol.* **84**:1177-1188 (2012).
975
976 41. R. Green *et al.* Rapid evolution of an overt metabolic defect restores balanced growth. *BioRxiv*
977 doi.org/10.1101/498543 (2018).
978
979 42. M. J. Penninckx. An overview on glutathione in Saccharomyces versus non-conventional
980 yeasts. *FEMS Yeast Res.* **2**:295-305 (2002).
981
982 43. K. Sugiyama, S. Izawa, & Y. Inoue. The Yap1p-dependent induction of glutathione synthesis
983 in heat shock response of Saccharomyces cerevisiae. *J. Biol. Chem.* **275**:15535-15540
984 (2000).

44. S. A. Golladay, S. H. Park, & A. E. Aust. Efflux of reduced glutathione after exposure of human lung epithelial cells to crocidolite asbestos. *Environ. Health Perspect.* **105**:1273-1277 (1997).

45. S. Iyer-Biswas *et al.,* Scaling laws governing stochastic growth and division of single bacterial cells. *Proc. Natl. Acad. Sci. USA* **111,** 15912-15917 (2014).

46. M. Scott, T. Hwa. Bacterial growth laws and their applications. *Curr. Opin. Biotechnol.* **22,** 559-565 (2011).

47. M. Kafri, E. Metzl-Raz, F. Jonas, N. Barkai. Rethinking cell growth models. *FEMS Yeast Research* **16,** fow081 (2016).

48. A. R. Zomorrodi, D. Segrè. Genome-driven evolutionary game theory helps understand the rise of metabolic interdependencies in microbial communities. *Nat. Commun.* **8,** 1563 (2017).

49. J. Ihmels, R. Levy, N. Barkai. Principles of transcriptional control in the metabolic network of Saccharomyces cerevisiae. *Nature Biotechnol.* **22**, 86-92 (2004).

50. D. A. Charlebois, K. Hauser, S. Marshall, G. Balázsi. Multiscale effects of heating and cooling on genes and gene networks. *Proc. Natl. Acad. Sci. USA.* **115**, E10797-E10806 (2018).

51. J. E. Goldford *et al.* Emergent simplicity in microbial community assembly. *Science* **361**, 469-474 (2018).

52. J. Liu *et al.* Metabolic co-dependence gives rise to collective oscillations within biofilms. *Nature* **523**, 550-554 (2015).

53. A. Z. Rosenthal, Y. Qi, S. Hormoz, J. Park, S. H.-J. Li, M. B. Elowitz. Metabolic interactions between dynamic bacterial subpopulations. *eLife* **7,** e33099 (2018).

54. A. R. Pacheco, M. Moel, D. Segrè,. Costless metabolic secretions as drivers of interspecies interactions in microbial ecosystems. *Nat. Commun.* **10**, 103 (2019).

1019 55. J. Garcia-Ojalvo, J. M. Sancho, L. Ramirez-Piscina. A nonequilibrium phase transition with
1020 colored noise. *Physics Letters A* **168**, 35-39 (1992).
1021
1022 56. H. Youk, W. A. Lim. Secreting and sensing the same molecule allows cells to achieve versatile
1023 social behaviors. *Science* **343**,1242782 (2014).
1024
1025 57. C. Trapnell *et al*. Differential gene and transcript expression analysis of RNA-seq experiments
1026 with TopHat and Cufflinks. *Nat. Protoc.* **7**, 562-578 (2012).
1027

1028 ## Figure captions:

1029

1030 **Figure 1. Conventional, cell-autonomous view of temperature-dependent cell-replications.**
1031 **(A)** The conventional view states that cells autonomously replicate at "habitable temperatures"
1032 (blue region) and that at sufficiently high temperatures (i.e., "unlivable temperatures"), cells fail to
1033 replicate and can eventually die (red region). This view states that whether a cell can replicate or
1034 not at a given temperature depends on the cell's autonomous ability to use its heat-shock response
1035 system to sufficiently deal with various heat-induced damages.
1036 **(B)** Growth rate as a function of temperature for populations of wild-type yeast cells. Black data
1037 points in the blue region are for populations with sustained, exponential growth over time and
1038 white data points in the red region are for populations without sustained exponential growth. 39
1039 ^{O}C is near a boundary of blue and red regions (also see Figure S1).
1040 **(C)** The conventional view (explained in (A)) applied to budding yeast, based on the data in (B).
1041 **(D)** Question that we investigated in our study: can cells (budding yeasts) cooperatively combat
1042 rising temperatures so that they can turn a temperature that is unlivable for a few cells (e.g., 40
1043 ^{O}C shown in (C)) into a habitable temperature if there are sufficiently many cells working together
1044 to fight off extinction?

1045

1046

1047 **Figure 2. Population density determines replicability of cells and habitability of each**
1048 **temperature.**
1049 **(A-C)** Population density (number of cells / mL) measured over time with a flow cytometer for
1050 populations of wild-type yeast of differing initial population-densities at (**A**) a conventionally-
1051 defined habitable temperature (38.4 ^{O}C), (**B**) near the edge of conventionally-defined habitable
1052 and unlivable temperatures (39.1 ^{O}C), (**C**) and at a conventionally-defined unlivable temperature
1053 (40.3 ^{O}C). Figure 1B sets the conventional definition of a temperature's habitability. For (**A-B**):
1054 Each color shows eight populations that start with the same initial population-density. Red curves
1055 show no-growth beyond initial transient growths (i.e., "no growth"). Green curves show
1056 unpredictable growths (i.e., "random growth"). Blue curves show deterministic, exponential
1057 growths whereby all populations identically grow (i.e., "deterministic growth"). For (**C**): Each color
1058 shows four populations with the same initial population-density. All colors except the red show
1059 growth by ~10-fold.
1060 **(D)** Phase diagram constructed from measurements. Colors represent the behaviors mentioned
1061 in (B) - blue region marks deterministic growth, green region marks random-growth, red region

1062 marks no-growth, and grey region marks populations not growing as they have more cells than
1063 the carrying capacity. Each triangle represents an experiment of type shown in (A-C), performed
1064 at a specific initial population-density and temperature (Figures S2-3). A triangle's color represents
1065 the phase exhibited by populations. See caption of Figure S3 for a description of how we deduced
1066 the phase boundaries from the measurements.
1067 **(E)** Growth rates of populations in the no-growth phase (red), random-growth phase (green) and
1068 deterministic-growth phase (blue) as a function of temperature (error bars are s.e.m., n = 6 or
1069 more for temperatures less than 40 ^{O}C, and n = 3 for higher temperatures). Grey data reproduces
1070 the growth rates of the conventional view shown in Figure 1B.
1071 **(F)** Phase diagrams constructed for engineered yeast strains that constitutively express GFP at
1072 the indicated levels (1x and 100x - see Figure S4A). Triangles indicate experimental data (samples
1073 of growth data represented by these triangles are in Figures S4B-I).
1074
1075
1076 **Figure 3. Cell deaths depend on initial population-density and are not autonomous:**
1077 **populations of higher initial densities decelerate and halt their approach to extinction more**
1078 **rapidly.**
1079 (**A**) We determined the number of survivors per mL over time in a non-growing population at 42.0
1080 ^{O}C (i.e., population in the no-growth phase) by transferring an aliquot of the liquid culture to an
1081 agar pad at different time points, incubating the agar pad at 30 ^{O}C, and then counting the number
1082 of colony forming units ("# of survivors/mL") (see Figure S6A). Circles represent measured
1083 numbers of survivors. Triangles are also from measurements and are overestimates (i.e., the
1084 aliquots did not yield any colonies at 30 ^{O}C, meaning that an aliquot of a larger volume was
1085 required to observe at least one colony. Hence the triangles represent an overestimate of the
1086 number of survivors per mL). Brown dashed line is an exponentially decaying function fitted to the
1087 three circles between 10 and 50 hours. Blue dashed curve is a power-law fit to the same circles.
1088 Also see Figure S6.
1089 (**B**) Number of survivors per mL for three populations of differing initial population-density - all in
1090 the no-growth phase at 41.0 ^{O}C - measured as in (A). Initial population-densities are 92,000 cells
1091 / mL (purple), 231,000 cells / mL (orange), and 312,000 cells / mL (blue). Dashed lines are
1092 exponentially decreasing functions fitted to first three timepoints that share the same color (i.e.,
1093 deaths that occur during the first day of incubation). Also see Figure S6.
1094 (**C**) The conventional view states that cells autonomously die and that every cell has the same
1095 probability of dying per unit time. This leads to the population half-life (i.e., the time taken for a

population density to be halved) to be independent of the initial population-density for a given temperature.

(**D**) Population half-life, plotted here as a function of initial population-density, is defined as the time taken for a population density to be halved, based on fitting exponentially decreasing functions to the number of survivors during the first 24 hours of incubation that follows a ~20-hours of transient growth (transient growth is due to the cells coming from 30 ^{O}C and adjusting to the new temperature). Hence, we measured the number of survivors at approximately 20 hrs, 28 hrs, 36 hrs, and 44 hrs after we incubated the populations at the desired high temperature. Usually, the 44-hr data already deviated from exponential decay and thus we usually omitted them from the exponential fits. Shown here are the half-lives of populations at 39.1 ^{O}C, 40 ^{O}C, 40.3 ^{O}C, 40.8 ^{O}C, 42 ^{O}C, and 43 ^{O}C. Error bars are the s.e.m. (n = 3 for all data points). Circles represent populations in the no-growth phase. The two squares (for 39.1 ^{O}C and 40 ^{O}C) represent populations that grew because they had sufficient densities to trigger their own growth, in accordance with the phase diagram (Figure 2D).

Figure 4. Cells secrete and extracellularly accumulate glutathione to help each other and future generations of cells replicate at high temperatures.

(A) Schematic description of experiments (in (B) and (C)) to distinguish two classes of mechanisms: transfer growing cells into a fresh medium (to determine if intracellular factors dictate population growth) or take out only the growth medium of a growing population and incubate fresh cells in it (to determine if extracellular factors dictate population growth).

(B) At ~39 ^{O}C. Blue curves show two populations of wild-type yeasts that start to exponentially grow when their population-density reaches ~10,000 cells/mL after a transient growth. Cells of a population marked by the boxed blue data point were transferred without their growth medium into a fresh medium that was pre-warmed to ~39 ^{O}C. This resulted in ~10,000 cells/mL in the new culture, represented by the two green curves (two replicate populations).

(C) At ~39 ^{O}C. Population density over time for populations of wild-type yeasts that were incubated in a growth medium that previously harbored a population of exponentially growing cells at ~39 ^{O}C for 0 hours (grey curves), 12 hours (red curves), and 16 hours (purple curves). Each color shows at least 6 replicate populations. Also see Figures S7A-D.

(D) At 39.1 ^{O}C. All populations start at 400 cells/mL, which is too low of a density to permit growth. Adding either ascorbic acid (5 mM - yellow) or glutathione (200 μM - green) to the growth media induces growths. Without adding either one, population does not grow (grey).

1130 **(E)** At 39.1 ^{O}C. Measured the concentration of extracellular glutathione for populations in no-
1131 growth phase (initially 400 cells/mL - red data), random-growth phase (initially 2,000 cells/mL),
1132 and deterministic-growth phase (10,000 cells/mL). Three biological replicates each phase (*n*=3;
1133 error bars are s.e.m.). Measured three timepoints for each phase. Plotted here are the
1134 concentrations of extracellular glutathione as a function of the population density over time. Arrow
1135 shows both population density and concentration of extracellular glutathione increasing together
1136 over time (see also Figure S10).
1137 **(F)** Sensitivity of no-growth populations (initially ~400 cells/mL) at 39.1 ^{O}C to glutathione that we
1138 added into the growth medium. Shown here is the fold-change of the population density after two
1139 days of incubation with added glutathione. as function of supplemented glutathione. Last two data
1140 points show ~200-fold change, which represents the populations having fully grown to reach the
1141 carrying capacity (see also Figure S10).
1142 **(G)** Cartoon illustrating the mechanism deduced by (A-F). Yeasts secrete glutathione at high
1143 temperatures. The extracellular glutathione accumulates. When its concentration reaches at least
1144 a threshold amount (~0.3 μM from (F)), the population replicates at high temperatures by
1145 noticeable amounts.
1146
1147
1148 **Figure 5. Mathematical model with just one free parameter recapitulates all the**
1149 **experimental data under one framework.**
1150 (**A-B**) Description of the mathematical model (see full description of the model in the Supplemental
1151 text). (**A**) Schematic description of the three states that a cell (yellow circle) can be in. In each time
1152 step, any alive cell either stays alive without replicating, replicates, or dies. Alive cells constantly
1153 secrete glutathione (green circle). (**B**) Schematic description of the probabilities that describe each
1154 of the state transitions shown in (A). Left panel: The probability of a cell dying (red line) is fixed by
1155 the temperature and does not change over time. It increases linearly with temperature and, beyond
1156 some temperature, it exceeds the maximum possible value that the probability of a cell replicating
1157 can have (grey line). Right panel: The probability of a cell replicating (blue curve) nonlinearly
1158 increases as the concentration of the extracellular glutathione increases. Thus, the probability of
1159 a cell replicating is initially zero and increases over time up to a maximum possible value (grey
1160 horizontal line) as the extracellular glutathione accumulates due to each alive cell constantly
1161 secreting glutathione.
1162 (**C-F**) Results generated by the model with one, fixed set of parameters. Model recapitulates (C)
1163 the population-growth curves (compare with Figure 2A), (D) the phase diagram (compare with

Figure 2D), (E) population-density dependent deaths (compare with Figure 3B), (F) population half-life (based on cell deaths during the first day of incubation - compare with Figure 3D), the number of survivors decaying over time as a heavy-tailed function (see Figure S11E), and single-cell-level data on growths (compare Figure S11B with Figures S5C). Also see Figure S11.

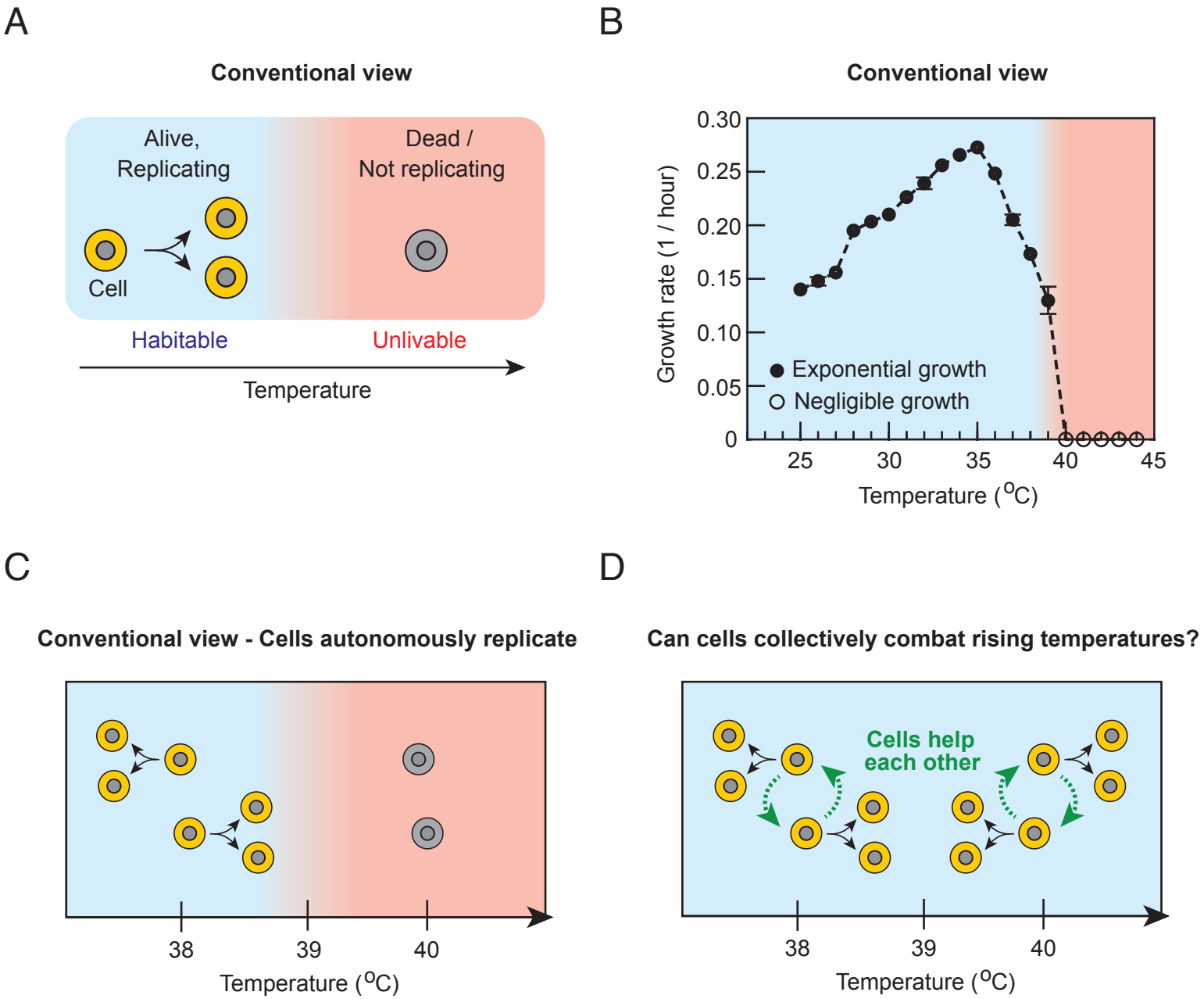
A
Conventional view
Alive,
Replicating
Dead /
Not replicating
Cell
Habitable
Unlivable
Temperature
B
Conventional view
Growth rate (1 / hour)
0.30
0.25
0.20
0.15
0.10
0.05
0
Exponential growth
Negligible growth
25
30
35
40
45
Temperature (°C)
C
Conventional view - Cells autonomously replicate
38
39
40
Temperature (°C)
D
Can cells collectively combat rising temperatures?
Cells help
each other
38
39
40
Temperature (°C)

Fig. 1

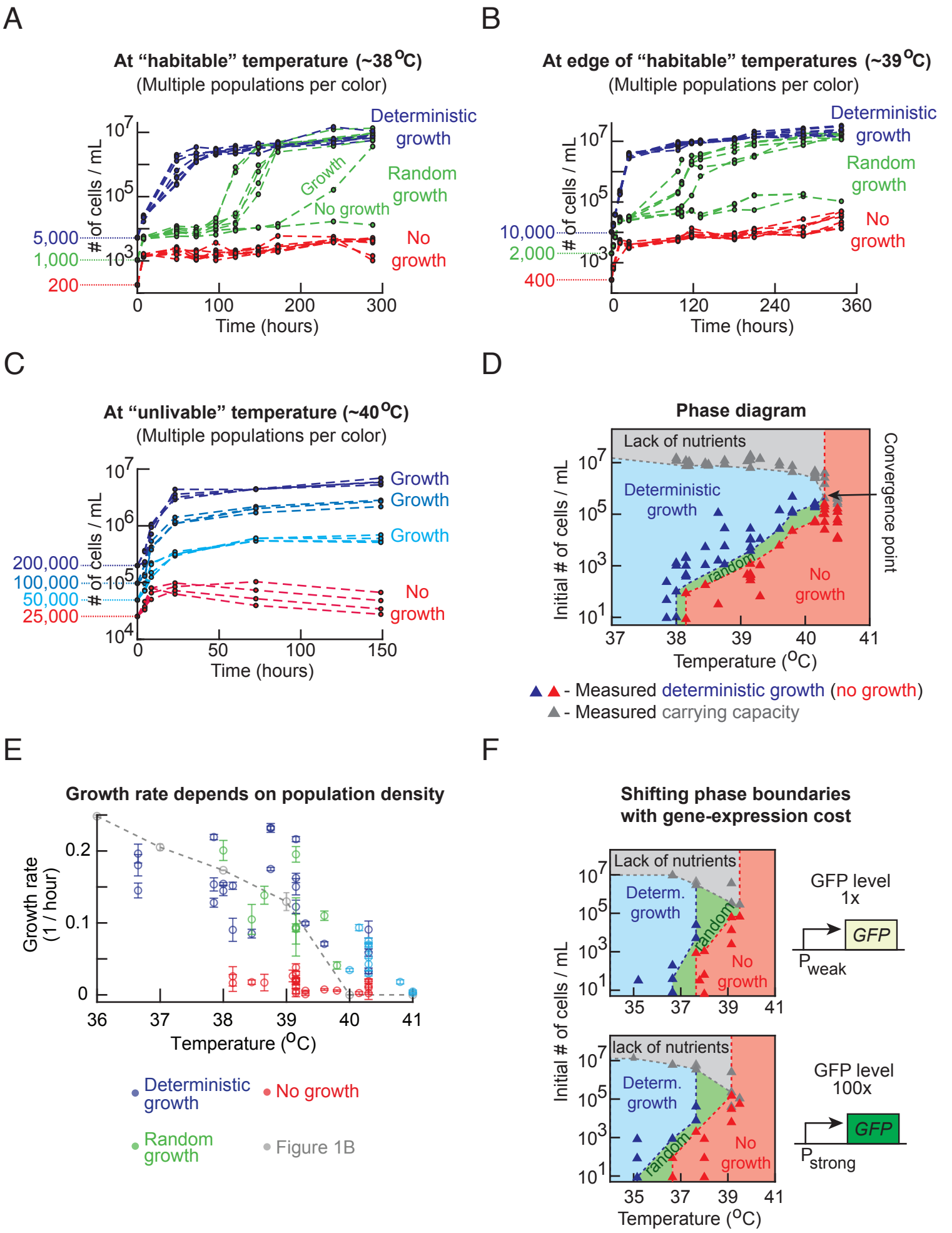
A
At "habitable" temperature (~38 °C)
(Multiple populations per color)
Deterministic growth
Random growth
Growth
No growth
No growth
5,000
1,000
200
# of cells / mL
Time (hours)
B
At edge of "habitable" temperatures (~39 °C)
(Multiple populations per color)
Deterministic growth
Random growth
No growth
10,000
2,000
400
# of cells / mL
Time (hours)
C
At "unlivable" temperature (~40 °C)
(Multiple populations per color)
Growth
Growth
Growth
No growth
200,000
100,000
50,000
25,000
# of cells / mL
Time (hours)
D
Phase diagram
Lack of nutrients
Deterministic growth
random
No growth
Convergence point
Initial # of cells / mL
Temperature (°C)
▲▲ - Measured deterministic growth (no growth)
▲ - Measured carrying capacity
E
Growth rate depends on population density
Growth rate (1 / hour)
Temperature (°C)
Deterministic growth
No growth
Random growth
Figure 1B
F
Shifting phase boundaries with gene-expression cost
Lack of nutrients
Determ. growth
random
No growth
GFP level 1x
GFP
P weak
lack of nutrients
Determ. growth
random
No growth
GFP level 100x
GFP
P strong
Initial # of cells / mL
Temperature (°C)

Fig. 2

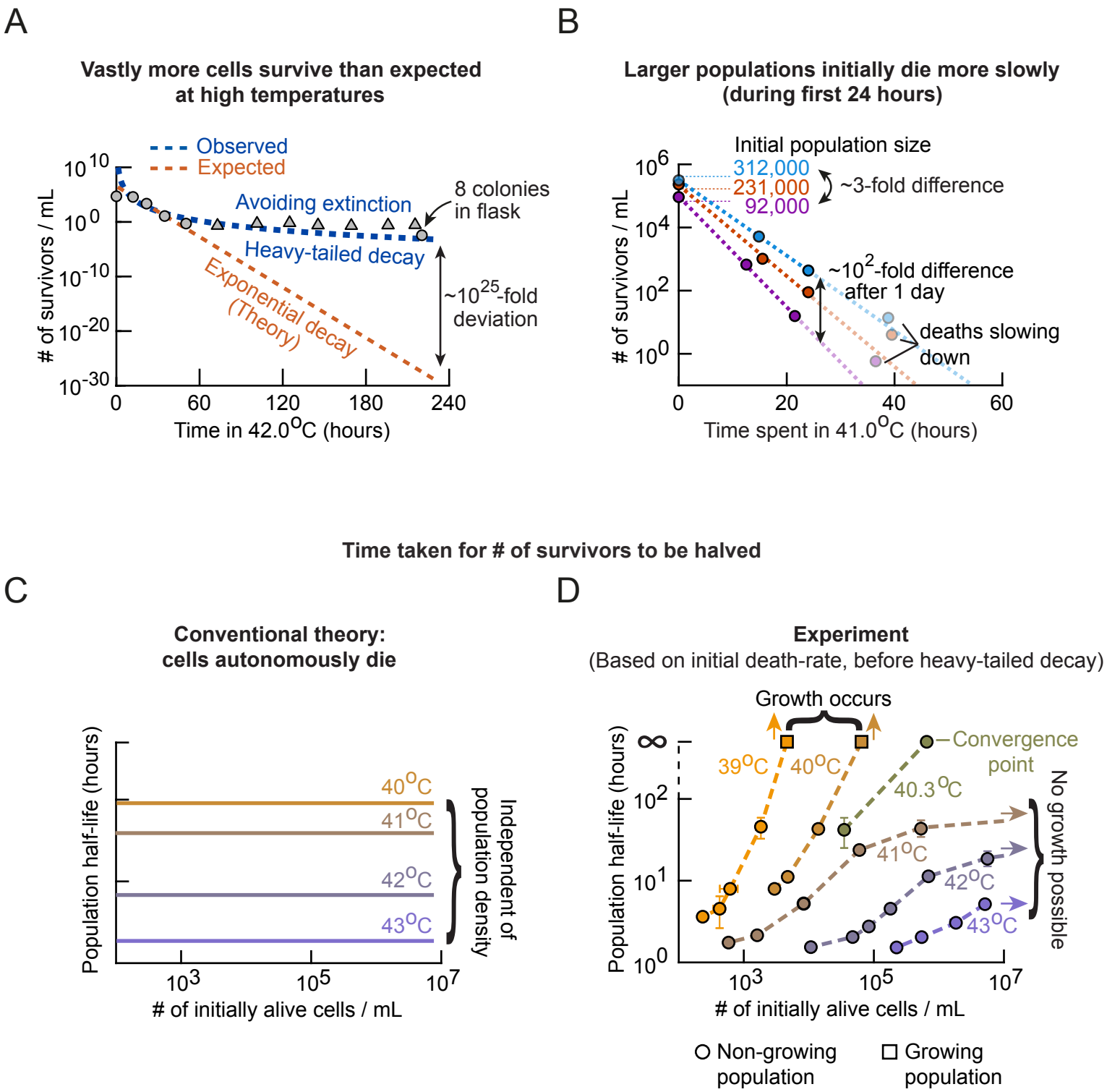
A
Vastly more cells survive than expected at high temperatures
Observed
Expected
Avoiding extinction
8 colonies in flask
Heavy-tailed decay
Exponential decay (Theory)
~10^25-fold deviation
# of survivors / mL
Time in 42.0°C (hours)
B
Larger populations initially die more slowly (during first 24 hours)
Initial population size
312,000
231,000
92,000
~3-fold difference
~10^2-fold difference after 1 day
deaths slowing down
# of survivors / mL
Time spent in 41.0°C (hours)
Time taken for # of survivors to be halved
C
Conventional theory: cells autonomously die
40°C
41°C
42°C
43°C
Independent of population density
Population half-life (hours)
# of initially alive cells / mL
D
Experiment
(Based on initial death-rate, before heavy-tailed decay)
Growth occurs
39°C
40°C
40.3°C
Convergence point
41°C
42°C
43°C
No growth possible
Population half-life (hours)
# of initially alive cells / mL
Non-growing population
Growing population

Fig. 3

A

Determining where factors for growth resides: Extracellular VS Intracellular

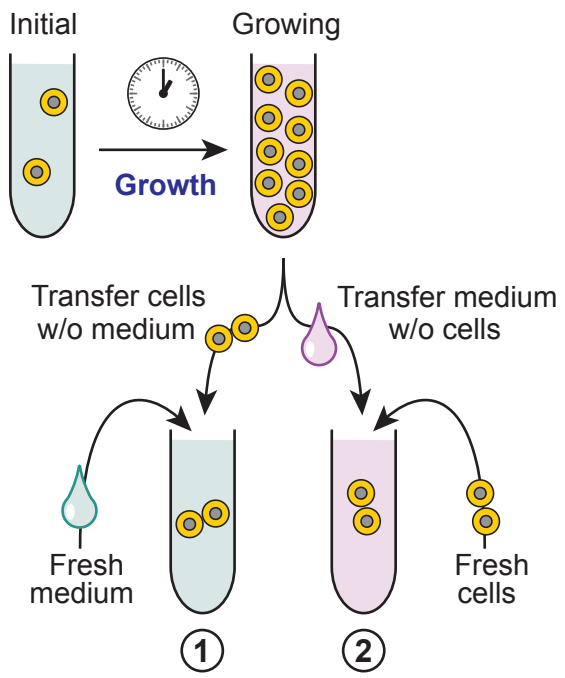

B

① Transferring growing cells to new medium stops growth

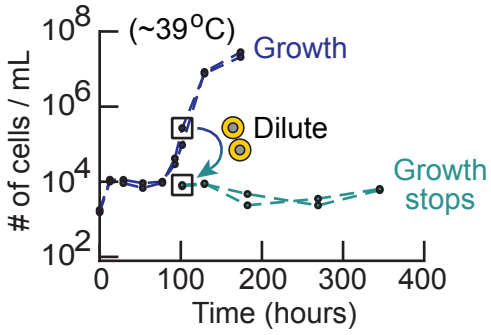

C

② Transferring medium of growing cells to fresh cells can induce growth

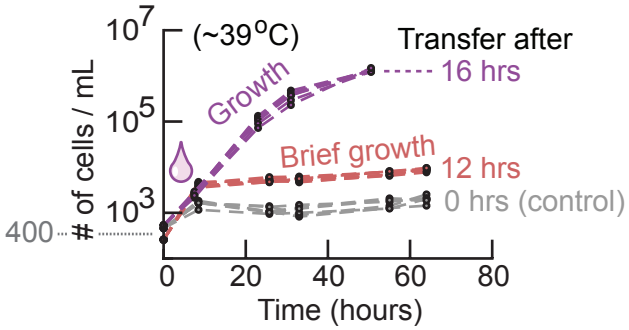

D

Extracellular antioxidants induce growth

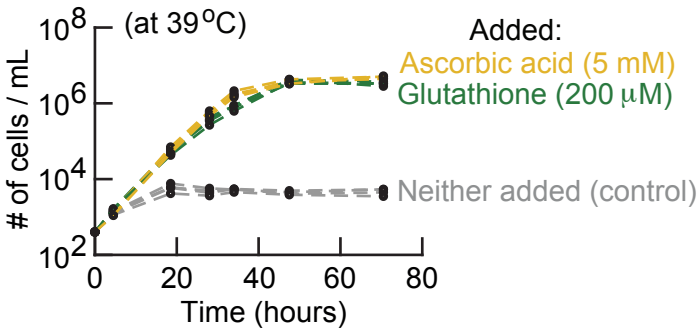

E

Randomly and deterministically growing cells secrete and accumulate glutathione

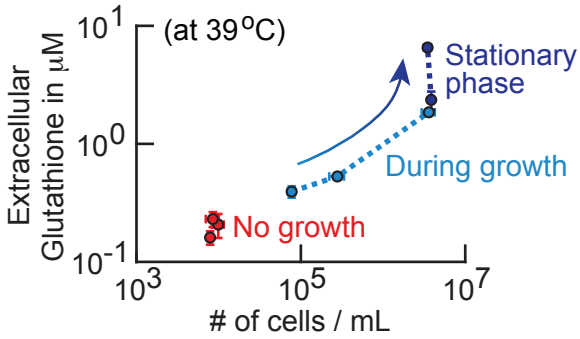

F

Sufficient extracellular glutathione is needed for population growth

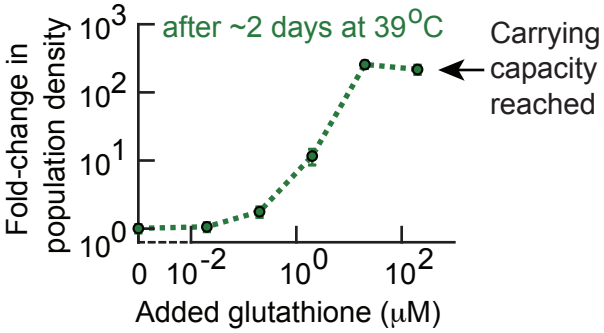

G

Cells secrete and extracellularly accumulate glutathione to help each other and future generations of cells replicate

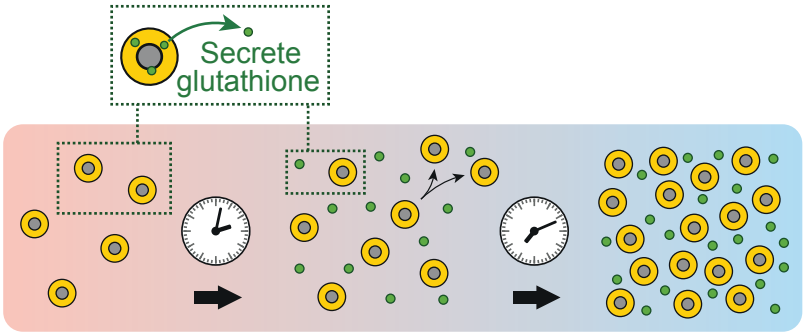

Fig. 4

Mathematical model: Schematics

A

Stochastic transitions of a cell

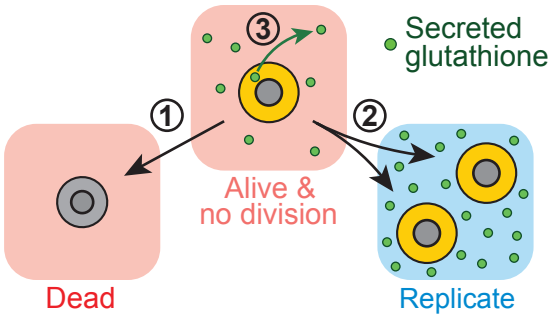

B

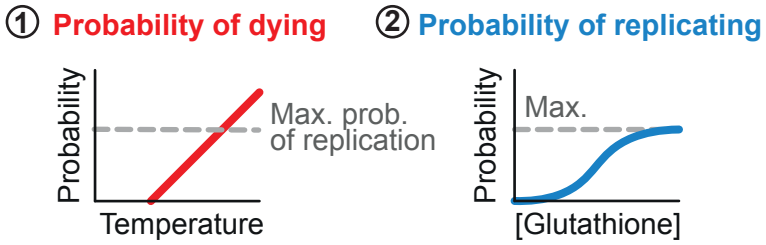

Mathematical model: Recapitulates key features

C

Calculated growth curves

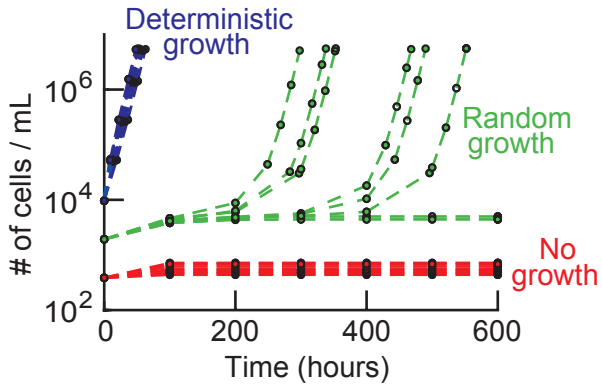

D

Phase diagram from model

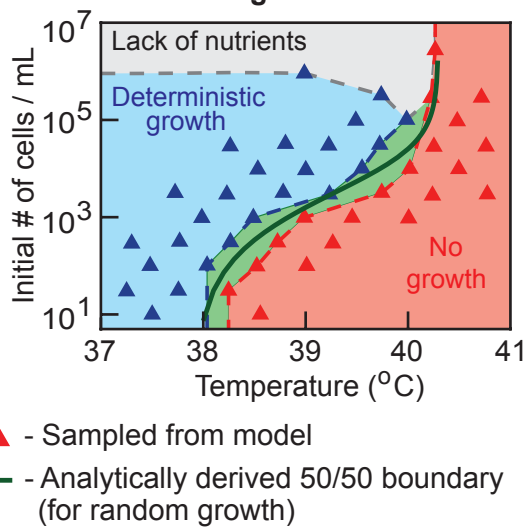

E

Calculated population-density dependent deaths and heavy-tailed decay

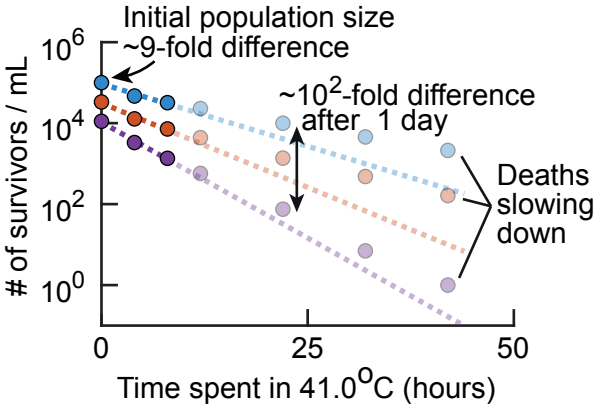

F

Calculated time taken for # of survivors to be halved

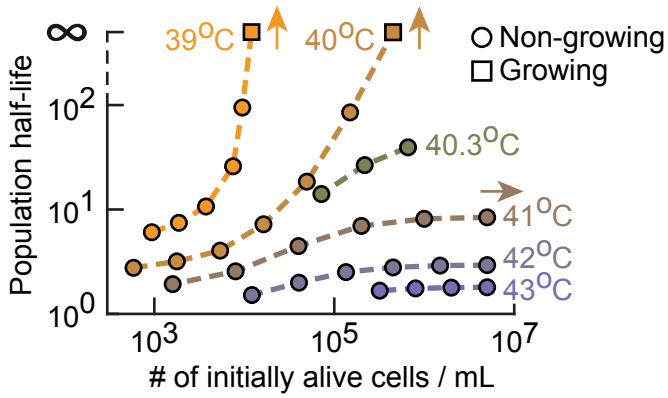

Fig. 5

Supplemental Information

Cells reshape habitability of temperature by secreting antioxidants to help each other replicate and avoid population extinction

Diederik S. Laman Trip[1,2] and Hyun Youk[1,2,3,*]

[1]Kavli Institute of Nanoscience,

[2]Department of Bionanoscience, Delft University of Technology, Delft 2628CJ, the Netherlands

[3]CIFAR, CIFAR Azrieli Global Scholars Program, Toronto ON M5G 1M1, Canada

[*]E-mail: h.youk@tudelft.nl

This document contains:

- **Figures S1 - S11**
- **Detailed description of the mathematical model**

Supplemental Figures

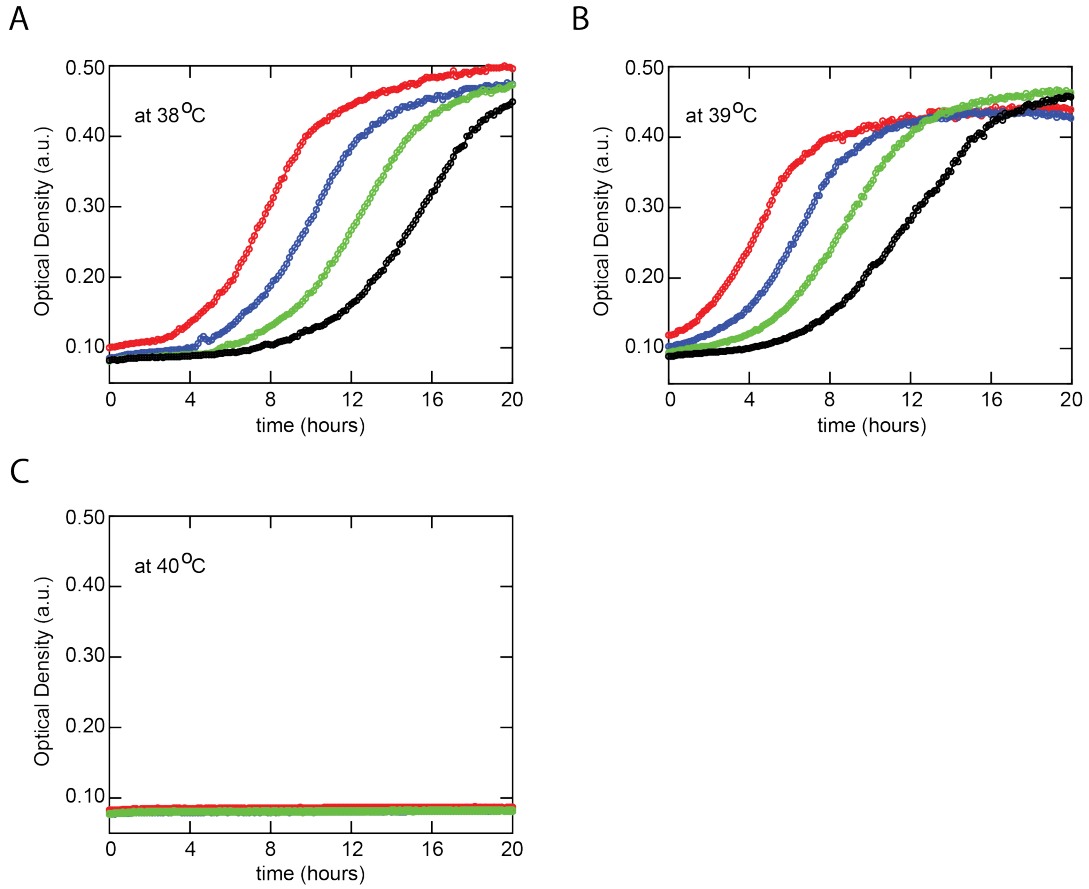

Figure S1. Conventional view of temperature-dependent cell-growth for populations of wild-type yeast defines habitable and inhabitable temperatures (Related to Figure 1B). (A-C) To obtain the conventional picture depicted in Fig. 1B, we performed a laboratory-standard growth-experiments in which we used a plate reader (BioTek Synergy HTX microplate plate reader, model S1LFA) to measure the Optical Density (OD) of liquid cultures of wild-type yeast cells over time (up to 20 hours shown here). OD represents the optical absorption of light at a wavelength of 600 nm and is directly proportional to the number of cells per volume, OD=0.10 corresponds to approximately 1.2 x 10^6 cells/mL. The plate reader cannot detect sufficiently small ODs (i.e., OD < 0.08). We show here representative data for 38 ^{O}C (**A**), 39 ^{O}C (**B**), and 40 ^{O}C (**C**). For each temperature, the different colors represent cell-populations with distinct starting ODs. To obtain these starting ODs for a given temperature, we diluted cells from a single liquid-culture of cells that grew in 30 ^{O}C (as we also did for growth experiments that appear in later figures). The relative starting ODs are approximately 1x (red), 0.5x (blue), 0.25x (green), and 0.125x

(black). The ODs for 1x-populations are similar (i.e., within a ~3-fold difference of each other) in (A-C) and are higher than 0.08. All cultures at 38 ^{O}C and 39 ^{O}C reach their carrying capacities (i.e., ODs plateau over time in (A-B)). None of the populations grew at 40 ^{O}C (i.e., OD remains flat over time in (C)).

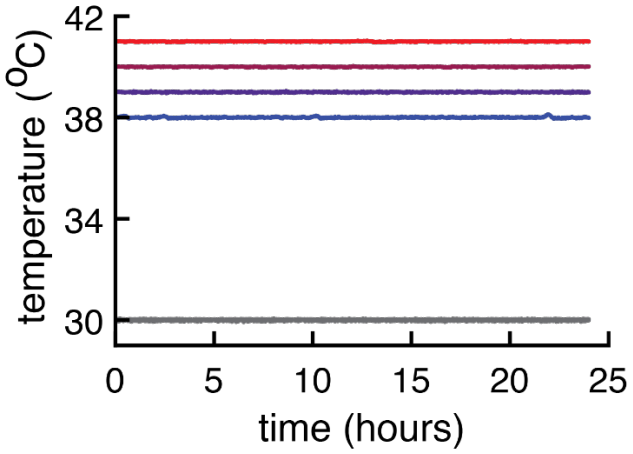

Figure S2. Temperature remains stable during all our growth-experiments (Related to Figure 2). In all our growth experiments described in Figure 2 and subsequent figures (performed with liquid cultures of cells incubated in compressor-cooled, high-precision thermostatic incubators (Memmert ICPs)), the incubators stably maintained their target temperature throughout the course of our growth-experiments, with a typical standard deviation of 0.017 ^{O}C over time (deviation measured over several days). As examples, shown here are temperatures recorded by the incubator's sensor, zoomed to 24 hours for five separate growth experiments: Starting from the top, the curves are for 41 ^{O}C, 40 ^{O}C, 39 ^{O}C, 38 ^{O}C and 30 ^{O}C. We also verified and aligned the incubators' temperatures by using a different thermocouple device. Thus, we measured temperature values with two different thermocouple devices and the temperature remained stably constant over the course of each growth-experiment.

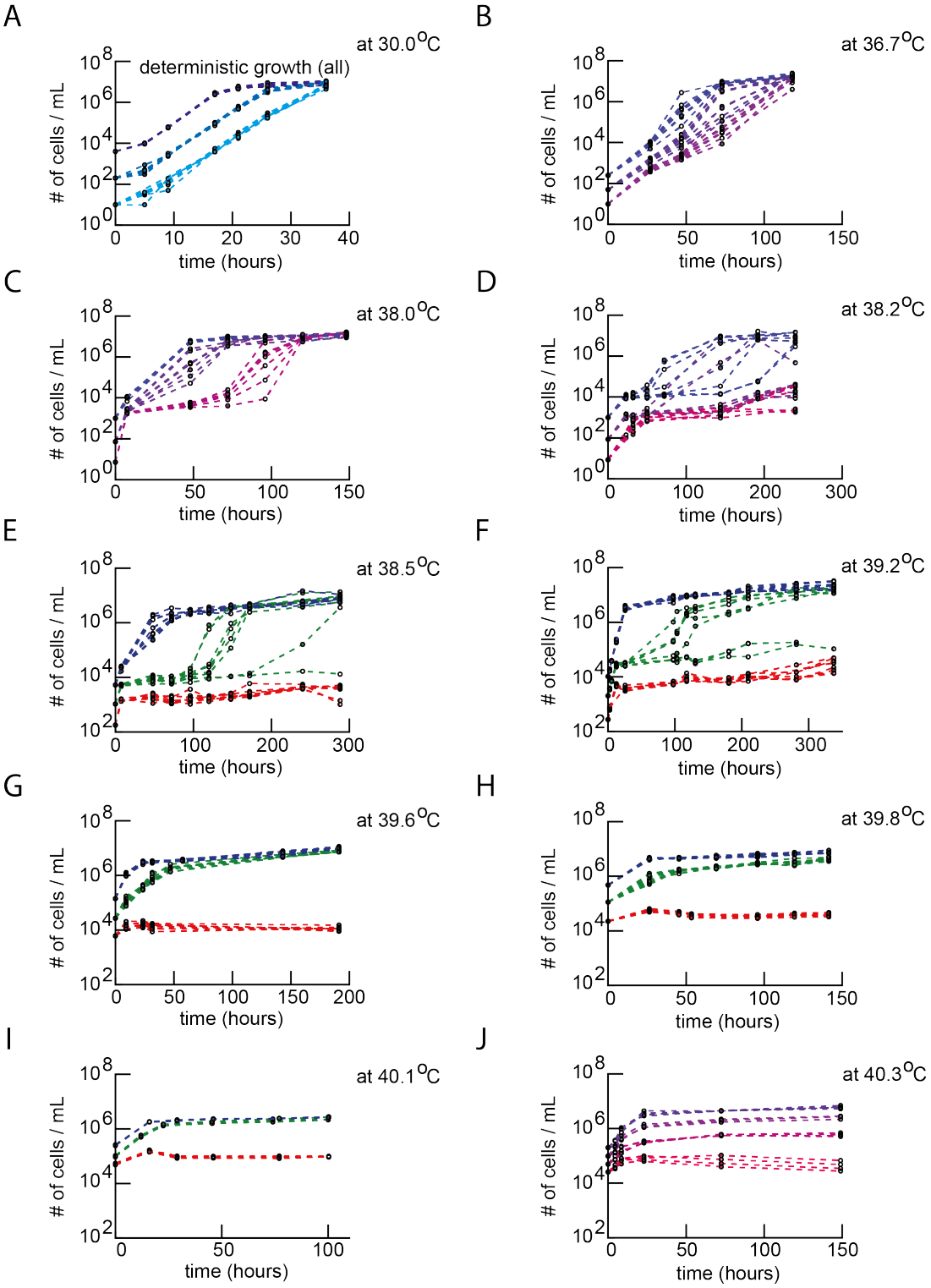

Figure S3. Initial population-density dependent growth of wild-type cell-populations for a wide range of initial population-densities and temperatures (Related to Figures 2A-E). (A-J) Population density (number of cells/mL) measured over time with a flow cytometer for wild-type

yeast populations of differing initial population-densities. Sample data shown for 30 ^{O}C (**A**), 36.7 ^{O}C (**B**), 38.0 ^{O}C (**C**), 38.2 ^{O}C (**D-E**), 38.5 ^{O}C and 39.2 ^{O}C respectively, copied here from Figure 2A-B for completeness, (**F**), 39.6 ^{O}C (**G**), 39.8 ^{O}C (**H**), 40.1 ^{O}C (**I**), and 40.3 ^{O}C (**J**). Each color shows populations that start with the same initial population-density and, for temperatures below 40.0 ^{O}C, there are eight replicates for each color that all start with the same initial population-density. For temperatures above 40.0 ^{O}C, there are at least three biological replicates for each color. To show multiple starting population-densities for populations having the same growth phase (e.g., random-growth phase), we used here a color scheme that is different from the one that we used in Fig. 2A-C. Based on these growth experiments, we constructed the phase diagram for the wild-type cells (Figure 2D). To construct the phase diagram, we determined whether a given initial population-density leads to a deterministic growth, a random growth or a no-growth from the data such as the ones shown here as follows: An initial population-density leads to deterministic growth in the phase diagram if all replicate populations, that start with the same initial population-density, grow exponentially in an identical manner over time (i.e. all curves overlap over time). As an example, (**A**) shows all three initial population-densities leading to a deterministic growth at 30 ^{O}C. An initial population-density leads to no-growth in the phase diagram if none of the replicate populations grow after an initial, transient growth that typically lasts at most ~10 hours due to the effect of cells being transferred from a 30 ^{O}C culture to their new temperature. As an example (**G**) shows the lowest initial population-density leading to no-growth (red curves). We classified an initial population-density, for a given temperature, as yielding a random growth in the phase diagram (Figure 2D) if the curves of replicate populations do not overlap or when some replicate populations do not grow while other replicate populations do grow. Here, the populations that do grow do not overlap due to growing at distinct rates or having different durations of stasis, leading to populations that grow reaching the carrying capacity at vastly different times (i.e., by 10s to 100s of hours) despite having the same initial population-density. As an example, (**C**) shows the intermediate initial population-density leading to random growths (green curves). We determined the phase boundaries in the phase diagram (Figure 2D) as follows: The boundary between the deterministic-growth and random-growth phases connects the minimum, measured initial-population-densities that yielded deterministic growth. The boundary between the random-growth and no-growth phases connects the maximum, measured initial-population-densities that yielded no growth. Finally, we determined the temperature above which a population-level growth is no longer possible by determining the lowest temperature for which the final population-density is always different when the initial population-density is different (i.e., populations never grow to the carrying capacity at which one or more essential nutrients has

been depleted). As an example, (**J**) shows that populations of any initial density never grow to the same population-density when they stop growing.

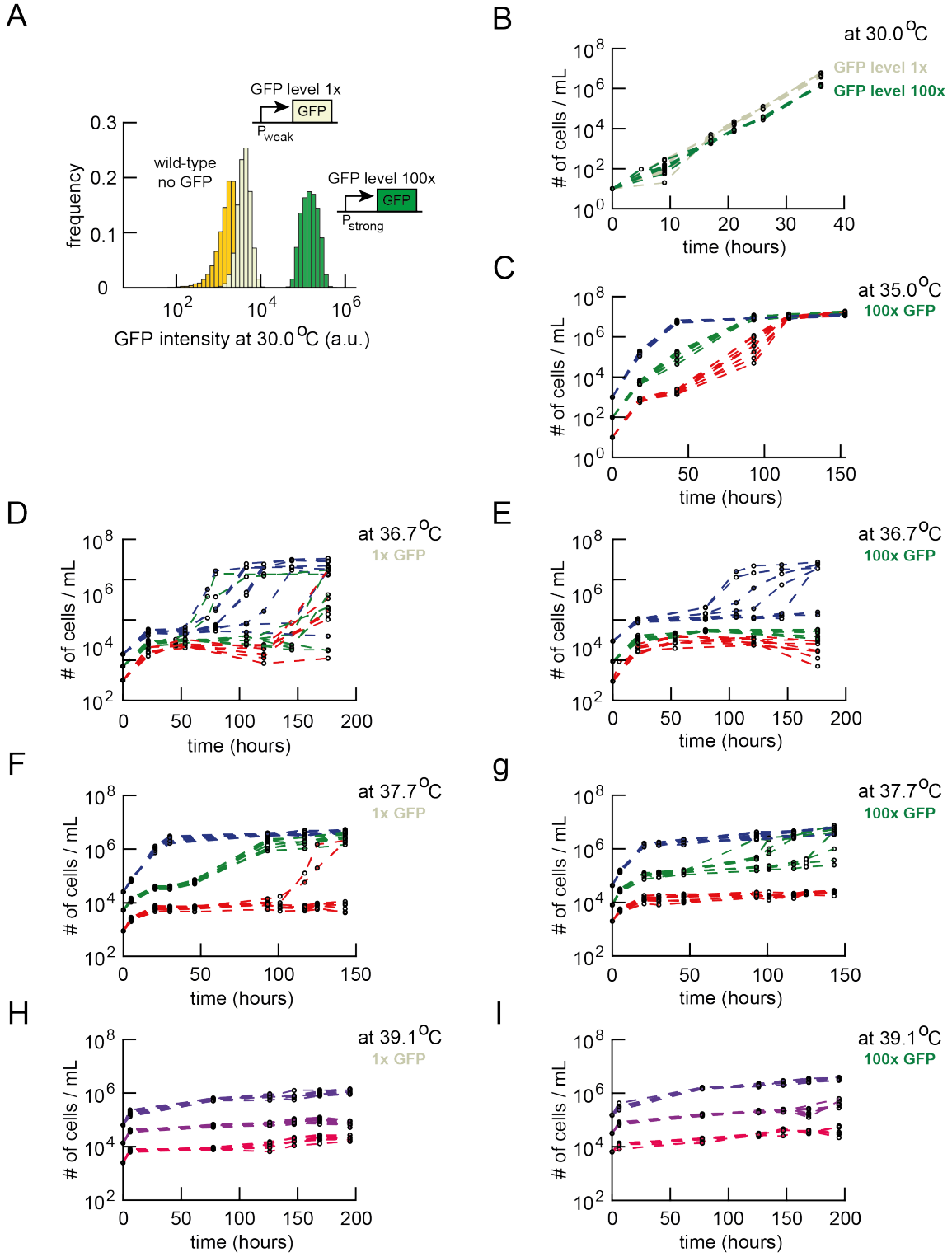

Figure S4. Initial population-density dependent growth by populations of engineered yeasts that constitutively express GFP for a wide range of initial population-densities and

temperatures (Related to Figure 2F). Characterization of the two yeast strains ("1x-GFP" and "100x-GFP" strains) that constitutively express GFP, which we used to construct the phase diagrams in Fig. 2F. **(A)** A histogram of GFP levels of the two engineered yeasts and the wild-type strain as measured by a flow cytometer. The 1x-GFP cells have a higher mean-fluorescence than the wild-type cells whereas the 100x-GFP cells have approximately 100-fold higher mean-fluorescence than the 1x-GFP cells. (**B-I**) As with the wild-type strain (Figure S3), we performed growth-experiments in which we used a flow cytometer to measure the population-density (number-of cells/mL) for the 1x-GFP and 100x-GFP strains. Sample data shown for 30 ^{O}C (**B,** 1x-GFP strain in grey and 100x-GFP strain in green), 35.0 ^{O}C (**C,** 100x GFP strain), 36.7 ^{O}C (**D,** 1x-GFP strain; **E,** 100x-GFP strain), 37.7 ^{O}C (**F,** 1x-GFP strain; **G,** 100x-GFP strain), and 39.1 ^{O}C (**H,** 1x-GFP strain; **I,** 100x-GFP strain). Each color shows multiple populations that all start with the same initial population-density. There are typically eight replicate populations for each color shown here. To show multiple initial-population-densities for each of the growth phases (e.g., random-growth phase), we used here a color scheme that is different from the one that we used in Figures 2A-C. To distinguish deterministic, random, and no-growth phases for the 1x-GFP and 100x-GFP strains, we used criteria that are similar to the ones that used for the wild-type strain (Figure 2D) which we described in the caption for Figure S3. Here, for a given temperature, if six of eight populations with the same initial population-density exponentially grew, then we classified that initial-population density as leading to the deterministic-growth phase in the phase diagram (for the wild-type cells, all eight populations had to exponentially grow). For a given temperature, if six out of eight populations with the same initial population-density did not grow, we classified that initial-population as yielding the no-growth phase in the phase diagram (for the wild-type cells had to not grow). These slight modifications do not qualitatively change the main features of the phase diagrams (Figure 2F).

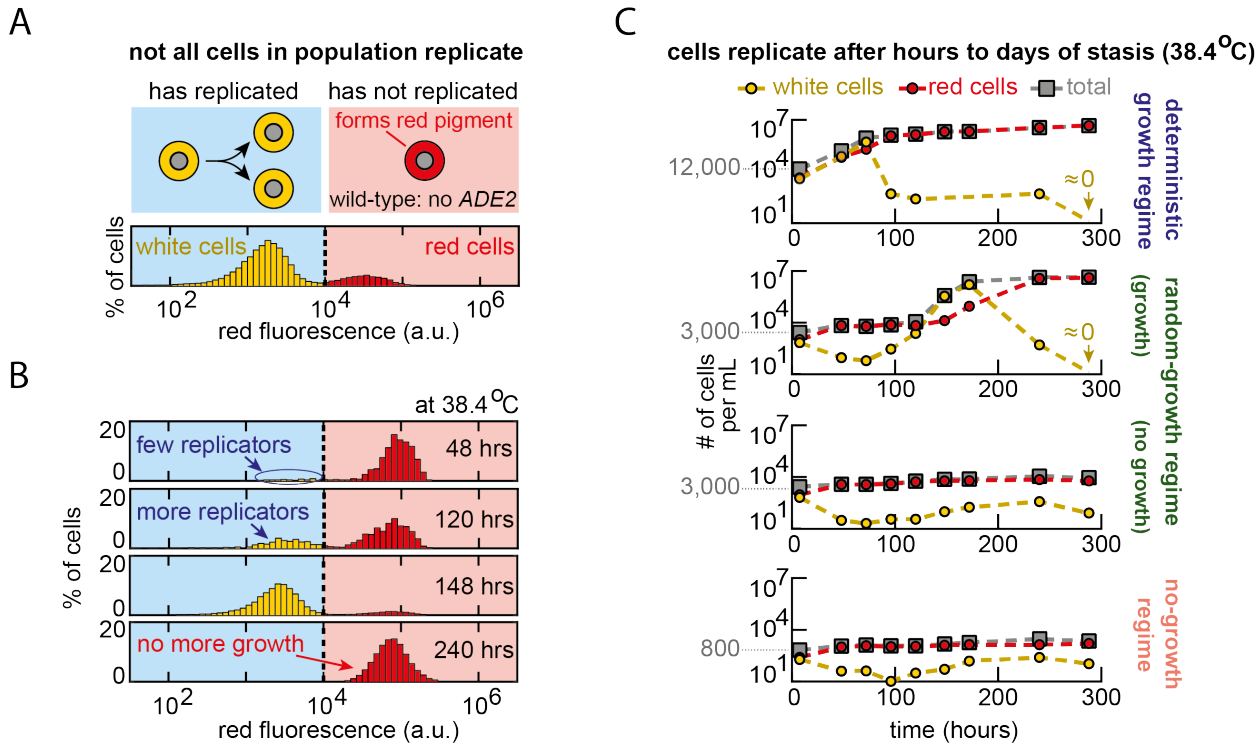

Figure S5. A few cells stochastically and transiently replicating in a no-growth and random-growth population (Related to Figures 2A-D). (A) Wild-type strain, with a defective *ADE2* gene, produces red pigments as by-products of the not-fully repressed adenine-biosynthesis. Red cells have not been dividing for some time. Non-red ("white") cells have been dividing. Histogram shows percentages of red and white cells in a population determined by a flow cytometer's red-fluorescence detector that quantified redness of individual cells. **(B)** Percentage of white and red cells over time measured with the flow cytometer for a population of wild-type yeasts. Time shows hours of incubation in 38.4 ^{O}C. These histograms show example time course for a population that grows at a high temperature. **(C)** Numbers of white and red cells in a population per mL, at various times for three different growth regimes indicated by the phase diagram (Figure 2D). Random-growth regime shows two replicate populations - one growing (second row) and one not growing (third row).

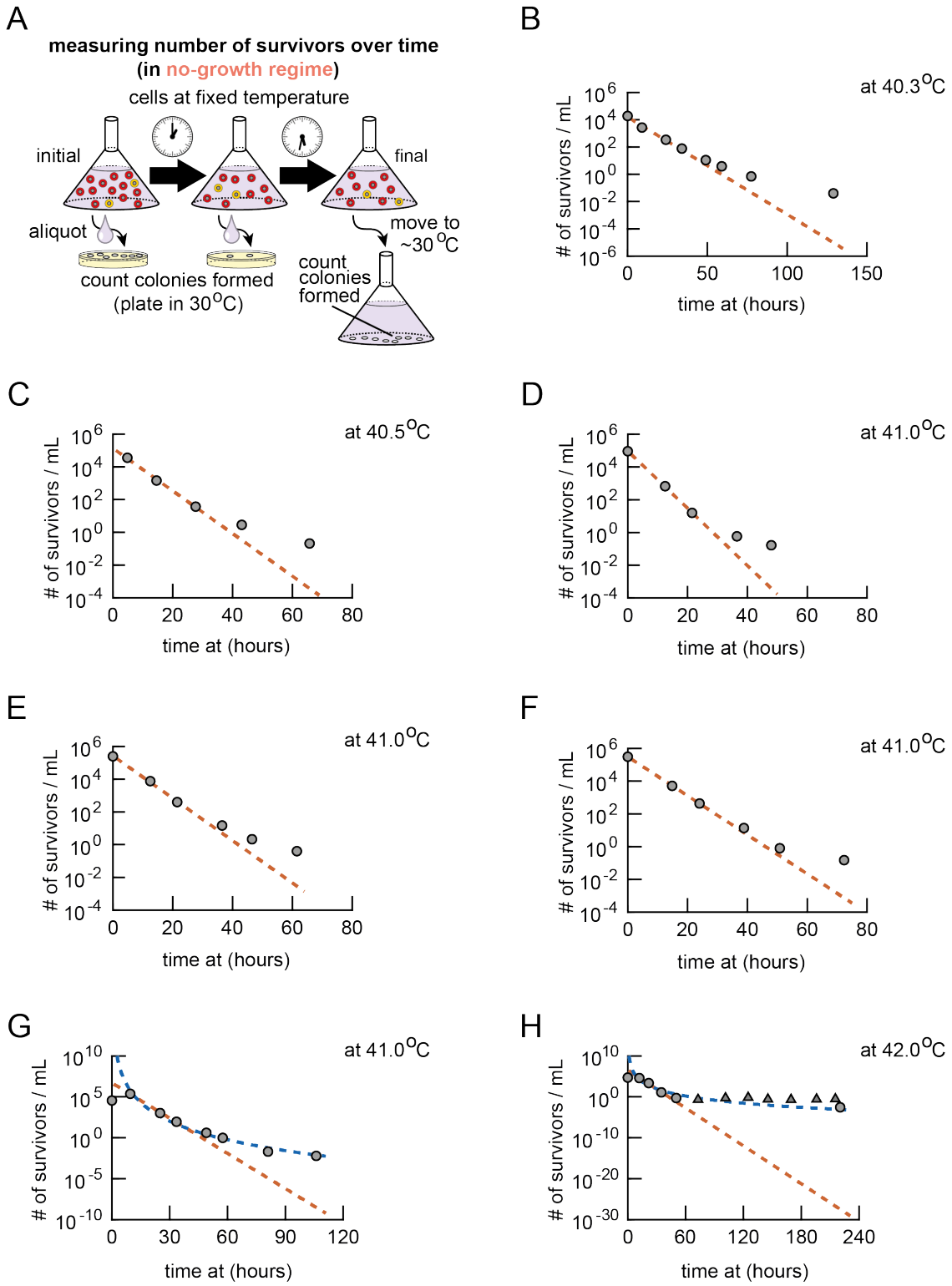

Figure S6. Unconventional death at high temperatures: number of survivors decreases over time as a heavy-tailed function (Related to Figures 3B-D). (A) Schematic description of the experiments that we performed to measure the number of surviving wild-type cells over time

in a population that was in the no-growth regime of the phase diagram (Figure 2D). At various times, we took an aliquot from a liquid culture of cells that we incubated at a high temperature. We then placed droplets of a serial dilution of the aliquot on an agar pad at 30 ^{O}C. We then counted the number of colonies that formed (colony forming units) on the agar at 30 ^{O}C. By counting the number of colony-forming units and knowing the dilutions and volumes of the aliquots that we took out various times, we determined the "# of survivors / mL" that we plotted in (B-H) and Figures 3E-F. For the last few time points in (B-H) and Figures 3E-F, in parallel to the plating on agar pads, we used a complementary method to count the number of survivors that remained in the liquid culture. Taking an aliquot whose volume is only a fraction of the total volume of the liquid culture would have yielded very few colonies on the agar pad, since there was typically less than one survivor per mL of the liquid cultures. Thus, we took out appropriate volumes (typically tens of mL) from the flask that contained the entire liquid culture at a high temperature, transferred it to an Erlenmeyer flask and then left it in ~30 ^{O}C for several days without shaking it so that all the cells settled down and formed colonies on the bottom of the flask. For the last time points in (B-H) and Fig. 3E-F, we took out the flask that contained the entire remaining liquid culture at high temperature instead. Counting the colonies formed by an aliquot on agar pads and counting the colonies formed by cells settled down in liquid yielded the same results when done in parallel. (**B-H)** We used the method in (A) to measure the number of surviving wild-type cells per volume (per mL) at 40.3 ^{O}C (**B**), 40.5 ^{O}C (**C**), 41.0 ^{O}C (**D-G**), and 42.0 ^{O}C (**H**). For (B-F), brown dashed-lines represent an exponentially decaying function that we fitted to the first three data points for each panel. For (G and H), the brown dashed-lines represent an exponentially decaying function that we fitted to the data points that lie between 10 and 50 hours for each panel. The blue dashed-curve is a power-law function that we fitted to the same data points as the exponentially decaying function. In each panel (B-H), we see that the data points vastly deviate from the brown dashed-line (i.e., data point at the final hour deviates by at least ~10^4 cells/mL in nearly all panels). Thus, contrary to the conventional view of cell death at high temperatures (*4*), the number of survivors does not exponentially decrease over time (i.e., cell-death is not completely autonomous and is not fixed by a single (exponential) rate-constant). Instead, it decreases over time as a heavy-tailed function.

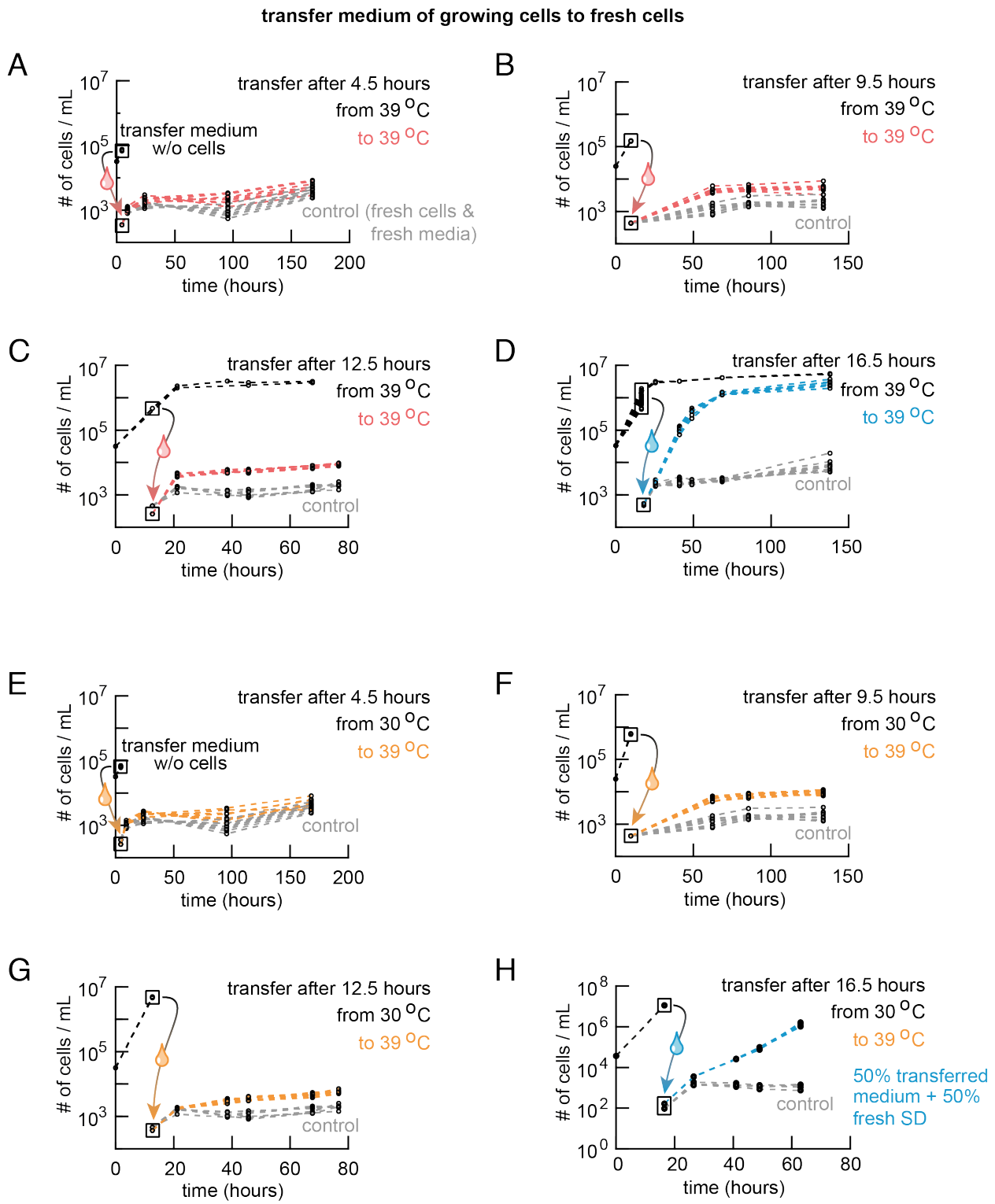

Figure S7. Ultra-sensitive growth at high temperatures is due to cells altering their shared extracellular environment (Related to Figures 4B-C). (A-D) From populations (black curves) whose initial population-density was 30,000 cells/mL and were deterministically growing at 39.1

^{O}C for 4.5 hours (**A)**, 9.5 hours (**B**), 12.5 hours (**C**), and 16.5 hours (**D**), we separated their growth media from all their cells by flowing them through filter papers that have 200-nm-diameter pores - we confirmed a complete separation of cells from their media by flowing the filtered media through a flow cytometer and detecting no cells in them at all. We then transplanted fresh cells into each of these filtered media, also at 39.1 ^{O}C and with an initial population-density of 400 cells/mL. We then measured the densities of these newly created populations over time (red curves for (A-C) and blue curves for (D)). As a control, we also incubated fresh cells in fresh media with the same initial population-density of 400 cells/mL and then measured their population densities over time (grey curves in (A-D)). For all colors in each panel, there are at least six replicate populations. Red curves in (A-C) show no appreciable growth beyond transient growths while the blue curve in (D) shows deterministic growth to the carrying capacity. (**E-H**) Same protocol as (A-D) except that the populations that gave away their media were growing at 30.0 ^{O}C for 4.5 hours (**E**), 9.5 hours (**F**), 12.5 hours (**G**), and 16.5 hours. After the media transfers, we still incubated the newly created populations at 39.1 ^{O}C as in (A-D) and with an initial population-density of 400 cells/mL, also as in (A-D). In (E-G), their population-densities over time at 39.1 ^{O}C are shown as orange curves and those of control populations (same as (A-D)) are in grey curves. Beyond the transient growths, none of the orange curves show sustained exponential growth (i.e., none reach the carrying capacity). (**H**) Population at 30 ^{O}C after 16.5 hours of incubation are in stationary phase, after a log-phase growth that ended with a diauxic shift. At this point, we transferred its growth medium to fresh cells at 39 ^{O}C. The population that received this medium grew at 39 ^{O}C to nearly reach its carrying capacity (blue curves). Taken together, these results (E-H) indicate that some factors that yeasts secrete during a stationary phase at 30 ^{O}C after - and perhaps during - diauxic shift, induce population growths at high temperatures.

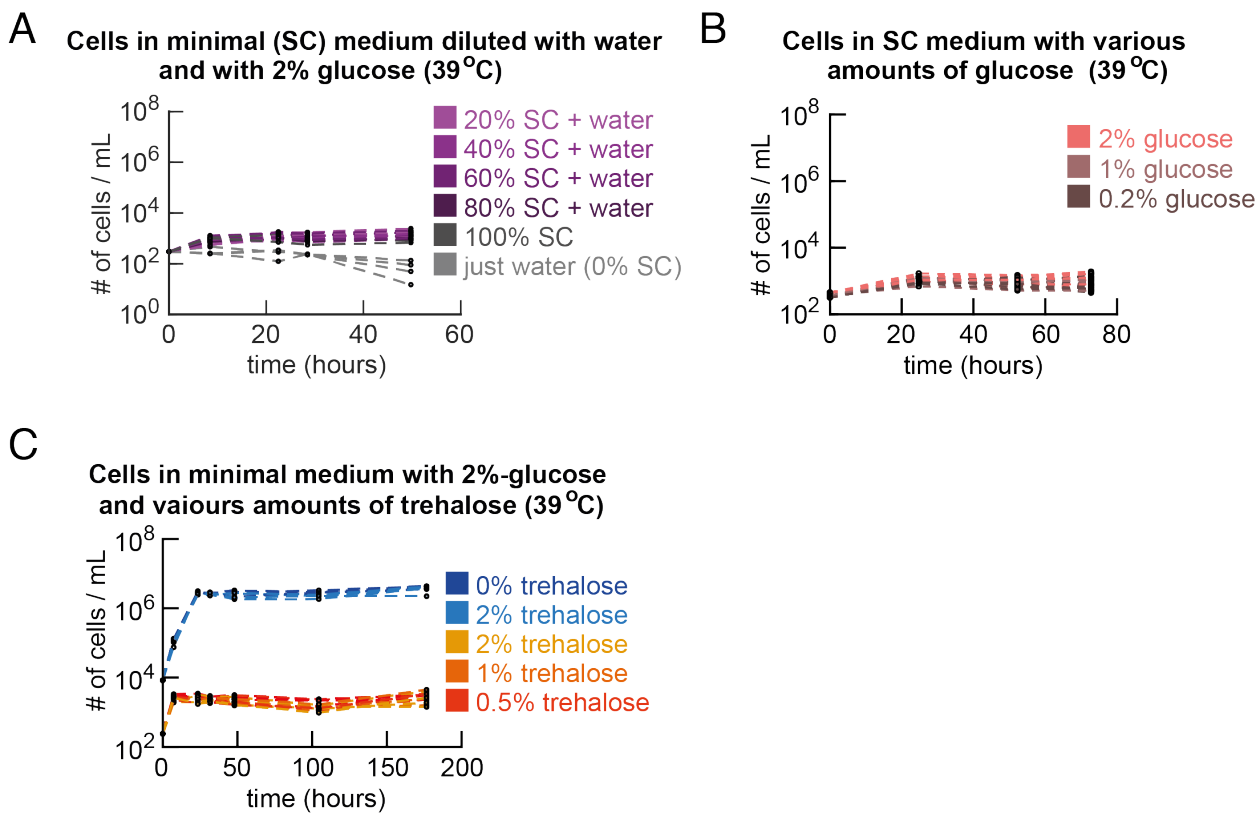

Figure S8. Population-density dependent growths at high temperatures are not due to cells depleting essential extracellular resources from the medium (Related to Figure 4C). (A) Initial population-density of ~400 cells/mL. Fresh cells were incubated in minimal media (SC media) that was diluted with water by various amounts as indicated (note: 100% means no dilution). All were supplemented with a saturating concentration (2%) of glucose. Graphs show fresh cells incubated in a 20%-SC medium (i.e., 20% SC + 80% water, supplemented with 2% glucose), 40%-, 60%-, 80%-, and 100%-SC medium. Also shown are data for fresh cells incubated just in water with a 2%-glucose (i.e., no essential amino acids since SC medium is water with all the essential amino acids and nitrogenous bases). In all these conditions, populations did not grow at all. Hence, population growths are not caused by to some extracellular components in the SC-medium being depleted by cells. (**B**) Complementary to (A), fresh cells were incubated in minimal media (SC -media) with various concentrations of glucose. Shown here are cells incubated in SC + 2% glucose, SC + 1% glucose, and SC + 0.2% glucose. None of these populations grew. Thus, population-density dependent growths that we observed are not due to depletions of glucose from the media. (A) and (B) together establish that depletions of any of the nutrients in the media are not the reason for the observed population-density dependent behaviors. (**C**) Fresh cells incubated in minimal media supplemented with various concentrations of trehalose at two different initial population densities (one that is too low for population-level

growth (400 cells/mL) and one that is sufficiently high for population-level growth (10,000 cells/mL)). These data show that trehalose does not inhibit population growths (at 10,000 cells/mL) and it also does not induce population growths (at 400 cells/mL). Trehalose is a common antioxidant. These results show that it plays no role in aiding or preventing populations growths at high temperatures.

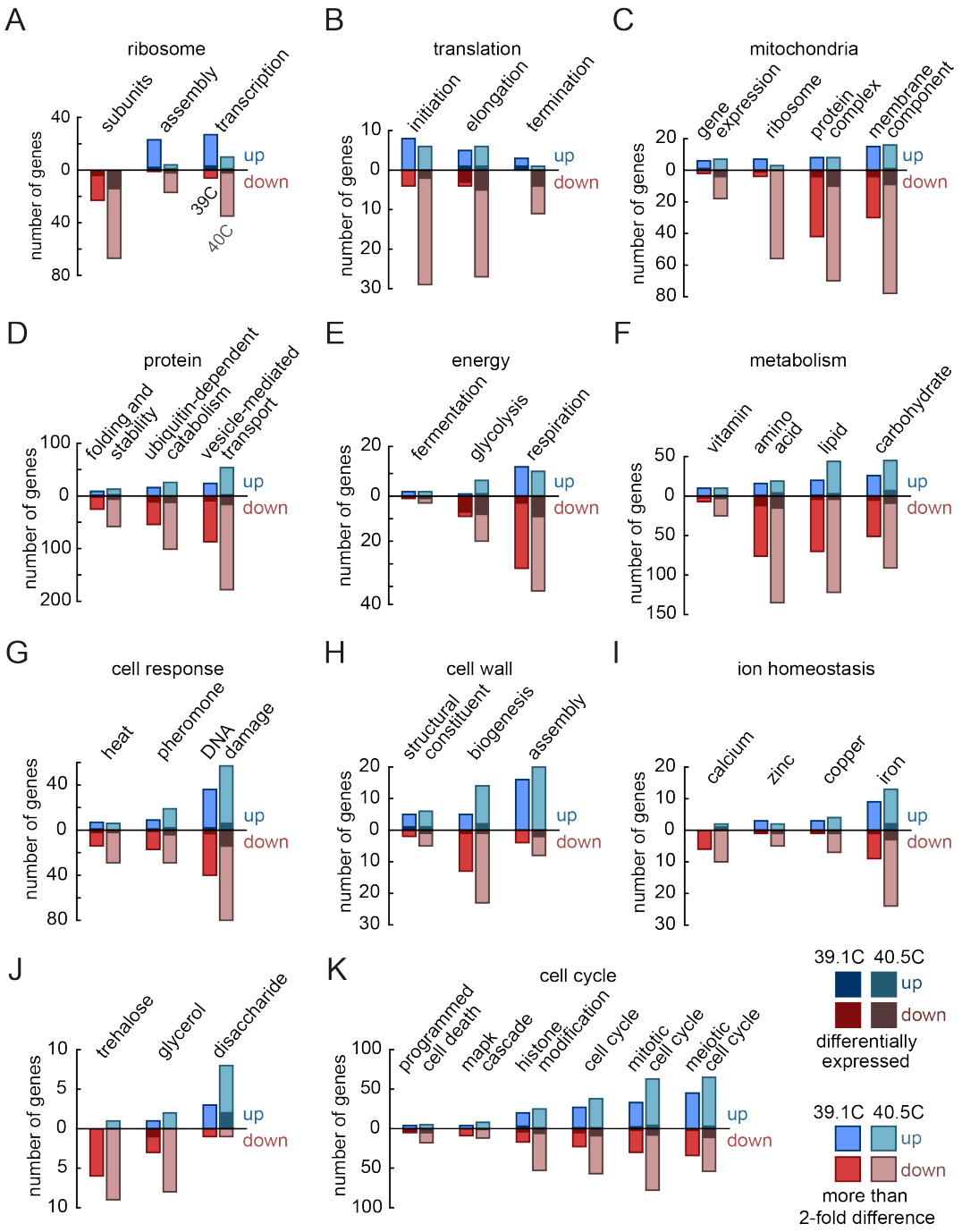

Figure S9. Transcriptome (RNA-seq) analysis reveals effects of high temperatures on gene expression in deterministic-growth and no-growth phases (Related to Figures 4D-F). Transcriptome (RNA-seq) analysis of wild-type yeast cells in mid-log phase growth at 39.1 ^{O}C after 75 hours and 100 hours of incubation (initial population-density: 11,000 cells/mL) and in no-growth-phase at 40.5 ^{O}C after 72 hours of incubation (initial population-density: 48,000 cells/mL). Genes were categorized based on the Gene Ontology (GO) annotations. Shown here are the

number of genes that are upregulated (blue) and downregulated (red) for the respective categories. Genes are classified as up- or down-regulated relative to their expression levels when they grow (always deterministically) at 30 ^{O}C. For the analysis, we averaged the expression levels of three (at 39.1 ^{O}C and 30 ^{O}C) or two (at 40.5 ^{O}C) biological replicates. The gene counts only include genes whose expression level differed by at least a 2-fold from their expression levels at 30 ^{O}C (shown in light colors) and differentially expressed genes (shown in dark colors). (**A)** For genes associated with the ribosome: Notably, ribosomal protein subunits were downregulated. Ribosome assembly, polymerases I and III and transcription of rRNA were upregulated for deterministically growing yeasts at 39.1 ^{O}C while they were downregulated for yeasts in the no-growth phase at 40.5 ^{O}C. (**B-C**) For genes associated with translation (**B)** and the mitochondrial genes (**C**): Almost all differentially expressed genes were downregulated. The ribosomal genes of mitochondria were upregulated for deterministically growing cells at 39.1 ^{O}C and downregulated for the no-growth-phase cells at 40.5 ^{O}C compared to their expression levels at 30 ^{O}C. (**D-F**) For genes associated with protein processing (**D**) and genes associated with the central carbon metabolism (**E**) and other metabolic activity (**F**), many of which are significantly differentially expressed: Most notably, genes of the glycolysis and respiration were downregulated at the high temperatures. (**G-H**) For cellular responses to heat and DNA damage (**G**) and genes associated with the cell wall (**H**): Strikingly, cell wall assembly was upregulated for both the deterministically growing cells and the no-growth-phase cells at high temperatures relative to their expression levels at 30 ^{O}C. **(I-J)** For genes associated with ion homeostasis (**I**), and other carbohydrates (**J**): Most genes involved in the turnover of trehalose (a metabolite involved in thermotolerance) were downregulated compared to their expression levels at 30 ^{O}C. Genes associated with metabolism of disaccharides such as maltose were upregulated, even though the minimal growth medium lacked disaccharides and our wild-type strain is unable to grow on maltose. (**K)** Genes associated with the cell cycle. (**A-K**) Overall summary: Our transcriptome analysis revealed that global gene-expression levels were predominantly downregulated for both deterministically growing cells (at 39.1 ^{O}C) and no-growth-phase cells (at 40.5 ^{O}C) compared to the expression levels at 30 ^{O}C. Moreover, we found that this global downregulation was more pronounced for the no-growth-phase cells at 40.5 ^{O}C than for the growing cells at 39.1 ^{O}C. Interestingly, the central carbon metabolism was downregulated for the no-growth-phase and deterministically growing cells and the ribosomal subunits were also downregulated, even for the deterministically growing cells at 39.1 ^{O}C. Furthermore, genes involved in the ribosomal transcription and assembly, the mitochondrial ribosome, and translation termination were upregulated for the deterministically growing cells at 39.1 ^{O}C and downregulated for the no-growth-phase cells at 40.5 ^{O}C.

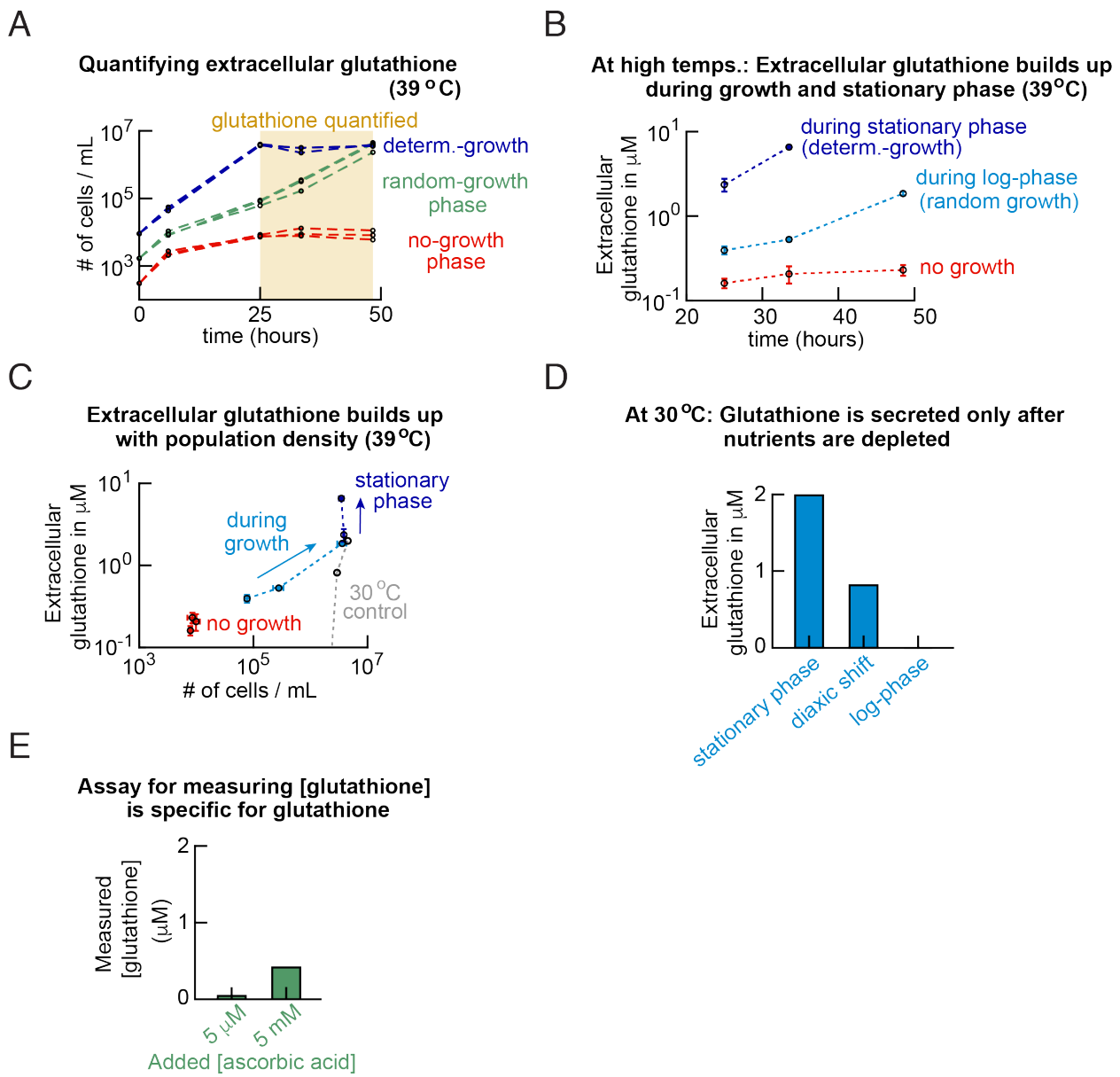

Figure S10. At high temperatures, cells of random and deterministic growth-phase populations secrete glutathione while they are in log-phase growth and stationary phase (Related to Figure 4E). (A) Populations with different staring densities at 39 ^{O}C (*n*=3). For each of these populations, we measured the extracellular glutathione concentration after 25, 33 and 48 hours of incubation in (B-C) (in the yellow region shown). **(B)** To quantify the extracellular glutathione concentration, we separated the cells from their medium by using a filter that removes the cells (VWR: 0.45-μm pore filter with a cellulose-acetate membrane). To ensure and verify that there were no cells in the filtered media, we flowed the filtered media through the flow cytometer. The flow cytometer did not detect any cells in the filtered medium. We measured the glutathione concentration in the filtered medium that we took from each population shown in (A) as described

in manufacturers' protocol (see Methods). We found that the extracellular glutathione concentration remained constant over time for no-growth populations (red curves). We found that the extracellular glutathione concentration increased over time during the log-phase growths (light blue curves). Moreover, we also found the extracellular glutathione concentration increasing over time after a population had reached stationary phase (due to reaching the carrying capacity) (dark blue curves). To check whether most of the extracellular glutathione was in the oxidized or the reduced form, we also determined the concentration of oxidized glutathione in the filtered media after 48 hours of incubation. For populations growing in log-phase (light blue), we found that most of the extracellular glutathione was in the reduced form (77% $\pm$ 3% (s.e.m., n=3), approximately 3:1 ratio of reduced-to-oxidized form). For the non-growing populations in the no-growth phase (red), we found that most of the extracellular glutathione was in the oxidized form (25% $\pm$ 24%, approximately 1:3 ratio of reduced-to-oxidized form). Hence, growing populations maintain an extracellular environment with more reduced glutathione than oxidized glutathione (note that the reduced form, not the oxidized form, is able to remove reactive oxygen species). **(C)** By combining (A) and (B), we determined the extracellular glutathione concentration as a function of the population density. This plot shows that the no-growth populations maintain both a nearly constant population density and extracellular glutathione concentration over time. While a population is growing in log-phase, the extracellular glutathione concentration increases with the population density over time and it continues to increase after the population reaches the carrying capacity and stops growing (i.e., during stationary phase). **(D)** As a control, we measured the concentration of extracellular glutathione for populations grown at 30 ^{O}C. We did not measure any extracellular glutathione for populations that were growing at log-phase (unlike in the case of higher temperatures such as 39 ^{O}C - see (C)). But as soon as the cells depleted glucose, they started to secrete glutathione, resulting in the glutathione accumulating in the extracellular medium over time while the cells were in stationary phase. This observation matches the fact that the media that we transferred from a population that was in stationary phase at 30 ^{O}C (16 hours after incubation in 30 ^{O}C) induced population growth at 39 ^{O}C. **(E)** Testing the specificity of the commercial glutathione assay kit. We added low and beyond-saturating (physiologically unrealistic) concentrations of ascorbic acid into minimal media and then flowed these ascorbic-acid containing media through the glutathione assay kit. This control reports the false positive signal observed for other antioxidants (that can also induce growth c.f. fig 4D). For physiological concentrations of ascorbic acid (e.g., 5 μM shown), the glutathione assay kit did not show any readings (i.e., it did not falsely report presence of glutathione). It only reported as false signal (i.e., presence of glutathione) for the non-physiological ascorbic-acid concentration of 5 mM - the kit

falsely reported ~0.4 μM of non-existent glutathione. Note that 0.4 μM is much lower than the 6 μM glutathione that we observed in the filtered media of cultures at high temperatures. Thus, for our purpose, we can say that the glutathione assay kit is specific for glutathione with negligible false positive readings.

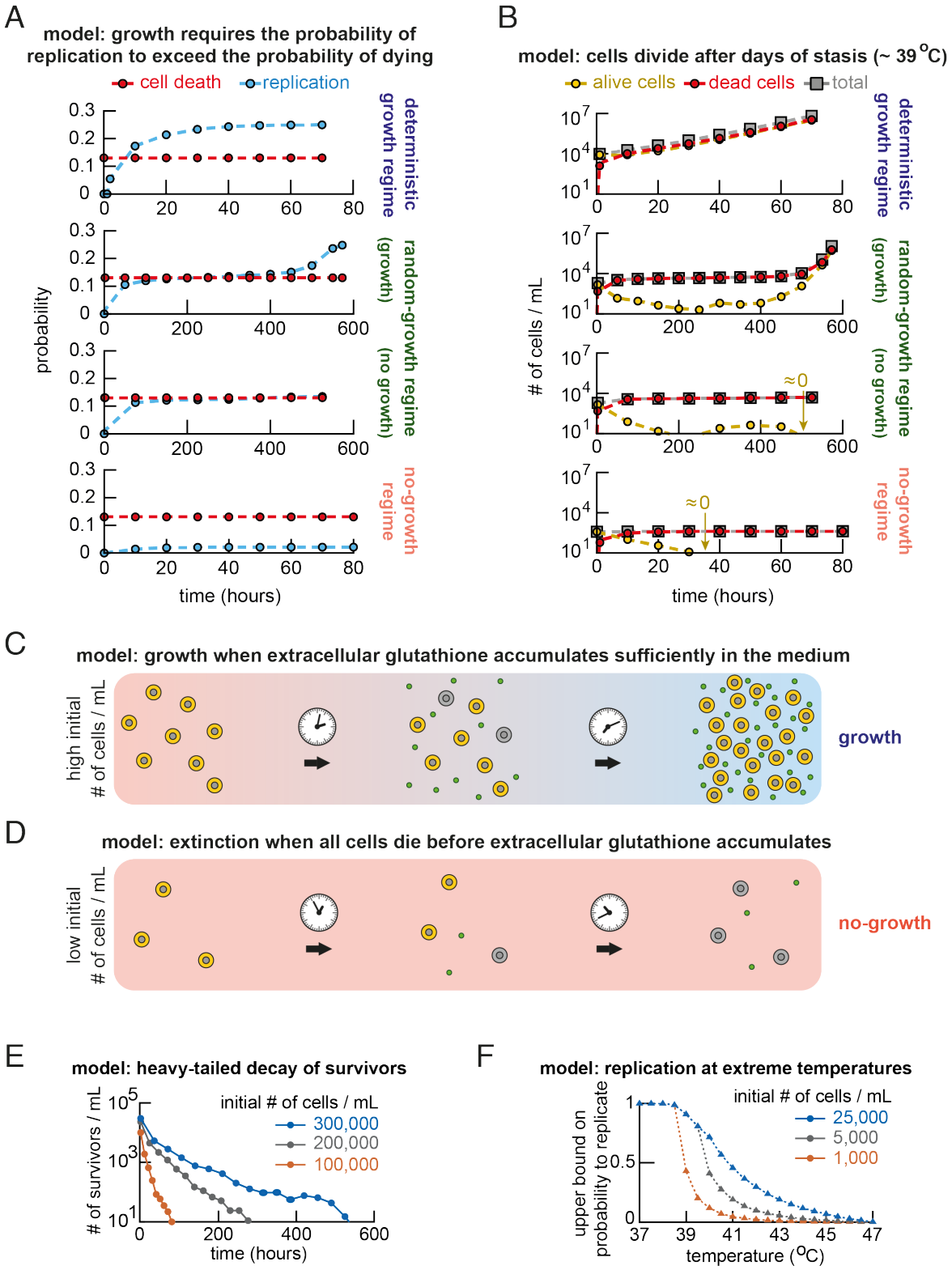

Figure S11. Schematics of the mathematical model that recapitulates all the main features of our data (Related to Figure 5). (**A**) The probability of replicating and the probability of dying

as a function of time for the deterministic growth (top row), random growth (2nd row), random no-growth (3rd row) and no-growth phases (4th row). Here, we used the same, fixed set of parameters as the ones that we used to reproduce all the other main experimental observations in Figure 5. By assumption, the probability of dying per unit time is fixed for a specific temperature as illustrated in Figure 5B. For all populations, the probability of replication is initially zero and increases over time depending on the number of alive cells in the population. With alive cells secreting the extracellular factor, the probability of replicating quickly exceeds the probability of dying for high initial population-densities in the deterministic growth phase after a few units of time (top row). Eventually the probability of replicating plateaus at the maximally allowed value. For initial population-densities in the random growth phase (2nd and 3rd rows), the number of alive cells initially decreases over time as the probability of replicating approaches – but is smaller than – the probability of dying. Simultaneously, this continuously decreasing pool of alive cells secretes the extracellular factor, resulting in the probability of replicating continuously increasing - albeit with decreasing rate - over time. After some point in time (around 300 hours in the graphs shown here), the probability of replicating is very close to the probability of dying, and very few alive cells are left in the population. Here, the probability of replicating either exceeds the probability of dying - leading to net growth of the population - or the probability of replicating comes close to but remains smaller than the probability of dying - leading to a population extinction. For initial population-densities in the no-growth phase (bottom row), the probability of replicating remains well below the probability of dying. Here, the population goes extinct before the alive cells can accumulate sufficient concentration of the extracellular factor to increase the probability of replicating. (**B**) Besides all other features (shown in Figure 5), the model also reproduces the number of red cells and white cells, including the sustained population of few white cells in the random growth and no-growth phase, that we observed in Figure S5. Shown here are the number of alive (yellow points) and dead cells (red points) over time that our model produced for the same populations as in (A). For initial population-densities in the deterministic-growth phase (top row), the population grows exponentially as the probability of replicating quickly exceeds the probability of dying. For initial population-densities in the random-growth phase (2nd and 3rd rows), the number of alive cells over time reflects the fine balance between the probability of replicating and probability of dying. Here the population is ultra-sensitive to the state transitions of the very few alive cells (at ~300 hours). Based on whether these alive cells stay alive without replicating, replicate, or die in the next time steps, the population can eventually either expand and grow exponentially or go extinct in subsequent times. Finally, for initial population-densities in the no-growth regime (bottom row), the number of alive cells decreases exponentially as the probability

of replicating remains close to zero and does not approach the probability of dying, leading to a net death until the population goes extinct. (**C - D**) Schematic summary that outlines the main features of the model. All cell populations eventually either grow exponentially (**C**) or go extinct (**D**). Whether a population grows exponentially or goes extinct is determined by the balance between a decreasing number of alive cells that continuously accumulate the extracellular factor, which in turn determines the probability of replicating for those alive cells. There is a net decrease per unit time in the number of alive cells as long as the probability of replicating is smaller than the probability of dying. If a sufficient amount of the extracellular factor accumulates, then the probability of replicating at some time exceeds the probability of dying, leading to net - exponential - growth if there are any alive cells remaining (C). As long as a sufficient amount of extracellular factor does not accumulate before all cells die, the probability of replicating remains below the probability of dying, leading to a decrease in the number of alive cells and eventually a population extinction (D). (**E**) A competition between two elements - a constant probability of dying and an initially lower probability of replicating that keeps approaching the probability of dying, evermore closing the gap between the two values - results in the population whose approach to extinction continuously slows down over time, leading to the number of survivors decreasing over time as a heavy-tailed (power-law-like) function (see Supplemental Notes). (**F**) Finally, a consequence of our model, which recapitulates all the main features of the experimental data, is that cells can, in fact, replicate, albeit with a vanishingly low probability, at extremely high temperatures (e.g. 45 ^{O}C) for which only the no-growth phase exists in the population-level phase diagram.

I. Model Summary

This section summarizes the most important analytical results on the model for yeast growth. Please refer to the subsequent sections below for further mathematical argumentation and all derivations. The simplest stochastic model for yeast growth at high temperature is that, per unit time, cells replicate and cells die with fixed probabilities. However, any such linear model is unable to reproduce the behavior of yeasts we observed experimentally. In our experiments, we use $c = 8$ replicate populations per condition, and the largest inital population size is $k = 25$-fold larger than the smallest one. An upper bound for the probability to observe the outcome of our experiments is then given by (see section III),

$$P_{c,k} \leq k^c \cdot \left(\frac{1}{k+1}\right)^{1+\frac{c}{k}} = 0.26. \tag{1}$$

We were able to produce these results many times (see Figs. 2A-C, Figs. S3A-J), such that the simple linear model cannot explain our experimental observations. Hence, we need an extended non-linear stochastic model to reproduce the data. To this end we use experimental observations (Figs. 4A-G). Our data suggests that cells secrete gluathione that allows for cell growth when glutathione accumulates sufficiently (Figs. 4A-G, Figs. S8-10). We therefore extend the simplest model, by assuming that the probability of replication of cells depends on the concentration of extracellular glutathione that cells secrete at a constant rate.

The full model is as follows. Let A_t be the population-size of alive cells at time t with initial population-size A_0. Per unit time, any cell dies with probability $p_d(T)$ linearly increasing with the temperature T. Moreover, assume that cells replicate with probability $p_a(t)$, where $p_a(t)$ is given by the maximum probability of replication μ that is scaled by a Hill equation depending on the concentration of the extracellular glutathione m_t and constant $k(T)$. Finally, the extracellular glutathione accumulates by secretion of alive cells with rate $r_m(T)$. We describe the total population size at time t with N_t and let $N_{birth}(t)$ and $N_{death}(t)$ be the number of births and deaths of cells at time t. Then the stochastic model describing yeast growth at high temperature is given by,

$$\begin{aligned}
N_{birth}(t) &\sim \text{Binom}\big(A_t, p_a(t)\big),\\
N_{death}(t) &\sim \text{Binom}\big(A_t, p_d(T)\big),\\
A_{t+1} &= A_t + N_{birth}(t) - N_{death}(t),\\
p_a(t) &= \mu \cdot \frac{m_t}{k(T) + m_t},\\
m_{t+1} &= m_t + r_m(T) A_t,
\end{aligned} \tag{2}$$

where A_0 is the initial population-size, and the initial probability of replication is given by $p_a(0) = 0$. The total population size changes according to,

$$N_{t+1} = N_t + N_{birth}(t). \tag{3}$$

This model reproduces all the main features we observed experimentally (Fig. 5, Fig. S11). All simulations were run using one single set of parameters, choosing the temperature T and initial population-size A_0 appropriately. The parameters used to fit the model to our experimental data are the maximum probability of replication $\mu = 0.25$ (approximating the maximum growth rate of our wild-type yeast), $K = k(T)/r_m(T) = 30,000$ (chosen such that order of magnitude of the phase boundary matches the boundary we found experimentally, Fig. 2D) and the probability of dying depending on temperature, $p_d(T) = \mu \cdot \frac{T - T_{min}}{T_{max} - T_{min}}$ with $T_{min} = 37.9$ and $T_{max} = 40.2$ (chosen such that the endpoints of the phase boundary match the boundary we found experimentally, Fig. 2D).

Using an deterministic approximation of the stochastic model allows us to derive an analytical expression for the phase boundary between the deterministic growth phase and the no-growth phase (Section VI). The analytical expression for the phase boundary is given by (simplified form of 72),

$$A_0 \propto \frac{K \cdot p_d^2(T)}{\mu - p_d(T)}. \tag{4}$$

Hence, the initial population-size required for growth diverges as the probability of dying approaches the probability of replication in the model. Finally, the deterministic approximation is used to show that - in the no-growth regime where the population does not grow - the decrease of the population of alive cells is not appropriately described by exponential decay (Section VII). Instead, the instanteneous death rate is continously decreasing as a result of the probability of replication increasing over time. Therefore the decay of the number of alive cells in the population follows a heavy-tailed function, as we also find in our experiments (Figs. 3A-B, Fig. S7).

II. Simple model description

First, we consider the simplest stochastic model for yeast growth at high temperature. To this end, we assume that all cells are identical and independent of each other (i.i.d.). Let A_t be a random variable representing be the number of alive cells at time t. Per unit time, cells replicate with probability p_a and cells die with a probability $p_d(T)$ that is monotonically increasing with temperature T. Then $\{A_t\}_{t\geq 0}$ is a discrete-time Markov process describing yeast growth at high temperatures. Let N_t be the total population size at time t and describe the number of births and deaths with $N_{birth}(t)$ and $N_{death}(t)$ respectively. Then the simple model is described by,

$$N_{birth}(t) \sim \text{Binom}\big(A_t, p_a\big), \tag{5}$$

$$N_{death}(t) \sim \text{Binom}\big(A_t, p_d(T)\big), \tag{6}$$

$$A_{t+1} = A_t + N_{birth}(t) - N_{death}(t). \tag{7}$$

with the total population size changing according to,

$$N_{t+1} = N_t + N_{birth}(t). \tag{8}$$

We can approximate the stochastic model as follows. As both cell replication and death follow a Binomial distribution with parameters p_a and $p_d(T)$ respectively, we have,

$$\mathbb{E}[A_{t+1}] = A_t + p_a A_t - p_d(T) A_t. \tag{9}$$

By approximation for large A_t, we then obtain the following linear differential equation describing the system,

$$A_{t+1} - A_t \approx \Big(p_a - p_d(T)\Big) \cdot A_t \tag{10}$$

$$\frac{dA}{dt} \approx \Big(p_a - p_d(T)\Big) \cdot A. \tag{11}$$

It follows that, for a sufficiently large initial population of replicating cells A_0, the number of alive cells in the population can be modeled by,

$$A(t) = A_0 \cdot \exp\Big((p_a - p_d(T))t\Big). \tag{12}$$

The behavior of the model is completely independent of the initial population-size of replicating cells A_0. When $p_a > p_d(T)$, the population will grow exponentially. In contrast, growth on average is impossible if $p_a < p_d(T)$

and then the population goes extinct. Hence, yeast growth ceases at the temperature where the probability of dying p_d exceeds the probability of replication p_a.

III. Necessity of a non-linear model

In this section we prove that we need a non-linear model to describe yeast growth at high temperature. Experimentally we observe populations of cells of some initial size N_0 that never grow (Figs. 2S-C, Figs. S3A-J). Therefore, these cultures never obtain the sufficiently large initial population of replicating cells A_0 required for growth. Moreover, in our experiments we use a $k = 25$-fold difference in initial population size. In contrast, these populations with intially $k \cdot N_0$ cells always grow and hence do obtain A_0. With any simple linear model as described above, the population with initially $k \cdot N_0$ cells can grow exponentially when $p_d(T) < p_a$. Hence, as all probabilities are independent of the behavior of the cells, the population with intitially N_0 cells is required to go extinct by chance, while $p_d(T) < p_a$ dictates that they should exponentially grow (on average in the limit of a large population size). To get a better understanding of wheter such a linear population-level model is able to fit our observed growth of yeasts at high temperature, we look at the probability to get the sufficiently large population of replicating cells A_0 via any mechanism, i.e. the probability to obtain a population that will grow exponentially.

Let A_0 be the population of alive cells that is sufficiently large, such that the population of cells will eventually grow exponentially. Consider populations of with intial population-sizes of N_0 and $k \cdot N_0$ cells. We assume that cells are identical and independent of all other cells (i.i.d.). Let $p_g > 0$ be the probability that a cell gives rise to A_0. Then the probability that the culture with initial population-size N_0 will never exponentially grow is the probability that none of the cells gives rise to the population A_0, given by,

$$P_{\text{no growth}}(N_0) = (1 - p_g)^{N_0}. \tag{13}$$

Moreover, the probability that the culture with initial population-size $k \cdot N_0$ will eventually exponentially grow is the probability that some cell gives rise to the population A_0, given by,

$$P_{\text{growth}}(k \cdot N_0) = 1 - (1 - p_g)^{k \cdot N_0}. \tag{14}$$

Hence, the probability to observe c cultures with initial population-size N_0 never grow exponentially, and simultaneously c cultures with initial population-size $k \cdot N_0$ to all grow exponentially is given by,

$$P_c(N_0) = \Big(P_{\text{no growth}}(N_0)\Big)^c \cdot \Big(P_{\text{growth}}(k \cdot N_0)\Big)^c \tag{15}$$

$$= \Big((1 - p_g)^{N_0}\Big)^c \cdot \Big(1 - (1 - p_g)^{k \cdot N_0}\Big)^c. \tag{16}$$

Here $P_c(N_0)$ gives the probability of the outcome we observe in our experiments: all cultures with low initial population-size do not grow, while all cultures with high initial population-size do grow exponentially. To maximize the probability of observing our experimental outcome, we therefore want to maximze $P_c(N_0)$ for the only free variable p_g. To simplify notation, let $x := (1 - p_g)^{N_0}$. Then,

$$P_c(N_0) = x^c \cdot (1 - x^k)^c \tag{17}$$

$$= \big(x - x^{k+1}\big)^c. \tag{18}$$

Taking the derivative to maximize $P_c(N_0)$,

$$\frac{dP_c}{dp_g} = \frac{dP_c}{dx} \cdot \frac{dx}{dp_g} \tag{19}$$

$$= c\big(x - x^{k+1}\big)^{c-1} \cdot \big(1 - (k+1)x^k\big) \tag{20}$$

$$\cdot N_0(1-p_g)^{N_0-1} \cdot -1$$

Notice that $\frac{dP_c}{dp_g}$ is zero for the trivial solutions $p_g = 0$ and $p_g = 1$. The nontrivial solution of $\frac{dP_c}{dp_g} = 0$ is described by,

$$1 - (k+1)x^k = 0, \tag{21}$$

which yields the following solution that maximizes $P_c(N_0)$,

$$x = \left(\frac{1}{k+1}\right)^{\frac{1}{k}}. \tag{22}$$

Therefore, the probability $P_c(N_0)$ that describes the outcome we observe in our experiments is maximized for,

$$(1-p_g)^{N_0} = \left(\frac{1}{k+1}\right)^{\frac{1}{k}}, \tag{23}$$

hence the most likely probability that a cell gives rise to the population A_0 that will grow exponentially is given by,

$$p_g = 1 - \left(\frac{1}{k+1}\right)^{\frac{1}{kN_0}}. \tag{24}$$

Finally, the actual probability $P_c(N_0)$ that describes the outcome we observe in our experiments is bounded by,

$$P_c(N_0) \leq \left(\frac{1}{k+1}\right)^{\frac{c}{k}} \cdot \left(1 - \frac{1}{k+1}\right)^c \tag{25}$$

$$= k^c \cdot \left(\frac{1}{k+1}\right)^{1+\frac{c}{k}}. \tag{26}$$

This upper bound for the outcome we observe in our experiments only depends on the number of replicate populations c per condition and the dilution factor k between these conditions. As described above, we use $c = 8$ replicate populations per condition and a $k = 25$-fold difference between the largest and smallest initial population-sizes in our experiments. Then an upper bound for the probability to observe the outcomes of our experiments is given by substituting $c = 8$ and $k = 25$ into 25, leading to $P_c(N_0) \leq 0.26$. As we consistently make these experimental observations (Figs. 2A-C, Figs. S3A-J), one of the assumptions must be incorrect: cells are not identical or not independent, and the simple model cannot explain our experimental data.

IV. Non-linear model definition

We conclude that the simplest model 12 is insufficient to describe the behavior of our yeast cells at high temperature. Moreover, our data suggests that cells secrete glutathione that accumulates extracellularly and allows for cell growth when a sufficient concentration has been reached (Figs. 4A-G, Figs. S8-10). As our cells are genetically identical, we can safely assume that cells are not independent (not autonomous). We therefore extend the simplest model with secretion of glutathione and an effective probability of replication that depends on the extracellular concentration of glutathione.

Similar to the simple model 12, let A_t be the population size of alive cells at time t. Per unit time, any cell dies with probability $p_d(T)$ depending on the temperature T. In contrast with the simplest model, we now

assume that the probability of replication is not constant, based on our observation that population-sizes can remain constant while still containing alive cells (random phase, Figs. 2A-B). Hence, assume that cells replicate with probability $p_a(t)$, where $p_a(t)$ is some maximum probability of replication μ scaled by a Hill equation (Michaelis-Menten) depending on the concentration of extracellular glutathione m_t and constant $k(T)$. Finally, the extracellular glutathione accumulates by constant secretion of alive cells with secretion rate $r_m(T)$. Again describe the total population size at time t with N_t and let $N_{birth}(t)$ and $N_{death}(t)$ be the number of births and deaths of cells at time t. Then the full stochastic model is described by,

$$\begin{aligned} N_{birth}(t) &\sim \text{Binom}\big(A_t, p_a(t)\big), \\ N_{death}(t) &\sim \text{Binom}\big(A_t, p_d(T)\big), \\ A_{t+1} &= A_t + N_{birth}(t) - N_{death}(t), \\ p_a(t) &= \mu \cdot \frac{m_t}{k(T) + m_t}, \\ m_{t+1} &= m_t + r_m(T) A_t, \end{aligned} \tag{27}$$

with the total population size changing according to,

$$N_{t+1} = N_t + N_{birth}(t). \tag{28}$$

The behavior of this model is completely different than the simplest model (Section II). Here, the probability of replication $p_a(t)$ increases (monotonically) over time as function of the number of alive cells. Hence, as $p_a(0) = 0$, there is no guarantee that any population of cells will grow exponentially, unless the cells accumulate sufficient extracellular glutathione m_t such that $p_a(\tau) > p_d(T)$ for some time $\tau > 0$. This model 27 is studied in more detail with simulations (Fig. 5 and Fig. S11) and analytically with an approximation in the following sections.

V. Deterministic approximation

We analytically study the model 27 next, for which we use a deterministic approximation to gain insight into some key features of the model. In our model both cell replication and death follow a Binomial distribution, such that the number of alive cells at the next time step can be estimated by,

$$\mathbb{E}[A_{t+1}] = A_t + p_a(t) A_t - p_d(T) A_t. \tag{29}$$

By approximation, we obtain the following nonlinear system of equations:

$$A_{t+1} = A_t + p_a(t) A_t - p_d(T) A_t, \tag{30}$$

$$p_a(t) = \mu \cdot \frac{m_t}{k(T) + m_t}, \tag{31}$$

$$m_{t+1} = m_t + r_m(T) A_t. \tag{32}$$

First, we rewrite this system into a more convenient form. We rescale the extracellular glutathione as $M_t = m_t / r_m(T)$ and $K(T) = k(T)/r_m(T)$. Here, $K(T)$ now represents the constant relative to the production rate. Thus we obtain the following simplified determinist approximation of te stochastic model 27 describing growth

at high temperature,

$$A_{t+1} = A_t \cdot \Big(1 + p_a(t) - p_d(T)\Big) \tag{33}$$

$$p_a(t) = \mu \cdot \frac{M_t}{K(T) + M_t} \tag{34}$$

$$M_{t+1} = M_t + A_t. \tag{35}$$

A. Interpretation

The relative change of the number of alive cells is determined by the factor $1 + p_a(t) - p_d(T)$ which depends on time (probability of replication) and temperature (probability of dying). Here the number of alive cells on average increases when $p_a(t) > p_d(T)$ and decreases when $p_a(t) < p_d(T)$. Notice that $p_a(t) \leq \mu$ for all $t > 0$ by choice of the Hill function. Moreover, as $p_a(0) = 0$, the population of alive cells initially decreases exponentially (approximately with a factor $1 - p_d(T)$ per unit time). For the maximum probability of replication μ and probability of dying p_d we can destinguish three cases:

- $p_d < \mu$: In the limit of the concentration of the extracellular glutathione that accumulates ($M_t \to \infty$) we have $p_a(t) \to \mu$, such that $p_a(t) > p_d$ for some $t > 0$ and therefore the population could grow exponentially.
- $p_d \approx \mu$: Here the probability of dying is very close to the maxium probability of replication for a cell. Hence, only large populations of alive cells can sustain the population as $p_a(t) \to p_d$ only when the concentration of extracellular glutathione increases ($M_t \to \infty$).
- $p_d > \mu$: The probability of dying is higher than the maxium probability of replication, and the population of alive cells decreases on average, and is eventually guaranteed to go extinct.

B. Probability of dying depends linearly on temperature

The behavior of the model is fixed for a given probability of dying $P(death)$ independent of at what temperature T one sets $p_d(T) = P(death)$. Without loss of generality, a sensible assumption is to let the probability of dying for a cell increase monotonically with temperature - for two different temperatures, the probability of dying for the highest temperature is at least the probability of dying for the lowest temperature. Therefore the dependence of $p_d(T)$ on temperature T does not determine the qualitative behavior of the model, but merely when the model displays what kind of behavior. Since we know that all populations grow at $T = 37.9C$ and all populations do not grow at $T = 40.2C$ (Fig. 2D), the simplest assumption is to linearly increase the probability of dying between these values such that $p_d(40.2) = \mu$. Any non-linear choice for the probability of dying as function of temperature yields the same qualitative behavior of the model, but displays these behaviors at different temperatures.

C. Glutathione secretion rate is constant

Instead of being a constant, one can set the glutathione secretion rate $r_m(T)$ to be dependent on, for example, the population size A_t or glutathione concentration m_t. This changes the treshold $K(T)$, which in turn merely changes the shape (sharpness) of the Hill function which the probability of replication $p_a(t)$ depends on (33). Hence, choosing a non-constant secretion rate of glutathione modifies the behavior of the system by changing the sensitivity of the probability of replication for the extracellular glutathione concentration. Since a constant secretion rate is the simplest assumption, we used a constant $r_m(T)$ in our model. The qualitative behavior of the model does not change upon a different, sensible, choice for the glutathione secretion rate $r_m(T)$. For example, making $r_m(T)$ linearly dependent on the population size A_t - higher population sizes secrete more

glutathione - makes the system more sensitive to the initial population size; no growth populations secrete even less glutathione, growth populations secrete even more. Reversely, setting the secretion rate $r_m(T)$, for example, inversely proportional to glutathione concentration - low glutathione concentrations trigger a higher secretion rate than high glutathione concentrations - decreases sensitivity of the system to initial population size. This behavior arises because low initial population sizes are helped by secreting more glutathione that is initially not present.

VI. Description of the phase boundary

The goal of this section is to derive an description of the phase boundary of our model that we observe in simulations (Fig. 5). In contrast to the simple model 12, the non-linear model 27 allows for a population of cells with $p_a(0) < p_d(T)$ that can still exponentially grow for some $t > 0$ due to the accumulation of extracellular glutathione. Although the model 27 is stochastic, we can use the deterministic approximation 33 to gain some insight into the shape of the phase boundary and how the behavior of the model depends on the variables of the model. To this end, notice that any cell population eventually either exponentially grows or goes extinct. Therefore, without loss of generality, assume that there exists some $\epsilon > 0$ such that a cell population will (on average) grow exponentially when $p_a(t) > \epsilon p_d$ for some $t > 0$. Equivalently, a cell population will go extinct if $p_a(t) \leq \epsilon p_d$ for all $t > 0$. For now we ignore the dependence of cell populations on temperature, and write $K = K(T)$ and $p_d = p_d(T)$. The approach here is as follows: First we derive upper and lower bound on the number of alive cells in the population, followed by bounds for the concentration of the extracellular glutathione. Finally, all bounds are used to derive an approximate description of the phase boundary in the simulated phase diagram (Fig. 5).

A. Bounds on number of alive cells

First, we determine a lower and upper bound on the population of alive cells when the population is not growing exponentially ($1 + p_a(t) - p_d(T) < 1$ for 33). Notice that, by recursive substitution of 33,

$$A_{t+1} = A_0 \cdot \prod_{s=0}^{t} \Big(1 + p_a(s) - p_d\Big), \tag{36}$$

where A_0 is the initial population-size of alive cells at time $t = 0$. Moreover, the probability of replication is bounded by $p_a(s) \geq 0$, such that,

$$\begin{aligned} A_t &= A_0 \cdot \prod_{s=0}^{t-1} \Big(1 + p_a(s) - p_d\Big) && (37)\\ &\geq A_0 \cdot \prod_{s=0}^{t-1} \Big(1 - p_d\Big) && (38)\\ &= A_0 \Big(1 - p_d\Big)^t. && (39) \end{aligned}$$

Next, suppose that the cell population will go extinct. Then $p_a(s) < \epsilon p_d$ for all $s > 0$ by assumption, and,

$$\begin{aligned} A_t &= A_0 \cdot \prod_{s=0}^{t-1} \Big(1 + p_a(s) - p_d\Big) && (40)\\ &< A_0 \cdot \prod_{s=0}^{t-1} \Big(1 - p_d(1-\epsilon)\Big) && (41)\\ &= A_0 \Big(1 - p_d(1-\epsilon)\Big)^t && (42) \end{aligned}$$

Hence, when a cell population will go extinct, then the number of alive cells in the population at time t is bounded by,

$$A_0\Big(1-p_d\Big)^t \leq A_t < A_0\Big(1-p_d(1-\epsilon)\Big)^t. \tag{43}$$

B. Bounds on concentration of extracellular glutathione

Next, we determine a lower and upper bound on the concentration of the extracellular glutathione when the population of cells is not exponentially growing, similarly to the bound of the number of alive cells. Recursive substitution of M_t and using 36 yields,

$$M_{t+1} = \sum_{s=0}^{t} A_s \tag{44}$$

$$= A_0 + \sum_{s=1}^{t} A_s \tag{45}$$

$$= A_0 + A_0 \sum_{s=1}^{t} \prod_{k=0}^{s-1} \Big(1 + p_a(k) - p_d\Big) \tag{46}$$

Moreover, we can bound the probability of replication by $p_a(k) \geq 0$, such that,

$$M_{t+1} \geq A_0 + A_0 \sum_{s=1}^{t} \prod_{k=0}^{s-1} \Big(1 - p_d\Big) \tag{47}$$

$$= A_0 + A_0 \sum_{s=1}^{t} \Big(1 - p_d\Big)^s \tag{48}$$

$$= A_0 \sum_{s=0}^{t} \Big(1 - p_d\Big)^s. \tag{49}$$

Equation 49 represents the first $t+1$ terms of a geometric series that converges as its ratio satisfies $|1-p_d(T)| < 1$. Hence,

$$M_{t+1} \geq A_0 \cdot \frac{1-\big(1-p_d\big)^{t+1}}{p_d}. \tag{50}$$

Next, we seek an upper bound on the concentration of the extracellular glutathione. To this end, suppose that $p_a(k) < \epsilon p_d$ for all $k > 0$ such that the population is will go extinct by assumption. Then, starting from 46, and substituting $p_a(k) < \epsilon p_d$ and simplifying as in 49,

$$M_{t+1} = A_0 + A_0 \sum_{s=1}^{t} \prod_{k=0}^{s-1} \Big(1 + p_a(k) - p_d\Big) \tag{51}$$

$$< A_0 + A_0 \sum_{s=1}^{t} \prod_{k=0}^{s-1} \Big(1 - p_d(1-\epsilon)\Big) \tag{52}$$

$$= A_0 \sum_{s=0}^{t} \Big(1 - p_d(1-\epsilon)\Big)^s. \tag{53}$$

Substituting the known sum of a geometric series we obtain,

$$M_{t+1} < A_0 \cdot \frac{1-\big(1-p_d(1-\epsilon)\big)^{t+1}}{p_d(1-\epsilon)}. \tag{54}$$

Hence, when the cell population goes extinct, 50 and 54 yield the following bounds for the concentration of the extracellular glutathione M_t at time t,

$$A_0 \cdot \frac{1-\big(1-p_d\big)^t}{p_d} \leq M_t < A_0 \cdot \frac{1-\big(1-p_d(1-\epsilon)\big)^t}{p_d(1-\epsilon)}. \tag{55}$$

C. Growth vs extinction regime

The bounds 43 and 55 provide us with estimates of the number of alive cells in the population and the concentration of the extracellular glutathione when knowing that the population will go extinct. These bounds are usefull, as they provide the worst-case estimate for the accumulation of extracellular glutathione and population-size of alive cells. Using these bounds we seek a contradiction next. Assuming the worst-case scenario (extinction), we seek the initial population-size of alive cells A_0 for which the probability of replication still exceeds the probability of dying before extinction. Hence the population cannot (on average) go extinct as - even in the worst-case - the population will accumulate sufficient extracellular glutathione.

More specifically, we first determine a lower bound for the probability of replication $p_a(t)$ at the time the cell population is not yet extinct as function of A_0. Here, the cell population is not yet extinct when 43,

$$A_t \geq A_0(1-p_d)^t = 1. \tag{56}$$

Let τ be the time of extinction. Then, by solving 56, the time of extinction is lower bounded by,

$$\tau > \frac{\log(1/A_0)}{\log(1-p_d)}. \tag{57}$$

Substitution in the lower bound for the concentration of the extracellular glutathione when the population will go extinct yields 55,

$$M_\tau \geq A_0 \cdot \frac{1-\big(1-p_d\big)^\tau}{p_d} \tag{58}$$

$$> \frac{A_0-1}{p_d}. \tag{59}$$

Hence the worst-case concentration of the extracellular glutathione right before extinction is lower bounded by 59. Finally, substitution of 59 into the probability of replication in our model 33 gives,

$$p_a(\tau) > \mu \cdot \frac{A_0-1}{Kp_d+A_0-1}, \tag{60}$$

as $p_a(t)$ is monotonically increasing in M_t. Recall that we assume that the cell population will exponentially grow when $p_a(t) > \epsilon p_d$ for some $t > 0$. Therefore the cell population will at some point grow exponentially when,

$$p_a(\tau) > \mu \cdot \frac{A_0-1}{Kp_d+A_0-1} > \epsilon p_d, \tag{61}$$

which yields the following lower bound on the initial population-size of alive cells in order to be able to grow exponentially,

$$A_0 - 1 > K \cdot \frac{\epsilon p_d^2}{\mu - \epsilon p_d}. \tag{62}$$

Next, again using 43 and 55, we determine an upper bound for A_0 for which the cell population will go extinct. Recall that the cell population will go extinct when $p_a(t) \leq \epsilon p_d$ for all $t > 0$. Specifically, when τ is the time

of extinction, we require $p_a(\tau) \leq \epsilon p_d$ as $p_a(t)$ is monotonically increasing. The number of alive cells when the population will go extinct is bounded by 43,

$$A_t < A_0\Big(1 - p_d(1-\epsilon)\Big)^t. \tag{63}$$

Then the cell population is extinct when t solves,

$$A_0\Big(1 - p_d(1-\epsilon)\Big)^t = 1. \tag{64}$$

Let τ be the time of extinction. Then, by solving 64 we obtain an upper bound for the time of extinction,

$$\tau < \frac{\log(1/A_0)}{\log\big(1 - p_d(1-\epsilon)\big)}. \tag{65}$$

Substitution into the upper bound for the concentration of the extracellular glutathione 55 when the population goes extinct yields,

$$M_\tau < A_0 \cdot \frac{1 - \big(1 - p_d(1-\epsilon)\big)^\tau}{p_d(1-\epsilon)} \tag{66}$$

$$< \frac{A_0 - 1}{p_d(1-\epsilon)}. \tag{67}$$

Finally, substituting 67 into the probability of replication yields,

$$p_a(\tau) < \mu \cdot \frac{A_0 - 1}{Kp_d(1-\epsilon) + A_0 - 1}. \tag{68}$$

Recall that we assume that the cell population will go extinct when $p_a(\tau) \leq \epsilon p_d$. Therefore the cell population indeed goes extinct if, by substitution into 68,

$$p_a(\tau) < \mu \cdot \frac{A_0 - 1}{Kp_d(1-\epsilon) + A_0 - 1} < \epsilon p_d, \tag{69}$$

which yields the following upper bound on the initial population-size of alive cells that guarantees that the population goes extinct,

$$A_0 - 1 < K \cdot \frac{\epsilon(1-\epsilon)p_d^2}{\mu - \epsilon p_d}. \tag{70}$$

In summary, we now found a boundaries for the initial population-size of alive cells that guarantees extinction 70 and for which the population is able to grow exponentially 62. For any initial population-size of alive cells in between, growth and extinction are unpredictable. Hence the random phase in our phase diagram (Fig. 5) is described by,

$$K \cdot \frac{\epsilon(1-\epsilon)p_d^2}{\mu - \epsilon p_d} < A_0 - 1 < K \cdot \frac{\epsilon p_d^2}{\mu - \epsilon p_d}. \tag{71}$$

Interpretation: suppose that we want cell populations to eventually grow when $p_a(t) > \epsilon p_d$ and to go extinct when $p_a(t) \leq \epsilon p_d$. Then, the initial population-size of alive cells that describes the phase boundary scales according to 71,

$$A_0 \propto 1 + K(T) \cdot \frac{p_d^2(T)}{\mu - p_d(T)} \tag{72}$$

Moreover, for the cell populations that go extinct, a lower bound for the extinction time is given by 57.

VII. Heavy-tailed decay to extinction

In this final section, we consider the extinction of cell populations. More specifically, we study the instantaneous rate of death of the number of alive cells in the population. A common assumption is that the number of alive cells follows some exponential decay over time. This is indeed the case when the probability of replication $p_a(t)$ is constant, as then $1 + p_a(t) - p_d(T)$ is constant 33. However, in our model $p_a(t)$ is monotonically increasing.

A. The instantaneous decay rate

First, we derive the instantaneous decay rate of the number of alive cells in the population. To this end, notice that the number of alive cells in the population is approximated by 33,

$$A_{t+1} - A_t = \Big(p_a(t) - p_d(T)\Big) \cdot A_t. \tag{73}$$

We will only be interested at the decay rate of the number of alive cells at time very close to some $\tau > 0$, and therefore temporarilly assume that $p_a(t) = p_a(\tau)$ independent of time. For insight, we further approximate 73 with the following linear differential equation,

$$\frac{dA}{dt} \approx \Big(p_a(\tau) - p_d(T)\Big) \cdot A. \tag{74}$$

Solving this differential yields,

$$A_t = A_\tau \cdot \exp\Big((p_a(\tau) - p_d(T))(t - \tau)\Big), \tag{75}$$

where A_τ is the population of alive cells at our chosen time τ. For $p_a(\tau) - p_d(T) < 0$, the above equation indeed returns exponential decay with instantaneous rate $p_a(\tau) - p_d(T)$ at any time $\tau > 0$. Crucially, this instantaneous rate is monotonically decreasing as $p_a(\tau)$ monotonically increases as we increase the time τ 75. Therefore, the rate of decay decreases although the number of alive cells in the population decays exponentially at each moment in time. We study this decay of the population of alive cells in more detail next.

B. The decay is not exponentially bounded

We show that the decay of the population of alive cells in the culture cannot be exponentially bounded. To this end, we consider the decay of the population of alive cells A_t. Our model states that 33,

$$A_{t+1} = A_t \cdot \Big(1 + p_a(t) - p_d\Big), \tag{76}$$

such that the decay of the number of alive cells is given by recursive substitution 40,

$$A_t = A_0 \cdot \prod_{s=0}^{t-1} \Big(1 + p_a(s) - p_d\Big). \tag{77}$$

Now suppose that the number of alive cells in the population decays at least exponentially. Let $1 > \alpha > 0$ and assume that,

$$A(t) \leq A_0 \cdot \alpha^t. \tag{78}$$

Then exponential boundedness requires from 77 and 78 for all $t > 0$ that,

$$A_0 \cdot \prod_{s=0}^{t-1} \Big(1 + p_a(s) - p_d\Big) \leq A_0 \cdot \alpha^t. \tag{79}$$

Taking the logarithm and eliminating common terms yields the following condition for the decay of the population of alive cells to be exponentially bounded,

$$\frac{1}{t}\sum_{s=0}^{t-1}\log\left(1+p_a(s)-p_d\right)\leq\log(\alpha),\qquad\text{for all } t>0. \tag{80}$$

In words, for the decay to be exponentially bounded, we need $\log(1+p_a(t)-p_d)$ to be on average remain smaller than $\log(\alpha)$ for some fixed $1>\alpha>0$. However, $p_a(t)$ is monotonically increasing in time. Therefore we have $p_a(t)\geq p_a(\tau)$ for any $t\geq\tau$ and some $\tau>0$. It follows that we can use the bounds $p_a(t)\geq 0$ for $t<\tau$ and $p_a(t)\geq p_a(\tau)$ for $t\geq\tau$. Hence we can further bound the left hand side of condition 80 as,

$$\frac{1}{t}\sum_{s=0}^{t-1}\log\left(1+p_a(s)-p_d\right) \tag{81}$$

$$\geq\frac{1}{t}\sum_{s=0}^{\tau}\log(1-p_d)+\frac{1}{t}\sum_{s=\tau}^{t-1}\log(1+p_a(\tau)-p_d) \tag{82}$$

$$=\frac{\tau}{t}\log(1-p_d)+(1-\frac{\tau}{t})\log(1+p_a(\tau)-p_d). \tag{83}$$

Next, substitution of the lower bound 83 into 80 yields the following condition for the decay of the population of alive cells to be exponentially bounded,

$$\frac{\tau}{t}\log(1-p_d)+(1-\frac{\tau}{t})\log(1+p_a(\tau)-p_d)\leq\log(\alpha), \tag{84}$$

for all $t>\tau$. For any $0<\alpha<1$ we can distinguish the following cases:

- $p_d<\mu$: These parameters allow for growth in our model. We can choose any A_0 such that $p_a(\tau)\geq p_d$ eventually for some $\tau>0$. Then $\log(1+p_a(\tau)-p_d)>0$ and substitution into 84 yields the condition,

  $$\frac{\tau}{t}\log(1-p_d)\leq\log(\alpha), \tag{85}$$

  which is violated as $\frac{\tau}{t}\log(1-p_d)\to 0$ as $t\to\infty$ for τ fixed. Hence, the decay cannot be exponentially bounded when $p_d<\mu$.
- $p_d>\mu$: The probability of dying is higher than the maxium probability of replication. We cannot obtain $p_a(t)\geq p_d$ and the population is guaranteed to go extinct. At time of extinction $\tau>0$ we have $p_a(\tau)<p_d$ and such that there exists some $1>\alpha>0$ for which the decay of the population of alive cells is exponentially bounded (we can choose $\alpha=1+p_a(\tau)-p_d$ in 79). However, the decay rate of the viability of the population monotonically decreases over time up to the point of extinction, starting with instantaneous rate $1-p_d(T)$ at $t=0$ decreasing to $1+p_a(\tau)-p_d(T)$ at time of extinction.

In summary, the instantaneous decay rate of the number of alive cells in the population is monotonically decreasing in time, starting at $1-p_d(T)$ at time $t=0$ and decreasing to $1+p_a(\tau)-p_d(T)$ in case of extinction at time τ or to zero when the culture grows exponentially. Hence, the change of the population of alive cells in the culture cannot be appropriately modeled by exponential decay. Experimentally, we find that the decay of the population of alive cells is indeed heavy tailed (Figs. 3A-B, Fig. S7), and appropriately modelled by a power-law function.